

NMR ANALYSIS OF  
5'-5' PHOSPHODIESTER BONDED  
rCUG

NMR ANALYSIS OF  
5'-5' PHOSPHODIESTER BONDED  
rCUG

by

GARRY WALTER BUCHKO, B.Sc.

A Thesis

Submitted to the School of Graduate Studies  
in Partial Fulfilment of the Requirements  
for the Degree  
Master of Science  
McMaster University

Master of Science (1986)  
(Chemistry)

McMaster University  
Hamilton, Ontario

Title: NMR Analysis of a 5'-5' Phosphodiester Bond  
Author: Garry W. Buchko, B.Sc. (University of Manitoba)  
Supervisor: Professor R.A. Bell  
Number of Pages: xiv, 197

## ABSTRACT

A mixture of two isomers of rCUG was separated by HPLC, 5'C3'-5'U3'-5'G3' (low Rf) and 3'C5'-5'U3'-5'G3' (high Rf). These were characterized by proton, carbon-13, and phosphorus-31 NMR and enzymatic methods. This allowed for the first detailed analysis of the effect of a 5'-5' phosphodiester bond upon the solution structure of a ribo-oligonucleotide trimer.

The proton spectra of both isomers were assigned with the aid of COSY, NOE, RCT, and decoupling experiments. Variable temperature chemical shift plots and the use of first order coupling constants in various "Karplus-styled" equations allowed for the building of a solution structure model of the CUG high molecule that proved to adhere to Sundaralingam's "rigid" nucleotide concept (1973). The 5'-5' phosphodiester bond adopted a zig-zag right handed helical conformation with the terminal ribose oriented with the H-1' away from the center of base-stacking. This placed the C more distant from U and resulted in U/G base-stacking taking precedence over the dominant C/U base-stacking present in CUG low. The presence of the 5'-5' phosphodiester did not greatly effect the backbone structure of the adjacent 3'-5' linked phosphodiester bond.

Both trimers were digested with Phy M to remove the G. Dimers with 2'/3' cyclic Us were obtained and compared with 3'-5' CpU.

The presence of a 5'-5' phosphodiester bond allowed for a near complete assignment of the C-13 spectra of the two isomers. These spectra represent an addition to the small number of C-13 spectra available on ribo-oligonucleotide trimers.

The P-31 spectrum of CUG low was unambiguously assigned by selective CW proton decoupling. The high isomer spectrum was interpreted on the basis of this assignment and revealed a substantial downfield movement in the chemical shift of the phosphorus involved in the 5'-5' bond.

## ACKNOWLEDGEMENTS

I would like to acknowledge the guidance of my supervisor, Dr. R.A. Bell, in the completion of this work.

The assistance of Dr. D. Alkema and Dr. D.W. Hughes was instrumental in accomplishing the experimental aspects of this research and I am very grateful for it.

I deeply appreciate Dr. T. Neilson for allowing me to live in his laboratory and for his many suggestions.

Discussions with B. Allore, Dr. J. Orban, A. Sinclair, B. Sayer and even D. Neilson were also appreciated.

I wish to acknowledge Dr. A. Bain and Dr. C. Rogers of Bruker Spectrospin in Milton for assistance in acquiring 500 MHz spectra at their facilities.

In indirect assistance I thank my track coach, W. Urie, and the people of the Hamilton Olympic Club for their company on and off the track. I thank my aunt and uncle, Ann and Bill Buchko, for allowing me to live with them during most of my stay. Finally I would like to thank my parents back in Manitoba, whose love and support spanned the Great Lakes and vast wilderness of northern Ontario everyday.

## TABLE OF CONTENTS

	Page
ABSTRACT	iii
ACKNOWLEDGEMENTS	v
LIST OF FIGURES	viii
LIST OF TABLES	xii
ABBREVIATIONS	xiii
1.1.1 INTRODUCTION	1
1.2.1 Nucleic Acid Nomenclature	3
1.3.1 Nucleic Acid Analysis	8
1.3.2 X-Ray Crystallography	9
1.3.3 NMR Analysis of Nucleic Acids	13
1.3.3.1 The Furanose Ring	16
1.3.3.2 Heterobase-ribose Ring Torsion Angle, $\chi$ (C1'-N)	17
1.3.3.3 Dihedral Angle Between C-5' and C-4', $\gamma$	18
1.3.3.4 Dihedral Angle Between O-5' and C-5', $\beta$	20
1.3.3.5 Dihedral Angle Between C-3' and O-3', $\epsilon$	23
1.3.3.6 Dihedral Angle Between P and O-3', $\delta$ , and O-5'	25
1.4.1 The "Rigid" Oligomer	26
2.1.1 NUCLEAR MAGNETIC RESONANCE	29
2.2.1 Relaxation	34
2.3.1 Double Resonance Experiments	38
2.3.2 Spin Decoupling	38
2.3.3 The Nuclear Overhauser Effect	41
2.3.4 Exchangeable Proton Detection	44
2.3.5.1 Two Dimensional NMR	48
2.3.5.2 Correlated Spectroscopy (COSY)	51
2.3.5.3 The Relay Coherence Transfer Experiment	54
3.1.1 EXPERIMENTAL	57
3.1.1 Deblocking of the Fully Blocked Ribo-Oligonucleotide	57
3.1.2 Deblocking Procedure	57
3.2.1 High Performance Liquid Chromatography	60
3.3.1 Enzymatic Digestions	63

3.4.1	Proton NMR Spectroscopy	65
3.4.2	Decoupling Experiments	67
3.4.3	NOE Experiments	68
3.4.4	The 1:1 Pulse Experiment	69
3.4.5	The COSY Experiment	71
3.4.6	The RCT Experiment	72
3.4.7	P-31 Spectra Acquisition	74
3.4.8	C-13 Spectra Acquisition	75
4.1.1	RESULTS AND DISCUSSION	76
4.1.1.1	Chemical Synthesis of the Trimers	76
4.1.1.2	Overview of the Phosphotriester Method	76
4.2.1	Trimer Proton Assignment	79
4.2.2	CUG Low Proton Assignments	80
4.2.3	CUG High Proton Assignments	91
4.2.4	Trimer Exchangeable Proton Spectra	104
4.3.1	Enzymatic Analysis	108
4.3.2	The Enzymatic Results	111
4.4.1	Dimer Proton Assignments	114
4.5.1	Phosphorus NMR	123
4.5.2	Phosphorus Referencing and Assignments	125
4.6.1	Carbon-13 Spectroscopy	132
4.7.1	Solution Behaviour	143
4.7.2	Trimer Base Region	143
4.7.3	Trimer H-1' Proton Regions	148
4.7.4.1	Dimer Behaviour	152
4.7.4.2	Aromatic Region	158
4.7.4.3	H-1' Region	159
4.8.1	The Phosphodiester Backbone	161
4.9.1	The N/S Equilibrium	171
5.1.1	CONCLUSIONS	179
	BIBLIOGRAPHY	185

## LIST OF FIGURES

Figure		Page
1.	Primary structure of CUG, numbering scheme, and IUPAC-IUB nomenclature.	4
2.	Torsion angle nomenclature as defined by Klyne and Prelog (organic) and by spectroscopists (Saenger, 1984).	5
3.	A) N/S ribose equilibrium. C) Syn/anti glycosidic orientation.	6
4.	Watson-Crick base pairing of C•G and U•A together with the additional base pairing possible with U•A. Major and minor grooves also defined.	11
5.	Newman projections of the torsion angles $\gamma$ , $\beta$ , $\epsilon$ , $\alpha$ , and $\zeta$ plus schematic representation of their interrelationship.	18
6.	A) Vector model of the alignment of spins in a magnetic field. B) Vector description of a $90^\circ$ pulse. C) Vector model of $T_2$ relaxation. D) Chemical shift anisotropy as it relates to benzene.	33
7.	Spin decoupling experiments. A) Pulse sequence. B) Effective magnetic field due to $B_2$ . C) Ideal decoupling effect on spectrum.	40
8.	The Nuclear Overhauser Experiment. A) Energy level diagram for a two spin system, I and S, with one half spins. B) NOE pulse sequence.	42
9.	Vector diagram of the 1:1 hard pulse sequence.	45
10.	A) Schematic pulse sequence for a heteronuclear 2D experiment. B) Vector representation for a C-H system. C) 2D heteronuclear spectrum for C-H.	49
11.	The Cosy experiment. A) General pulse	52

sequence. B) 2D COSY spectrum. C)  
Possible magnetization transfer pathways  
in a pyrimidine nucleoside.

12.	Schematic route for the phosphotriester synthesis of cytidyl-3',5'-uridylyl-3',5'-guanine.	78
13.	2D contour plot of the COSY-45 experiment on CUG low, 5.89 mM, at 30.8°C.	82
14.	500 MHz spectrum of the ribose region of CUG low, 3.31 mM, 30.0°C.	85
15.	Comparison of the downfield proton spectral region of CUG high and low at 70°C.	89
16.	Comparison of the upfield ribose proton spectral region of CUG high and low at 70°C.	90
17.	Difference NOE experiment on the G(H-8) proton of CUG high.	95
18.a	2D contour plot of the RCT experiment on CUG high, 7.90 mM, at 60.1°C.	96
18.b	Comparison of F1 slices of the 2D RCT experiment on CUG high, 7.90 mM, with a normal proton spectrum obtained at 60.1°C.	98
19.	2D contour plot of CUG high, 1.81 mM, in a 1:1 solution of D <sub>2</sub> O:pyridine.	99
20.	Result of a decoupling experiment involving the irradiation of the C(H-1') proton of CUG low.	102
21.	Exchangeable proton spectra of CUG high and low, -3.4°C.	105
22.	Enzymatic digestion products of CUG low: A) Snake venom phosphodiesterase. B) Phy M.	110
23.	HPLC chromatograms of various spleen phosphodiesterase digests (1 OD samples).	113
24.	250 MHz comparison of the lowfield proton spectra of CU>P high and low at 60.6°C.	117

25.	250 MHz comparison of the upfield ribose proton region of CUG high with CU>P high at 60°C.	118
26.	250 MHz comparison of the lowfield proton spectra of CUG high and CU>P high at 60°C.	119
27.	250 MHz comparison of the lowfield proton spectra of 3'-5' linked CpU with CU>P low at 30.0°C.	120
28.	500 MHz proton spectrum of the ribose region of CU>P high at 30.0°C.	121
29.	Phosphorus variable temperature plot of both CUG isomers.	127
30.	Results of the selective proton CW decoupling experiments to assign the phosphorus signals.	130
31.	Carbon-13 spectrum of the ribose region of CUG low, 50.6 mM, at 22°C.	135
32.	Carbon-13 spectrum of the ribose region of CUG high, 65.4 mM, at 55°C.	136
33.	Variable temperature plots comparing the H-8 and H-6 protons of CUG high and low.	144
34.	Variable temperature plots comparing the H-5 protons of CUG high and low.	145
35.	Variable temperature plots comparing the anomeric H-1' protons of CUG high and low.	149
36.	Plot of the chemical shift of the C H-1' proton of CUG low versus its $3J(H1',H2')$ coupling constant.	151
37.	Variable temperature plots comparing the H-6 protons of CU>P high, CU>P low and CpU (3'-5').	154
38.	Variable temperature plots comparing the H-5 protons of CU>P high, CU>P low and CpU (3'-5').	155
39.	Variable temperature plots comparing	156

	the H-1 protons of CU>P high, CU>P low, and CpU (3'-5').	
40.	Variable temperature plots comparing the effect of salt on selective protons of CUG high and low.	157
41.	Variable temperature plots comparing the H-5'/H-5" protons of CUG high and low.	165
42.	Variable temperature plots comparing the H-5'/H-5" protons of CUG high (3.31 mM) and CU>P high (3.90 mM).	166
43.	Schematic comparison of the different behaviour of the oligoribonucleotides depending on the phosphodiester bond.	170
44.	Variable temperature plots of the $^3J(H1',H2')$ coupling constants of CUG high and low.	172
45.	Variable temperature plots of the H-2' and H-3' protons of CUG low.	173
46.	Variable temperature plots comparing the G H-2 protons of CUG high and low.	174
47.	Variable temperature plots comparing the H-2' protons of U and the H-3' protons of U and G in CUG high and low.	175

## LIST OF TABLES

Table		Page
1.	HPLC Program for separating the fully blocked CUG isomers.	61
2.	HPLC purification yields in OD units (at 260 nm).	62
3.	CUG low H-1' chemical shift comparisons in ppm.	63
4.	Chemical shifts of CUG low, 5.89 mM, no salt, at four different temperatures.	86
5.	First order coupling constants observed CUG low (3.31 mM) in no salt at 47.7°C.	87
6.	Chemical shifts of CUG high, 7.90 mM, no salt, at four different temperatures.	88
7.	First order coupling constants observed for CUG high (7.90 mM) in 1M salt at 47°C.	101
8.	Phy M digestion products as eluted by descending paper chromatography.	112
9.	Comparison of the coupling constants of the 2' and 3' protons of 2'-3' cyclic U with those present in the PhyM dimers.	116
10.	C-5' chemical shifts in ppm.	140
11.	Carbon-13 chemical shifts (ppm) and phosphorus-31 coupling constants (Hz).	142
12.	Aromatic and H-1' chemical shift differences over temperature for CUG high and low in ppm.	146
13.	CUG high and low torsion angle comparison at 47.7°C.	162

## ABBREVIATIONS

A*	adenosine
Å	angstrom ( $10^{-8}$ cm)
BB	broadband decoupling
B <sub>0</sub>	static magnetic field
bz	benzoyl group
C*	cytosine
°C	Celsius
COSY	coherence spectroscopy
CW	continuous wave decoupling
D	deuterium
D <sub>2</sub> O	deuterium oxide
DNA	deoxyribonucleic acid
G*	guanosine
HD	homo-decoupling
HG	homo-gated decoupling
Hz	Hertz
J	coupling constant in Hz
M	Mega ( $10^6$ )
mRNA	messenger RNA
MST	mesitylenesulfonyl 1,2,4-triazole
NOE	nuclear Overhauser effect
NMR	nuclear magnetic resonance
OD	optical density unit
p	2,2,2-trichloroethyl phosphate

p	phosphorus
>P	2'/3' cyclic phosphate
ppm	parts per million
RCT	relay coherence transfer
Rf	ratio of distance travelled by solute to that of solvent
RNA	ribonucleic acid
T*	thymidine
thp	tetrahydropyranyl
tlc	thin layer chromatography
T <sub>m</sub>	melting temperature of a duplexing or base-stacking structure. It is the point where 50% of the molecules are duplexed or stacked
trac	trityloxyacetyl
U*	uridine
UV	ultra-violet
δ	chemical shift
1D	one dimensional
2D	two dimensional

---

\* IUPAC-IUB Joint Commission on Biochemical nomenclature (1983).

### 1.1.1 INTRODUCTION

The importance of nucleic acids within living organisms has been known for a relatively short time. Avery et al. in 1944 were the first to show that nucleic acids played a role in the transportation of genetic information. They showed that the "transforming principle" from heat killed normally infectious pneumococcus Type III cells (S) to mutant non-pathogenic (R) cells was a "nucleic acid of the deoxyribose type." In 1947 Astbury succeeded in acquiring X-ray pictures of DNA fibres. However it took six years before Watson and Crick, with the aid of additional information, proposed their double helical model (1953a) and its semiconservative mode of replication (1953b). The replication model was not confirmed conclusively until 1958 by Meselson and Stahl's density centrifugation experiments with N-15 labelled DNA. Two years later Kornberg (1960) actually isolated and characterized an enzyme, DNA polymerase I, capable of synthesising DNA from nucleotide 5' triphosphates when given a primer and a template. Progress since then has evolved to the point today where it is possible to excise particular genes from eucaryotes with restriction enzymes and induce prokaryotes to produce the gene products (Glover, 1980).

Even if nucleic acids were not directly critical to life by their generation to generation transmission of genetic information, their many other functions within a cell would still warrant their investigation. For instance, the transcription of DNA to messenger RNA (mRNA) that is eventually translated to protein which carries out the reactions of life. In the process transfer ribonucleic acids (tRNA) composed of a number of unique nucleotides bring individual amino acids together. These reactions are carried out on structures called ribosomes which themselves are composed of various sized strands of RNA.

In addition to their importance in protein synthesis, nucleic acids perform yet further cellular tasks. Adenine triphosphate (ATP) is a major energy carrier in cells. Cyclic adenine monophosphate (cAMP) is called a "second hormonal messenger" involved in the amplification cascade of epinephrine induced glycogen breakdown. Various co-enzymes contain nucleic acids, such as nicotinamide adenine dinucleotide (NAD), which belong to a group of enzymes called pyridine-linked dehydrogenases. Many antibiotics, such as puramysin, are derivatives of "normal" nucleic acids and inhibit normal cellular reactions.

Obviously nucleic acids play a multi-functional role in the life process. It is this importance that makes their structure determination in solution a useful tool in understanding the mechanisms of their action.

### 1.2.1 Nucleic Acid Nomenclature

To describe a molecular structure it is important to convey the information to others in terms that are mutually understandable. As a result, the nomenclature used to describe the angles and bonds of a nucleic acid structure will be those agreed upon by the IUPAC-IUB Joint Commission on Biochemical Nomenclature (1983).

A nucleoside is composed of a sugar and a base. In RNA the sugar unit is  $\beta$ -D-ribose (r), while in DNA it is  $\beta$ D-2'deoxyribose (d). The heterocyclic bases consist of two branches, the purines and pyrimidines. The purine bases are guanine (G) and adenine (A). The pyrimidine bases are uracil (U), cytosine (C), and thymine (T). The later pyrimidine is found naturally only in DNA with the non-methylated (C-5) counterpart, U, existing in RNA. The sugar-base linkage is through a  $\beta$ -glycosyl C1'-N bond. The addition of a phosphate group via an ester bond to any of the ribose hydroxy groups produces a nucleotide. This is the repeating unit of RNA and DNA oligomers.

The linkage of these nucleotide units to each other is via phosphodiester bonds. Normally this is from the C-3' position of one nucleotide to the C-5' position of the next nucleotide's ribose. Figure 1 depicts a trimer, cytidylyl-3',5'-uradiylyl-3',5'-guanine. It may be

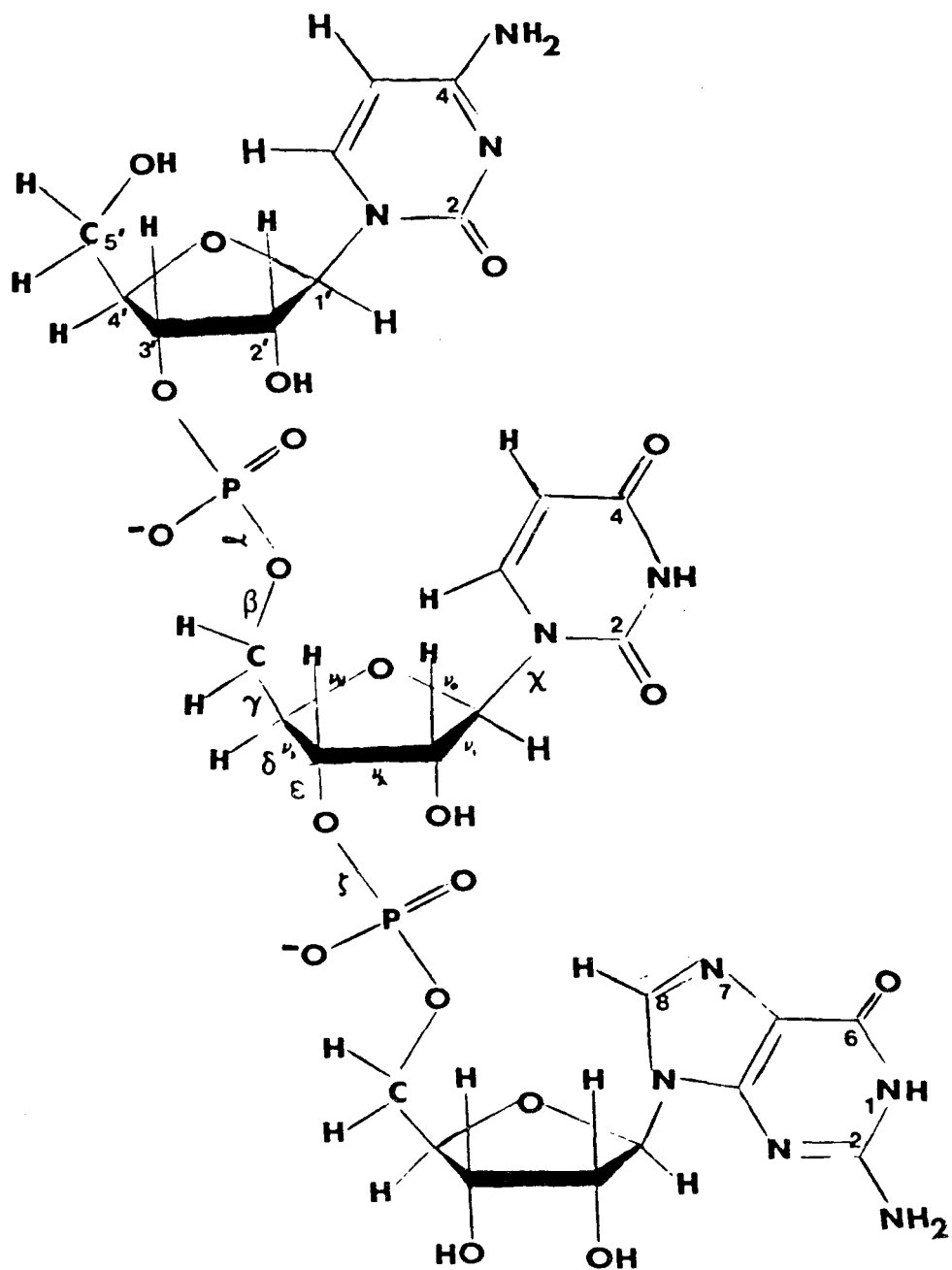


Fig. 1.

Primary structure of CUG, numbering scheme, and IUPAC-IUB nomenclature.

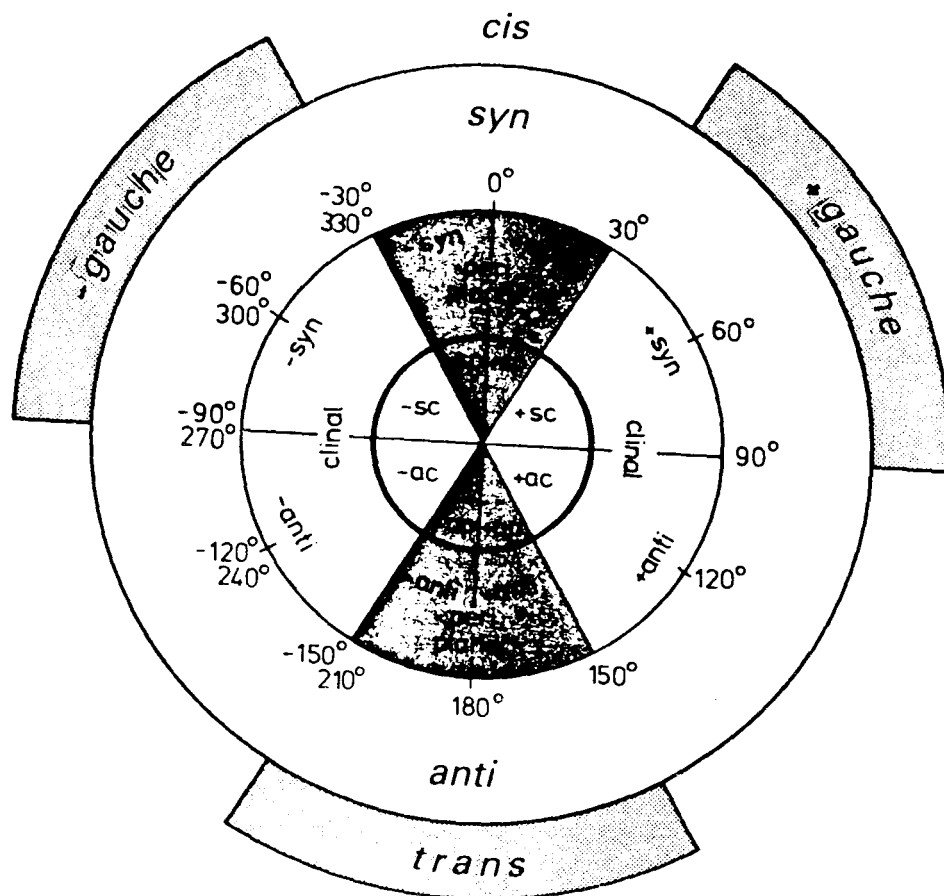
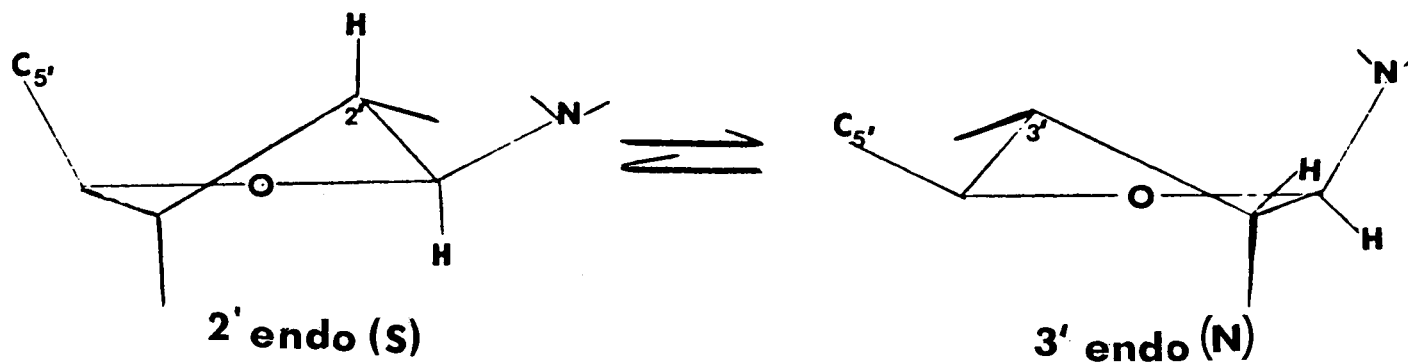


Fig. 2.

Torsion angle nomenclature as defined by Klyne and Prelog (organic) and by spectroscopists (Saenger, 1984).

A



C

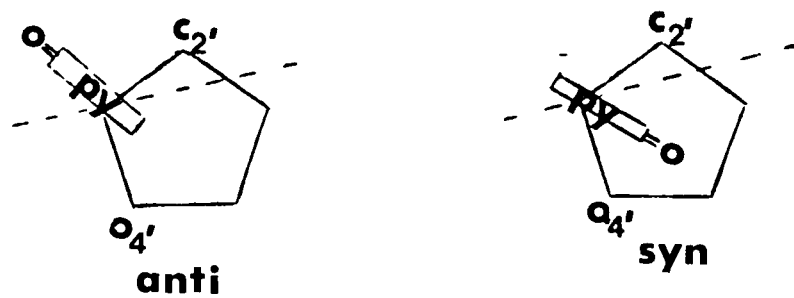


Fig. 3.

A) N/S ribose equilibrium. C) Syn/anti glycosidic orientation.

abbreviated rCpUpG, or CUG, with the understanding that the free 5' hydroxyl end is to the left (C) and the free 3' hydroxyl to the right (G).

Figure 1 describes a few other nomenclature conventions as well. The bases are numbered as indicated for pyrimidines and purines. The sugar atoms are distinguished by the use of a prime symbol. Around the ring it is C1'-C2'-C3'-C4'-O4'. Ribose atoms other than carbon are given the same primed number when bond to these atoms. When two identical atoms are attached, as the hydrogens on C-5', they are distinguished by a double prime, H-5' and H-5''.

To describe the 3D position of the atoms, it is necessary to define the torsion angles that relate 4 positions in space, A-B-C-D. This angle is the one produced by A and D when looking along the B-C bond. A related definition, called the dihedral angle, involves the angle produced by the normals to the ABC plane and the BCD plane.

The accepted IUPAC-IUB convention is to define torsion angle ranges of the orientation of A relative to D as first introduced by Klyne and Prelog (1960). Figure 2 defines these ranges along with the spectroscopists' nomenclature on the outside (Saenger, 1984).

As a result it is possible to define six torsional angles along the oligomer backbone,  $\alpha$ ,  $\beta$ ,  $\gamma$ ,  $\delta$ ,  $\epsilon$ , and  $\zeta$ , as designated in Figure 1 along P-O5'-C5'-C4'-C3'-O3'-P. Five torsion angles may be defined around the ribose ring as well,

$\psi$ ,  $\psi_2$ ,  $\psi_3$ , and  $\psi_4$  as described for the second sugar in the same diagram. Additionally there is the torsion angle  $\chi$  that defines the ribose-base orientation about the C1'-N glycosidic bond. Two general positions exist as illustrated in Figure 3. The syn form has the bulk of the base over the top of the ribose (the six membered ring in the case of the purines, or the O2 keto of the pyrimidines). In the Klyne-Prelog convention this is called sp. In the anti form, ap, the bulk of the base is pointed away from the sugar.

Figure 3 also illustrates the 2 major puckering modes of the furanose ring. If one considers atoms C-4', O-4', and C-1' forming a plane then one defines the pucker with regards to the position of the C-2' and C-3' carbons in relation to it. A carbon towards the C-5' atom and above the plane is considered to be in the endo position. A carbon away from the C-5' carbon and below the plane is designated to be in the exo position (Jardetzky, 1960). An infinite number of variations exist between the two extremes. Hence the concept of pseudorotation is applicable to the furanose ring with preferred conformations being defined by energy minimum conferred by the bases and nucleotides bound to it in oligomers (Altona and Sundaralingam, 1972).

### 1.3.1 Nucleic Acid Analysis

Many techniques have been employed to obtain

information on the torsion angles and conformations of nucleic acids. These include optical rotary dispersion (ORD), circular dichroism (CD), infrared (IR) spectroscopy, fluorescence spectroscopy, ultra-violet (UV) spectroscopy, calorimetric studies, temperature jump studies, nuclear magnetic resonance (NMR) spectroscopy, and X-ray crystallography. All these methods, except for X-rays, involve the study of nucleic acids in solution. However this exception is the technique which can most accurately define the orientation of all the atoms within a molecule. Therefore, though the solution structure may not always be identical to the image expressed via X-ray studies (Seeman, 1980), it is the best method to acquire a first approximation of the preferred orientation of the nucleic acid. Then one may use other solution methods to confirm these structures.

### 1.3.2 X-Ray Crystallography

The basic principle behind X-ray crystallography is that electron dense areas in the sample reflect the electromagnetic radiation applied in a consistent pattern dependent on the position of the repeating unit. Analysis of such patterns, aided today by large computers, allows one to define the position of each atom or group of atoms. With good crystals of molecular weights less than 2000 daltons it is possible to define bond lengths and angles with a standard

deviation of .005 to .01 Å and .3 to 1° (Saenger, 1984). For bigger molecules, such as tRNA, resolution becomes a problem. Instead of defining the position of atoms one is now defining only the position of the phosphates, riboses, and bases. For larger molecules yet, such as DNA or RNA double helical fibres, the resolution is poorer because only quasi-crystals exist and the individual helices are disordered about the fibre axis.

The first dimer to be crystallized and examined by X-rays was UpA (Sussman et al., 1972). Because of the acidic conditions used, normal Watson-Crick pairing was not observed. However, the sugar pucker was found to be C3'-endo with the bases in the anti position as observed by Arnott's group for RNA "A-type" fibres (1969). The next year the same group succeeded in crystallizing a dimer, ApU, which actually formed a Watson-Crick mini double helix (Rosenberg et al., 1973). Again it existed in the C3' endo form with  $\chi$  in the anti position. The only major difference was in the  $\alpha$  and  $\zeta$  torsion angles. The important feature of this result was in it being the first case where Watson-Crick hydrogen bonded base pairing was actually seen at the atomic level. Figure 4 illustrates this Watson-Crick base pair plus three other unusual types possible with A-U. Also illustrated is a G-C base pair, crystallized and its structure determined by X-ray analysis later that year, which contained many of the same features as the A-U double helix (Arnott et al., 1973).

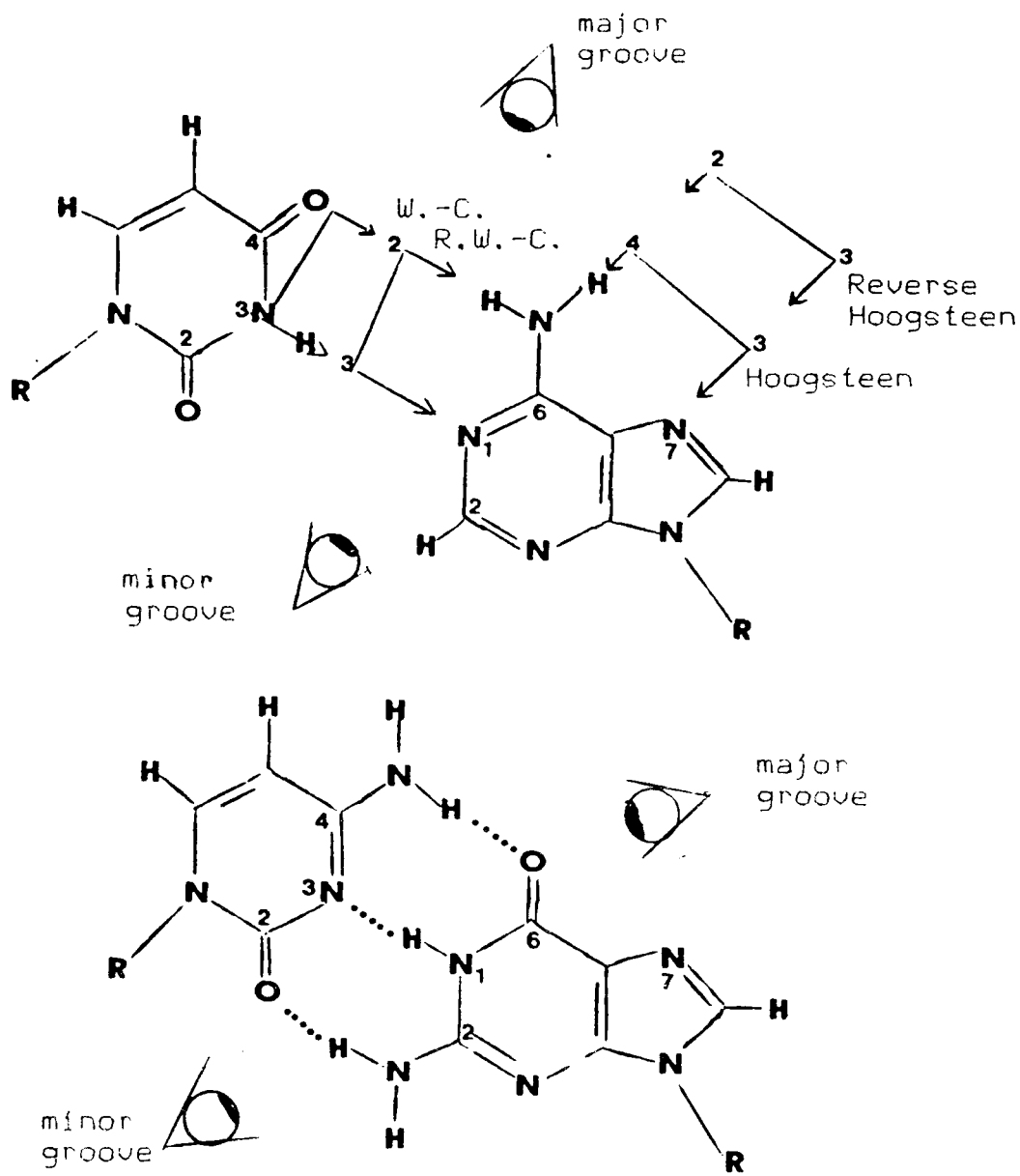


Fig. 4. Watson-Crick base pairing of C•G and U•A together with the additional base pairing possible with U•A. Major and minor grooves also defined.

Note that only one type of base pair is capable of forming in this later situation.

Eventually longer ribose sequences (Mizuno et al., 1981) and tRNA (Kim et al., 1974) were crystallized and studied in this fashion and the same basic features arose as in the RNA mini double helices. The sugars existed in the C3'-endo form (except for isolated cases in tRNA) with the bases in the anti orientation. No "B-type" RNA has ever been seen, most likely due to the presence of the 2'-OH group which prevents the C2'-endo pucker present in the B form (Kallenbach et al., 1977). The most likely explanation is that the 2'-OH and the C5'-OH or 5' phosphate group clash in this endo form (Bridge et al., 1975).

This A-RNA consists of 11 base pairs per turn with a rotation of 30 to 32.7° per residue. The intra-strand phosphate distance is 5.9 Å and the base pairs are dislocated 4.4 to 4.9 Å from the helical axis in the major groove. The base pair tilt is positive and between 10 to 20.2°. As a result of the "hole" in A-RNA and its underwinding, intra- and inter-strand interactions are possible (Saenger, 1984). A slightly different form of A-RNA has also been recognized, called A'-RNA (Arnott et al., 1973). It exists only in high salt concentrations (20%). It has 12 base pairs per turn and a pitch height of 36°.

Left handed Z-DNA has been reported in crystals by Wang et al. (1979) for a dCGCGCG oligomer. This form exists

only in high salt concentrations. It is characterized by an alternating pyrimidine-purine sequence with the purines in the syn and C3'-endo positions while the pyrimidines are in the anti and C2'endo orientations. There is no major groove and the helix axis crosses the minor groove. Recently such a structure has been suggested for RNA in high salt solutions (Hall et al., 1984, Cruz et al., 1985). As yet no crystalline forms of such RNA have been detected. The presence of Z-RNA may be important biologically in situations where double stranded RNA exists, such as in ribosomes and some viruses.

Most of this information on RNA single and double stranded structures have arisen from crystal studies. Although these solids are believed to reflect quite closely the solution structures of molecules, some differences may exist (Seeman, 1980). Furthermore, it is not always possible to synthesise enough oligomer to successfully crystallize it. For both reasons a solution analysis is necessary. While a number of techniques are useful, the most informative of such methods involves the use of nuclear magnetic resonance (Chapter 2).

### 1.3.3 NMR Analysis of Nucleic Acids

One of the strengths of proton NMR spectroscopy is that it allows one to probe specific sites of nucleic acids

in solution. Because of the large number of protons present in nucleic acids, methods to simplify the spectra are useful. The most often used technique is to deuterate exchangeable proton positions (Kearns and Shulman, 1974). As a result one is left with only the H-5 and H-6 base protons in U and C. In purines, both G and A contain a signal due to H-8 while adenine has an additional resonance for H-2. All these aromatic signals are downfield (approximately 5-9 ppm) due to deshielding effects. In a double helical state, H-5, H-6, and H-8 reflect the environment in the major groove while H-2 possesses information on the minor groove (Figure 4). Generally, upfield sigmoidal shifts of these resonances with temperature indicate duplex formation (Gralla and Crothers, 1973) or strong base stacking interactions (Stannard and Fesenfeld, 1975). The midpoint of such curves is called the  $T_m$  of duplex or base stacking formation. These values are sequence dependent and attempts have been made to predict such numbers (Borer et al., 1974). However these predictions are not reliable, especially for short sequences (Romaniuk, 1979) where end effects add to the uncertainty encountered in predicting ideal nearest neighbour effects. Additional efforts have been made to predict the chemical shifts of these resonances from nearest neighbour effects at high temperatures (Bell et al., 1985) with some success.

The only ribose proton readily observable in proton NMR is H-1'. This is because it appears about 1 ppm

downfield of the region usually cluttered by the other ribose resonances (3-5 ppm). Its chemical shift is also a reflection of duplex formation or stacking. More important is its coupling constant ( $3J$ ) to the H-2' proton which is often the only source of information on the preferred sugar conformation in oligomers. Such an insight into  $\chi$ , the percent N or S character, and various other torsion angles arise due to Karplus' finding (1969) that the three bond coupling constants are related to the torsion angle between the two nuclei.

Karplus' original equation was derived for vicinal proton couplings:

$$3J(H,H) = A' \cos^2 \theta + C' \quad (1)$$

where  $A'$  and  $C'$  are constants and  $\theta$  corresponds to the torsion angle between the protons.

Although theoretical attempts have been made to predict the form of "Karplus styled" equations, these efforts have largely failed. As a result most equations are empirical in nature. They differ for various situations as  $3J$  depends on the bond angle, bond length, and the electronegativity and orientation of attached substituent groups. This has lead to a number of different equations to define the many torsion angles needed to model the structure of nucleic acids in solution. A lot of them use X-ray data and/or more simplified molecular systems as their basis. Generally the method of choice throughout this thesis will be

the system presented by Davies (1978) in his review of the subject.

### 1.3.3.1 The Furanose Ring

The form of the Karplus equation suited for the analysis of ribose  $^3J(H,H)$  coupling constants is:

$$^3J(H,H) = A \cos^2 \theta - B \cos \theta + C \quad (2)$$

where A, B, and C are constants (Barfield and Grant, 1965).

A number of different values have been proposed for A, B, and C over the years depending on the data available. The conclusion drawn by Davies (1978) using the analysis of 140 different nucleotides and nucleosides is that the best values for A and B are 10.2 and 0.8 assuming C=0.

It should be realized that the  $\theta$  value obtained by the use of equation (2) is not a reflection of a rigid, non-moving conformation. Instead, it is the average torsion angle of a dynamic equilibrium between all possible conformations. To a good approximation one may assume this equilibrium is a reflection of only two states, N and S (Hruska, 1973). A more detailed analysis of all possible configurations involves the use of pseudorotational analysis (Altona and Sundaralingam, 1973). Such a study uses two calculated values, P, the angle of pucker, and  $\tau$ , the degree of pucker. Such values can be put through an equation to obtain  $\theta$ , but the easiest method is to turn to plotted graphs

of these numbers and read off the % N/S character given 3J (Gushchlbauer and Son, 1975).

Such an analysis may be avoided with the use of two general equations that offer good approximations to the N/S percentages. Given the error normally encountered in acquiring 3J(H,H), such an approximation is usually justified:

$$\%N = 10 \times 3J(H1', H2') \quad (3)$$

$$\%S = 10 \times 3J(H3', H4') \quad (4)$$

(Altona and Sundaralingam, 1973).

It follows that a good approximation to the equilibrium constant between the two states is given by:

$$K_{eq} = 3J(H1', H2') / 3J(H3', H4') \quad (5)$$

(Altona and Sundaralingam, 1973).

In RNA oligomers one encounters only the N conformation in perfect A-type duplexes (Arnott, 1970). Additionally it has been assumed that an increase in base stacking results in an increase in the %N character (Lee et al., 1976). As a result one may follow base stacking or duplexing by monitoring the %N character shifts with temperature changes (Lee and Tinoco Jr., 1980). Thus one possesses another handle other than sigmoidal curves from the aromatic and H-1' protons to follow the behaviour of RNA oligomers with temperature.

#### 1.3.3.2 Heterobase-ribose ring torsion angle, $\chi$ , (C1'-N)

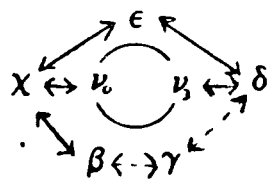
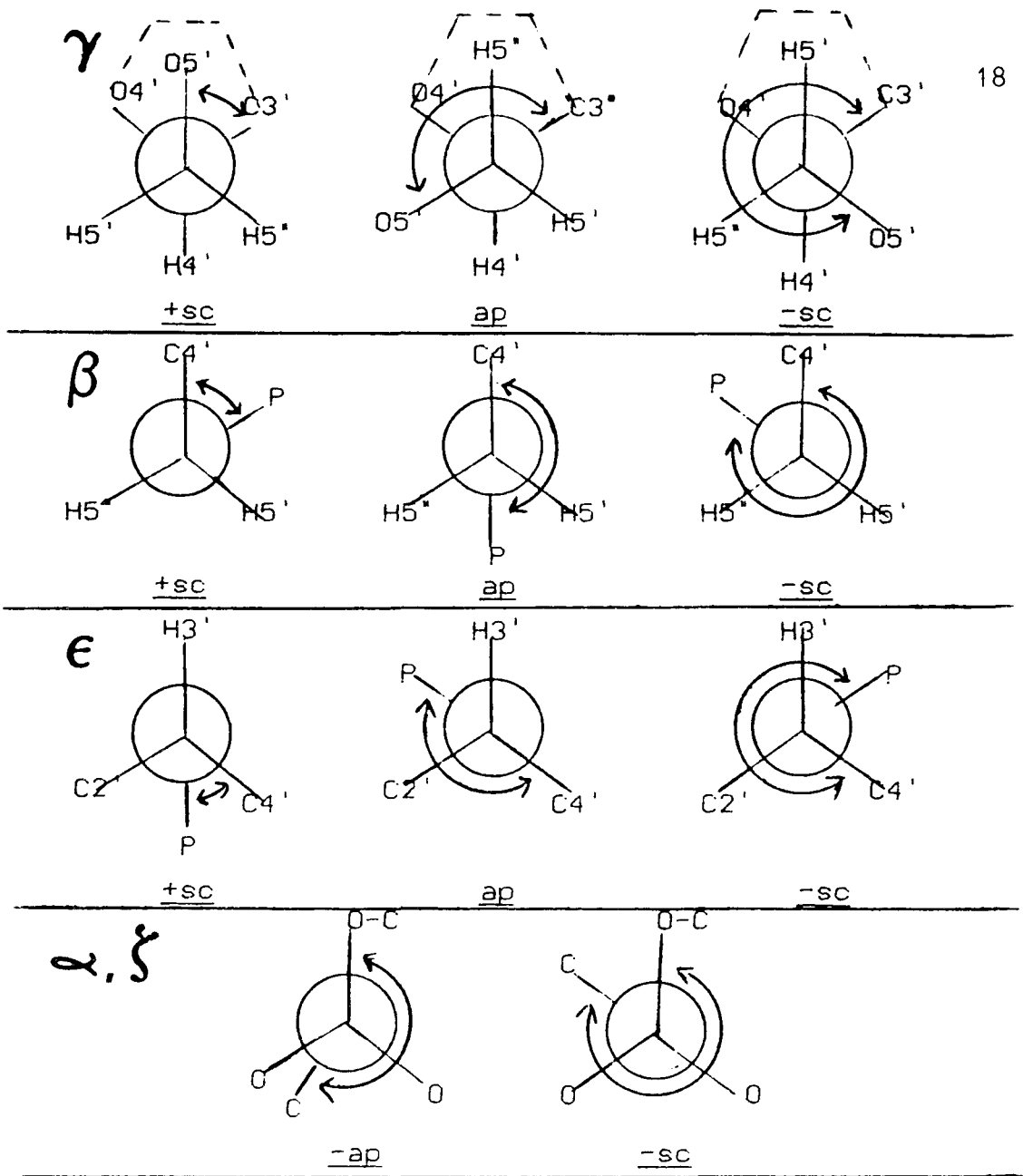


Fig. 5. Newman projections of the torsion angles  $\gamma$ ,  $\beta$ ,  $\epsilon$ ,  $\alpha$ , and  $\xi$  plus schematic representation of their interrelationship.

In this situation no proton/proton coupling constants exist except for hard to find long range couplings between H-1' and the base protons (4 bonds or greater). As a result one must use proton/carbon coupling constants to acquire information on  $\chi$ . The problem with this is the low abundance of natural C-13 and the assignment of resonances if one has enough oligomer to obtain such a coupled spectrum. If these problems are overcome then some general conclusions can be drawn about the orientation of the base about the ribose.

For pyrimidines it has been shown that  $3J(C6, H1') \gg 3J(C2, H1')$  when  $\chi$  is in the anti conformation (Davies, 1976). The opposite is true if the base is in the syn orientation. More specifically:

$$J_{\text{free}}(\text{anti}) < J < J_{\text{free}}(\text{syn}) \quad (6)$$

where  $J_{\text{pyr}} = (3J(C6, H1') - 3J(C2, H1'))$  with  $J(U) = .6$  Hz and  $J(C) = .9$  Hz.

For purines:

$$J_{\text{pur}} = (3J(C8, H1') - 3J(C2, H1')) \quad (7)$$

with  $J_{\text{free}} = 1.2$  Hz.

This method generally agrees with other methods used to determine  $\chi$  such as; i) NOEs between H-1' and base protons H-6 and H-8 (Bell and Saunders, 1973), ii) deuterium substitution effects on  $T_1$  (Akusaka et al., 1975), iii) paramagnetic ion effects on  $T_1$  (Chan and Nelson, 1969),

and iv) ribose proton chemical shift changes brought about by shielding or deshielding effects of the base (Schweizer et al., 1973). In monomers, pyrimidines are generally in the anti position while purines are more a mixture of anti and syn. In double stranded or single stranded base stacked structures the anti form exists, except in Z-helices where purines are in the syn position.

### 1.3.3.3 Dihedral Angle Between C-5' and C-4', $\gamma$

X-ray structures have shown that three primary orientations about the C5'-C4' bond exist (Sundaralingam, 1973) as illustrated in Figure 5.

Values for the torsion angle  $\gamma$  can be best obtained from the H-4' to H-5' and H-5" coupling constants by using  $A=9.7$ ,  $B=1.8$  and  $C=0$  in Equation (2) (Hruska, 1973). As with the ribose conformation however, these states are not fixed and a dynamic equilibrium exists between them. However, by assuming a preference range for each conformation, it is possible to develop empirical formulae to describe the population of each state (+sc, ap, and -sc). Upon reviewing the literature, Davies (1978) concluded that the best expressions for these are:

$$3J(H4', H5') = 1.3P_{+sc} + 2.7P_{ap} + 11.7P_{-sc} \quad (8)$$

$$3J(H4', H5'') = 1.3P_{+sc} + 11.5P_{ap} + 5.8P_{-sc} \quad (9)$$

$$1 = P_{+sc} + P_{ap} + P_{-sc} \quad (10)$$

where P=probability.

The convention with regards to labelling the 5' and 5" protons is to assign the most upfield proton as 5" (Blackburn et al., 1970). If the assignment is reversed the probabilities of P<sub>ap</sub> and P<sub>-sc</sub> are essentially reversed as well.

To avoid calculations that involve solving three equations with three unknowns one may use a more simple procedure as proposed by Sarma et al. (1973a) that offer good correlations to Equations (8-10) for small J (2-3 Hz) but differ by about 10% for couplings in the 4-5 Hz range. Considering the inherent experimental error in the coupling constants, the latter equations often suffice.

$$P_{+sc} = (13 - (3J(H4', H5') + 3J(H4', H5'')))/10 \quad (11)$$

$$P_{ap} = (3J(H4', H5''))/10 \quad (12)$$

$$P_{-sc} = (3J(H4', H5'))/10 \quad (13)$$

Results from X-ray data and application of these empirical equations to solution studies show a large preference for the +sc state, followed by ap. The gauche/gauche interactions of the oxygens in both of these states does not appear to be an important factor, for the -sc situation, which places them both trans, is the least preferred. In oligomers, as duplexing and/or base stacking occurs, the amount of +sc character tends to increase. This can be correlated to an increased anti conformation about the glycosidic bond  $\chi$ . This is most likely because the  $\chi_{sp}/\gamma_{+sc}$

combination is unfavorable because of the steric repulsion between the pyrimidine keto group or the purine amino or keto group with O-5'.

#### 1.3.3.4 Dihedral Angle Between O-5' and C-5', $\beta$

Again there exists three possible conformational states for this bond to assume as illustrated in Figure 5.

Two different methods may be used to describe the situation. The most often used approach deals with the proton 5' and 5" couplings to phosphorus. Values for  $\theta$  are obtained with the use of  $A=18.1$ ,  $B=4.8$ , and  $C=0$  (Lee and Sarma, 1976). With the assumption of a three fold potential of the three states, it is possible to take a weighted average of the couplings these will produce while rotating rapidly and derive equations for the probability of each state:

$$P_{ap} = (25 - (3J(H5',P) + 3J(H5'',P)))/21 \quad (14)$$

$$P_{+sc} = (3J(H5'',P) - 2.1)/21 \quad (15)$$

$$P_{-sc} = (3J(H5',P) - 2.1)/21 \quad (16)$$

Alternatively, if one possesses a phosphorus coupled carbon spectrum, the following equation may be used to obtain a value for  $P_{ap}$  and  $P_{+sc}$  plus  $P_{-sc}$  (Davies, 1978):

$$3J(P,C4') = 10P_{ap} + 2.5(1 - P_{ap}) \quad (17)$$

Only a value for the sum of  $P_{+sc}$  and  $P_{-sc}$  is possible because of the lack of experimental data to draw any

reasonable conclusions.

The results of such studies with RNA oligomers show a large preference for the ap state, where the C-4' carbon and the phosphorus are trans to each other. Such an orientation maximizes the P-31/C-13 coupling at about 2.7 Hz. Consequently an increase in  $3J(P, C4')$  reflects an increase in  $\beta$  ap character. Then, with  $\gamma$  preferably in the +sc position, one acquires a W-type formation along the P-O5'-C5'-C4' backbone with base stacking or duplexing.

#### 1.3.3.5 Dihedral Angle Between C-3' and O-3', $\epsilon$

Three conformations exist to define the torsion angle as illustrated in Figure 5. Only one phosphorus/proton coupling exists hence it is not possible to define the population of all three states from proton spectra alone. Using values of  $A=18$ ,  $B=4.8$ , and  $C=0$  (Lee and Sarma, 1976) and assuming equal vicinal gauche couplings, the following equation has been proposed (Davies, 1978).

$$3J(P, H3') = 2.1(P-sc + P_{ap}) + 22.9P_{+sc} \quad (18)$$

A value of approximately 9 Hz corresponds to free rotation about  $\epsilon$ . However, X-ray and lanthanide probes have never shown the existence of the +sc conformation. This is most likely due to the steric repulsion of the phosphate groups and ribose moiety in this arrangement (Yokoyama et al., 1981). Hence, an alternative method to separate the -sc

and ap populations is needed. This may be supplied by phosphorus/carbon-13 couplings. Consequently the following equations have been produced to elucidate values for the populations of each state (Govil and Smith, 1973):

$$3J(C2'-P3')=2.1P+sc + 10.1Pap + 2.1 P-sc \quad (19)$$

$$3J(C4'-P3')=2.1P+sc + 2.1Pap + 10.1 P-sc \quad (20)$$

$$1=P+sc + Pap + P-sc \quad (21)$$

These equations contain expressions for the P+sc state which has never been shown to exist. As a result two state models excluding this possibility have been produced (Alderfer and Ts'O, 1977):

$$Pap=3J(C4',P3')/(3J(C2',P3') + 3J(C4',P3')) \quad (22)$$

$$P-sc=3J(C2',P3')/(3J(C2',P3') + 3J(C4',P3')) \quad (23)$$

With regard to RNA structures, it has been shown that the amount of ap character is closely related to the ribose conformation. For N puckers, as in A-RNA,  $\epsilon$  is entirely in the ap form. When more S character is introduced there is a tendency to shift towards more -sc character (Yokoyama et al., 1981., Lankhorst et al., 1985). Further, the exact magnitude of  $\epsilon$  is sequence dependent for the double helix.

The only shortcoming of procedures employing P-31/C-13 coupling constants is the availability of sufficient sample to acquire a C-13 spectrum together with an ability to assign it. However, from available C-13 data the following equation has been derived to give a more accurate estimation of  $\epsilon$  from  $3J(P,H3')$  if one knows the percent N/S character (Lankhorst

et al., 1985):

$$P(\text{ap}, S) = (C - 3J(\text{H}3', \text{P})) / 4.05 \quad (24)$$

where C = a linear constant equal to 4.48 for 100% S to 4.09 for 0%.

### 1.3.3.6 Dihedral Angle Between P and O-3', $\alpha$ , and O-5', $\zeta$

Of all the torsion angles,  $\alpha$  (P-O3') and  $\zeta$  (P-O5') appear to be the most variable ones from X-ray analysis (Arnott and Hukins, 1969). NMR provides little direct information on these angles because there are no nuclei attached to the phosphorus atom with appropriate spins for observable coupling. As a result X-ray data is the chief source of accurate information on this parameter. However, it is possible to infer conformational references from NMR if one can follow the chemical shifts of the H-5' and H-5" protons (Ezra et al., 1977).

Both Newman projections for  $\alpha$  and  $\zeta$  consist of a P-O bond with an oxygen on the front and back that can be orientated 0 - 360 degrees about each other. Fortunately only two ranges appear to exist in stacked or duplexed oligomers, -sc and -ap, as illustrated in Figure 5.

Evidence, other than X-ray analysis, comes indirectly from two sources. First, the chemical shifts of H-5' and H-5" are indicative of the type of helix being formed. In a right handed helix the H-5' will come much closer to O-2'

than H-5" will. As a result there will be greater deshielding of this proton as stacking occurs, hence a downfield chemical shift. In a left handed helix, both of these protons are almost equidistant from an oxygen, with H-5" being slightly nearer one than H-5'. Both chemical shifts will therefore change equally with a marginally greater change for H-5".

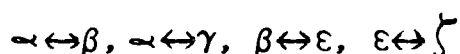
The second form of evidence comes from quantum mechanical considerations of the orientation of the two lone pairs of electrons on oxygen with the dipolar P-O bond. The energetically favoured conformation has the lone pairs of electrons anti-parallel to the P-O bond where it best donates its electrons to the dipole. This is termed the "gauche" or "anomeric" effect and is greatest when the molecule is in the -sc conformation (Saenger, 1984).

In dimers,  $\alpha$  and  $\zeta$  take on a -sc to -ap orientation with  $\zeta$  more confined to the -sc region. This arises from a greater steric hindrance. The O-3' oxygen is bonded directly to the ribose ring (C-3'). In  $\alpha$  it is one carbon (C-5') removed from it. As additional nucleic acids are added to the dimer, the confinement to the -sc region is more pronounced, especially when duplexing or single strand base stacking occurs.

#### 1.4.1 The "Rigid" Oligomer

In nucleotides, an orientation about one bond restricts the possible orientations about another bond. This has been shown with plots of various torsion angles versus each other (Kitamura et al., 1981., Davies, 1978). Such plots show a correlation coefficient of between .78-.89 for most angles except  $\gamma$ . This is presented schematically in Figure 5.

When one starts to form oligomers  $\gamma$  becomes more interrelated as well. Along the backbone the following relationships exist:



(Saenger, 1984).

The result is that the nucleotide units take up preferred positions in space whose degree of "rigidity" increases as oligomer length increases. This "rigidity" is conferred when base stacking or duplex formation takes place. For RNA this confines the molecule to  $\chi_{\text{anti}}$ , N,  $\gamma + sc$ ,  $\beta_{\text{ap}}$ ,  $\epsilon$  -ap to -sc (approximately 220°), with  $\alpha$  and  $\zeta$  in the ap hemisphere (-sc in tight double helices).

This concept of "rigidity" was first brought up by Sundaralingam (1973). Note the care taken in using this word. The molecules are "rigid" only in the sense that >70% of the population tend to be in a particular conformation. Generally, at high temperatures the probability of all conformations are roughly equal. As temperature is decreased one conformation becomes dominant. In a perfect double helix

many of the bonds approach the 100% probability level, but never actually attain it. This is because vibrations and rotations are constantly occurring. While the definitions for RNA alone in solution are generally quite predictable, the situation is more uncertain for DNA where exchange between A, B and Z forms may occur. In both cases the addition of protein, drugs, or metal ions to the solution, which interact with the helices, causes this concept to falter. Hence when discussing this model the double apostrophes will be kept in place around rigid to remind one that oligomers are "rigid" only in terms of probability limits.

### 2.1.1 NUCLEAR MAGNETIC RESONANCE

Nuclei possess "spin". As a result, one can classically treat this spin as a moving charge in a loop. This spinning charge possesses a magnetic dipole. The moment of this dipole can be expressed in terms of the area and current in the loop:

$$u=iA/c \quad (25)$$

where  $u$ =magnetic dipole moment,  $i$ =current,  $A$ =area, and  $c$ =speed of light.

Because current is charge divided by time, (25) becomes:

$$u=qA/tc \quad (26)$$

where  $t$ =time.

This spinning body possesses angular momentum as well:

$$P=mr^2\omega \quad (27)$$

where  $P$ =angular momentum,  $r$ =radius, and  $\omega$ =angular velocity in radians/second.

Equation (27) can be rewritten as:

$$P=mr^2 2\pi/t \quad (28)$$

since  $\omega=2\pi/t$ .

The area in equation (25) may be expressed as  $\pi r^2$ . This value can be obtained from (28):

$$\pi r^2 = Pt/2m \quad (29)$$

The substitution of (29) into (26) results in the following equation for  $u$ :

$$u = qP/2mc \quad (30)$$

where  $P$  is in units of  $\hbar$ , therefore:

$$u = qP\hbar/2mc \quad (31)$$

For a nucleus with angular momentum  $I$ , and mass  $M$ , the expression becomes:

$$u_I = g_I (e\hbar/2Mc) I \quad (32)$$

where  $g_I$  = nuclear  $g$  factor.

One can then simplify (32) by allowing  $\beta_N$  to equal  $e\hbar/2Mc$  where  $\beta$  is called the nuclear magneton for proton  $N$ :

$$u_N = g_N \beta_N I \quad (33)$$

This may be further simplified by allowing  $g_N \beta_N / \hbar$  to equal  $\gamma_N$ , the magnetogyric ratio:

$$u_N = \gamma_N I \hbar \quad (34)$$

From this, one can see that the magnetogyric ratio is really an expression for the ratio between the magnetic dipole moment and angular momentum:

$$u_N / I \hbar = \gamma_N \quad (35)$$

Placing this magnetic dipole in an external magnetic field results in the production of energy levels.

Classically:

$$E = -uB_0 \quad (36)$$

where  $E$  = energy,  $B_0$  = external magnetic field.

By substituting (33) into (36) one acquires:

$$E = -g_N \beta_N I B_0 \quad (37)$$

$$E = -\gamma_N I B_0 \quad (38)$$

From here it is necessary to enter the realm of quantum mechanics.

Spin angular momentum is quantized as:

$$P = \sqrt{I(I+1)} \hbar \quad (39)$$

It is impossible to physically observe all three components of angular momentum at once (x, y, and z) therefore one randomly uses  $P_z$  by convention:

$$P_z = m_1 \hbar \quad (40)$$

where  $m_1 = I, I - 1, I - 2, \dots -I$

A selection rule dictates that  $\Delta m_1 = \pm 1$ .

Now  $P_z$  can be substituted for  $I$  in (38):

$$E = -\gamma_N m_1 \hbar B_0 \quad (41)$$

For  $I = 1/2$ ,  $m$  is equal to  $+1/2$  ( $\alpha$ ) and  $-1/2$  ( $\beta$ ).

Therefore the energy difference between the two states is:

$$\Delta E = (1/2) \gamma_N \hbar B_0 - - (1/2) \gamma_N \hbar B_0 \quad (42)$$

$$\Delta E = \gamma_N \hbar B_0 \quad (43)$$

Because  $\Delta E$  is equal to  $h\nu$ :

$$h\nu = \gamma_N \hbar B_0 \quad (44)$$

$$h\nu = \gamma_N \hbar B_0 / 2\pi \quad (45)$$

$$2\pi\nu = \gamma_N B_0 \quad (46)$$

$$\nu_0 = \gamma_N B_0 \quad (47)$$

since  $\nu_0 = 2\pi \nu$ .

$\nu_0$  is called the Larmor frequency. Since  $\gamma_N$  is a fixed value for a particular nuclei, this value depends only

on  $B_0$ . Vectorially this is represented by the two magnetic dipole vectors for the  $\alpha$  and  $\beta$  spins, as illustrated in Figure 6, which behave differently when placed in a magnetic field. The  $\alpha$  state is aligned with  $B_0$  while  $\beta$  is opposed to it.

The energy difference between these two states is small, but enough to produce a net magnetization vector,  $M_0$ , aligned along the z-axis when a large number of nuclei are placed in the field.

To simplify the vector expressions used to describe a NMR experiment, one allows the Cartesian x, y, z coordinate system to rotate at the Larmor frequency  $\nu_0$ . This produces a static system, for now when the irradiating frequency  $B_1$  is applied along the x-axis, one simply finds  $M_0$  tilted into the x-y plane and not rotating about  $B_1$  as it does in the laboratory frame of reference. The degree of tilting is called the flip or pulse angle. A  $90^\circ$  pulse is one that tips the magnetization from the z-axis as illustrated in Figure 6.

The Larmor frequency depends on  $B_0$ . In a molecule each nuclei in a chemically different environment experiences a different effective magnetic field,  $B_e$ . Hence such nuclei precess at different Larmor frequencies. Modern spectrometers excite all these nuclei simultaneously with the  $B_1$  pulse. Therefore when the detector (receiver), in Figure 6 along the y-axis is turned on after the  $90^\circ$  pulse, it

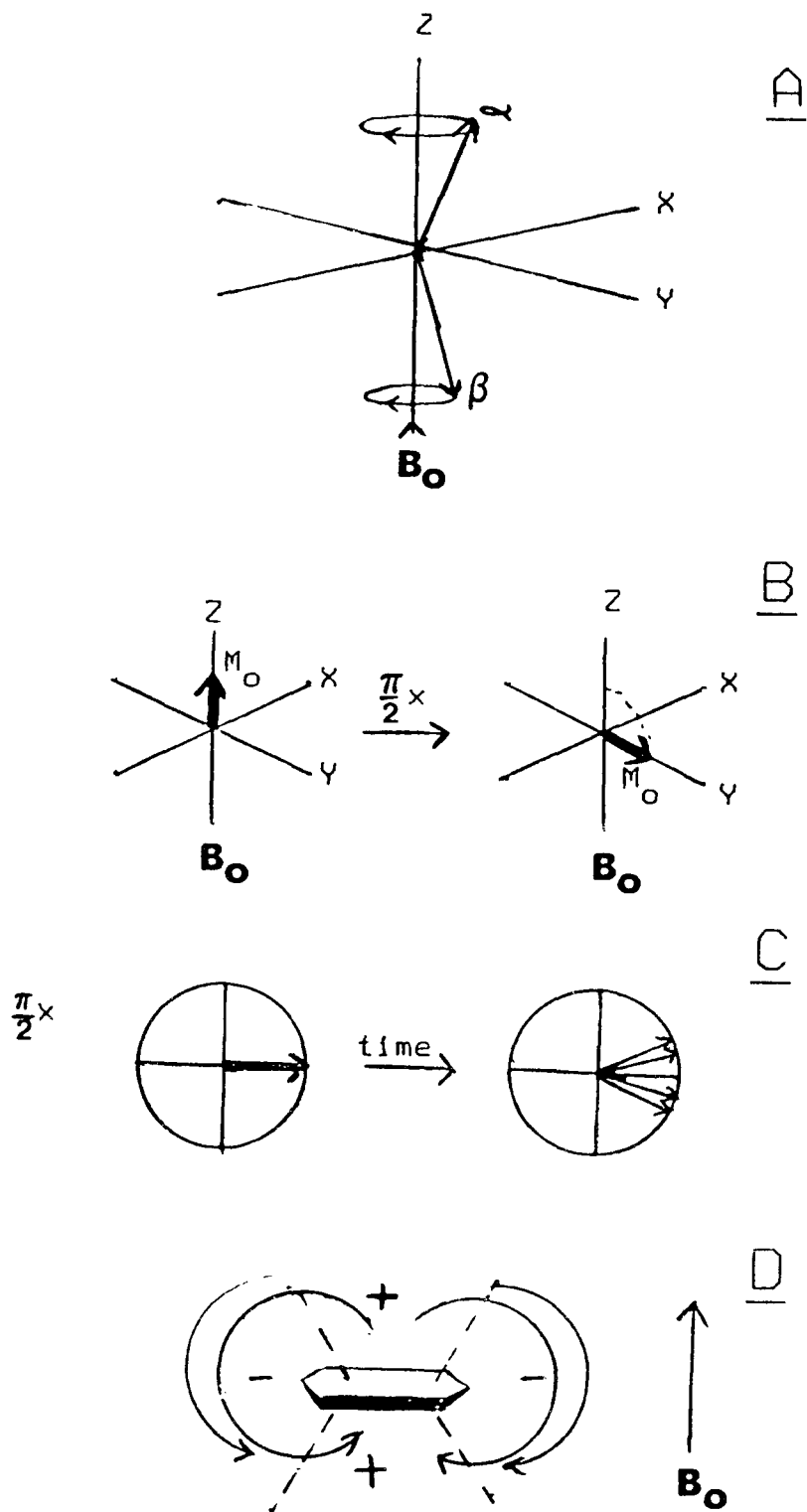


Fig. 6.

A) Vector model of the alignment of spins in a magnetic field. B) Vector description of a  $90^\circ$  pulse. C) Vector model of  $T_2$  relaxation. D) Chemical shift anisotropy as it relates to benzene.

records the sum of the free induction decays (FID) of the many different Larmor frequencies. With the use of high speed computers, a Fourier transformation of this, the time domain signal, is converted into a frequency domain one. The result is a spectrum which contains information dependent on the atomic environment of the nuclei being observed. In this sensitivity lies the power of NMR.

### 2.2.1 Relaxation

The bulk magnetization,  $M_0$ , tilted in Figure 6B, returns to equilibrium (relaxes) via various mechanisms grouped into two processes. One is called longitudinal or spin-lattice relaxation ( $T_1$ ). It involves returning  $M_0$  back to the z-axis after the  $90^\circ$  pulse is turned off. The second is called transverse or spin-spin relaxation ( $T_2$ ). It involves the fanning out of the magnetization transferred into the x-y plane around the x-y plane (Figure 6C) so that at equilibrium there is no net magnetization in this plane.

This later form of relaxation is basically an entropy effect and results primarily from inhomogeneities in  $B_0$ . It is this type of relaxation that makes  $180^\circ$  refocussing pulses useful in many NMR experiments (Morris and Freeman, 1979).

In solution  $T_1 \approx T_2$  but never smaller than it. However, of the two modes of relaxation,  $T_1$  values provide the most useful information on the dynamic and structural

properties of nucleic acid monomers (Chachaty et al., 1976) to nucleic acid polymers (Assa-Munt et al., 1984). This type of relaxation from the excited to the normal equilibrium state occurs with the release of the proper quanta of energy by the excited nuclei. This energy corresponds to the Larmor frequency and the transfer can either be stimulated or spontaneous. Because spontaneous emission depends on the cube of the frequency, it is not an important pathway in the radio frequency range. As a result the emission must be stimulated. Such stimulation occurs via fluctuating magnetic or electronic fields at the Larmor frequency of the excited nuclei. This later process governs the mode whereby quadrupole nuclei transfer energy to the lattice. This is accomplished when the fluctuating electric field gradient produced by the electrons in the rotating molecule interacts with the quadrupole. The former method, involving local magnetic field fluctuations, can be broken down into five different forms:

i) paramagnetic relaxation: an unpaired electron on a molecule tumbling in solution generates ever changing magnetic fields. For this reason dissolved oxygen in liquid samples often create problems when attempting to acquire absolute  $T_1$ s and Nuclear Overhauser Effects (NOEs) (Fukushima and Roeder, (1981)).

ii) chemical shift anisotropy: the nuclei in question is fixed in a region that either shields or deshields it from  $B_0$

(Figure 6D). For example, in an aromatic ring, like benzene, the  $\pi$  electrons circulate and this produces a local magnetic field. The position of a nucleus in relation to this field will effect its chemical shift ( $\delta$ ). Because the molecule is not rigidly fixed in position, bending and vibrating, it constantly changes the magnetic fields experienced by the particular nuclei, helping them to relax.

iii) spin rotation: involves a small molecular group (eg: methyl), the rapidly rotating bonds (electrons) of which, in relation to the rest of the molecule, produce local magnetic fluctuations. As a result nearby nuclei may be aided in relaxation. This is observed as a decrease in  $T_1$  with an increase in temperature. It is important for small symmetrical molecules and segments of large molecules, such as proteins.

iv) scalar coupling: two nuclei, AX, are coupled to each other only if the lifetimes of their spin states are both simultaneously large. If one relaxes considerably faster, no splitting is seen. Furthermore, the rapid relaxation of nuclei A will speed up the relaxation of X by creating local varying magnetic fields. Two forms exist. The first, scalar coupling of the first kind, involves the exchange of A at a site close enough to affect X. The second kind involves A being physically bonded near X.

v) inter- and intra-molecular dipole-dipole: two atoms united via a chemical bond will, when tumbling rapidly in

solution, produce a changing dipole moment. Due to its constantly moving position relative to  $B_0$ , local fluctuating magnetic fields will be produced to help relax bonded or nearby nuclei.

Of these  $T_1$  mechanisms, it is the type (v) relaxation that is most important for nucleic acids in solution. However, depending on the situation, other forms of relaxation can come into play. For example, bases are essentially aromatic systems. Hence in stacked or base pairing situations, the orientation of the nuclei about the base will reflect its relaxation rate and chemical shift. This effect has been used in the study of the base paired protons where the chemical shift dictates the orientation of a proton in the shielding or deshielding cones of the base (Figure 6D) (Perkins, 1982). Exchange of these protons with water increases the apparent relaxation rate of these protons and reflects the stability of the hydrogen bonds (Chou et al., 1984). Others have used various lanthanide ions as probes (Bury et al., 1971) to confirm X-ray data. Depending on the element used, its position in the molecule will have a distance and angle effect on the chemical shift and  $T_1$ .

Relaxation mechanisms are a useful tool in studying nucleic acids. Perhaps more importantly, their existence allows one to use NMR as an experiment. This is because the absence of a return to the ground state would soon lead to a saturation of the excited state and no further absorbance of

energy. Additionally, a comprehension of relaxation is necessary to more fully understand other types of NMR experiments, such as NOEs and spin decouplings which will be more fully discussed in the following sections.

### 2.3.1 Double Resonance Experiments

Three types of double resonance experiments are helpful in the study of oligonucleotide structures: spin decoupling (Lee and Tinoco Jr., 1980), Nuclear Overhauser Effect (NOE) (Patel et al., 1982, Clore and Gronenborn, 1984), and saturation transfer (Pardi and Tinoco Jr., 1982). All three techniques, as the name suggests, involve the use of two irradiating frequencies; one to perturb a part of the system and a second to observe the effect of this perturbation on the whole system. The difference in these three methods generally lie in the length of the perturbing irradiation, its power, and the delay between successive observing pulses. The most common use of these techniques is to determine connectivity between nuclei through bonds, space, or reaction (Saunders and Merish, 1982). In the course of elucidating the structure of the two isomers of CUG, spin decoupling and NOEs proved to be valuable double resonance methods.

### 2.3.2 Spin Decoupling

Selective homonuclear spin decoupling allows one to selectively remove the coupling,  $J$ , of one proton, or set of identical protons, from proton(s) it may be coupled to. It is used primarily to establish 2, 3 or even 4 bond connectivity. The general pulse sequence is illustrated on the top of Figure 7. As soon as the 90 pulse is applied the decoupler is turned on at the carrier frequency of the proton(s) one desires to perturb. Because the decoupler will usually react with the receiver in the homonuclear case, a time sharing scheme is used where the decoupler is on only between periods of digitization known as the dwell time. This is called homo-decoupling (HD).

Such an experiment is presented in Figure 7 for an A and B coupled system. The effect of the second irradiation,  $B_2$ , applied at the frequency of A, is to essentially quantize these spins along the x-axis because  $B_{eff}$  of A is laying almost upon x. The effect of this irradiation upon the other nuclei, B, is mild however, hence  $B_{eff}(B)$  remains essentially along the z-axis. These two systems are quantized in an orthogonal position relative to each other. Since the Hamiltonian energy term for coupling is  $J I(A) \cdot I(B)$  (Harris, 1983), this goes to zero and no coupling is observed.

A variation of this technique is spin tickling, where the decoupling power is not sufficient to completely remove the coupling. This is necessary where one does not wish to

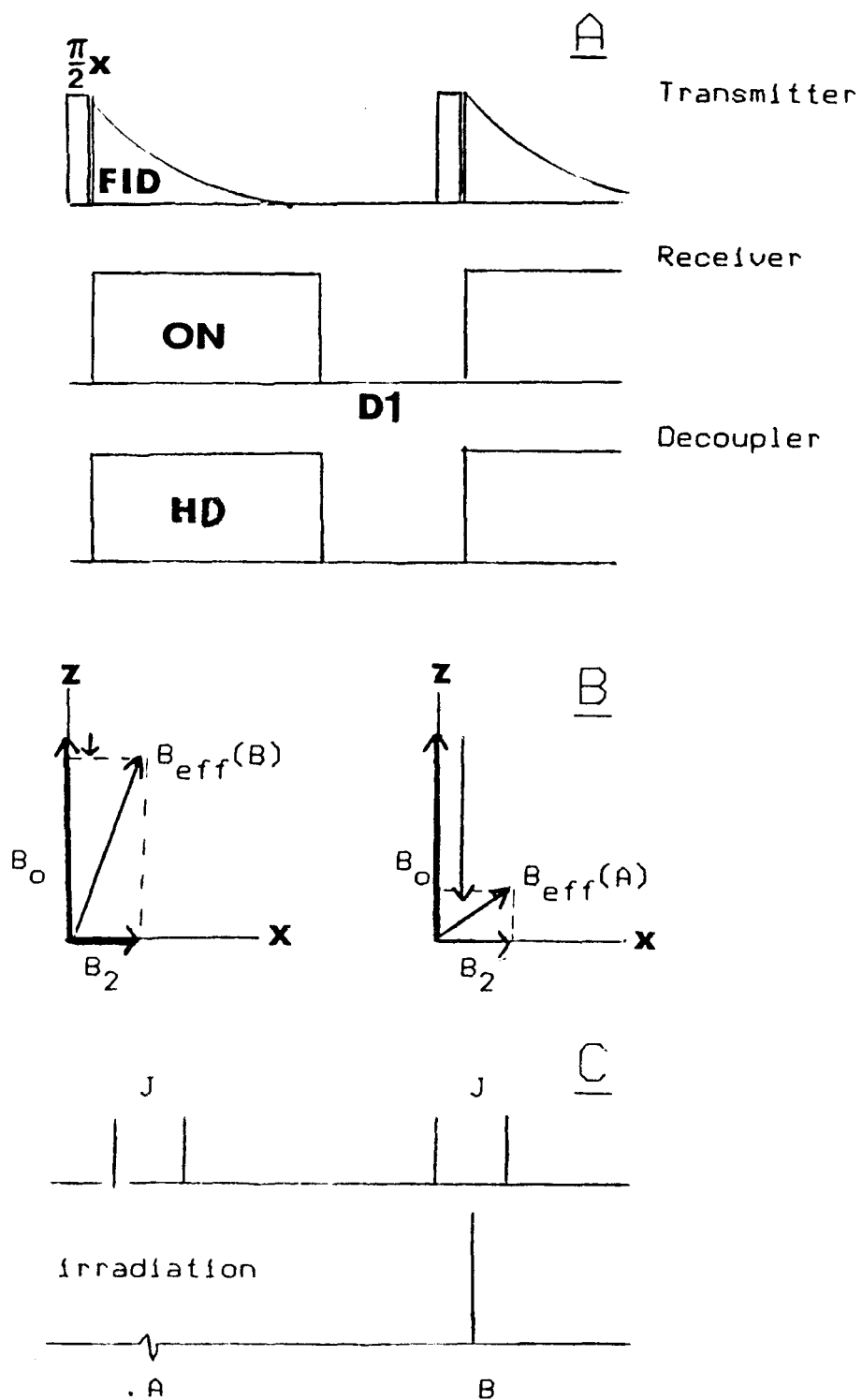


Fig. 7.

Spin decoupling experiments. A) Pulse sequence. B) Effective magnetic field due to  $B_2$ . C) Ideal decoupling effect on spectrum.

cross irradiate other nuclei with almost the same chemical shift. This will still produce a change in the appearance of the spectrum of the coupled nuclei as the apparent coupling constants will be altered.

### 2.3.3 The Nuclear Overhauser Effect

The Nuclear Overhauser Effect is used to detect nuclear connectivity through space. It arises through the process of spin lattice relaxation of the excited nuclei (Noggle and Schirmer, 1971). As described earlier, four possible pathways exist for these nuclei to disperse their energy to the lattice. Of these, it is usually dipole-dipole interactions that dominate. These result from local magnetic fields produced by the neighbouring nuclei, either intramolecularly or intermolecularly, which the excited nuclei can transfer their energy when the frequency distributions are correct. The NOE makes use of this relaxation mechanism as illustrated in Figure 8 for the simple two spin one-half case, I and S.

In a normal experiment, 1 and 2 are the most heavily populated states. Signals are the result of resonances  $W_{1I}$ . By irradiating S one equilibrates all the S spins. As a result, the pathways for the I spins (observing nuclei) to reach equilibrium are now influenced by  $W_2$  and  $W_0$ .  $W_2$  results in an increase in the intensity of the signal,  $W_0$  a

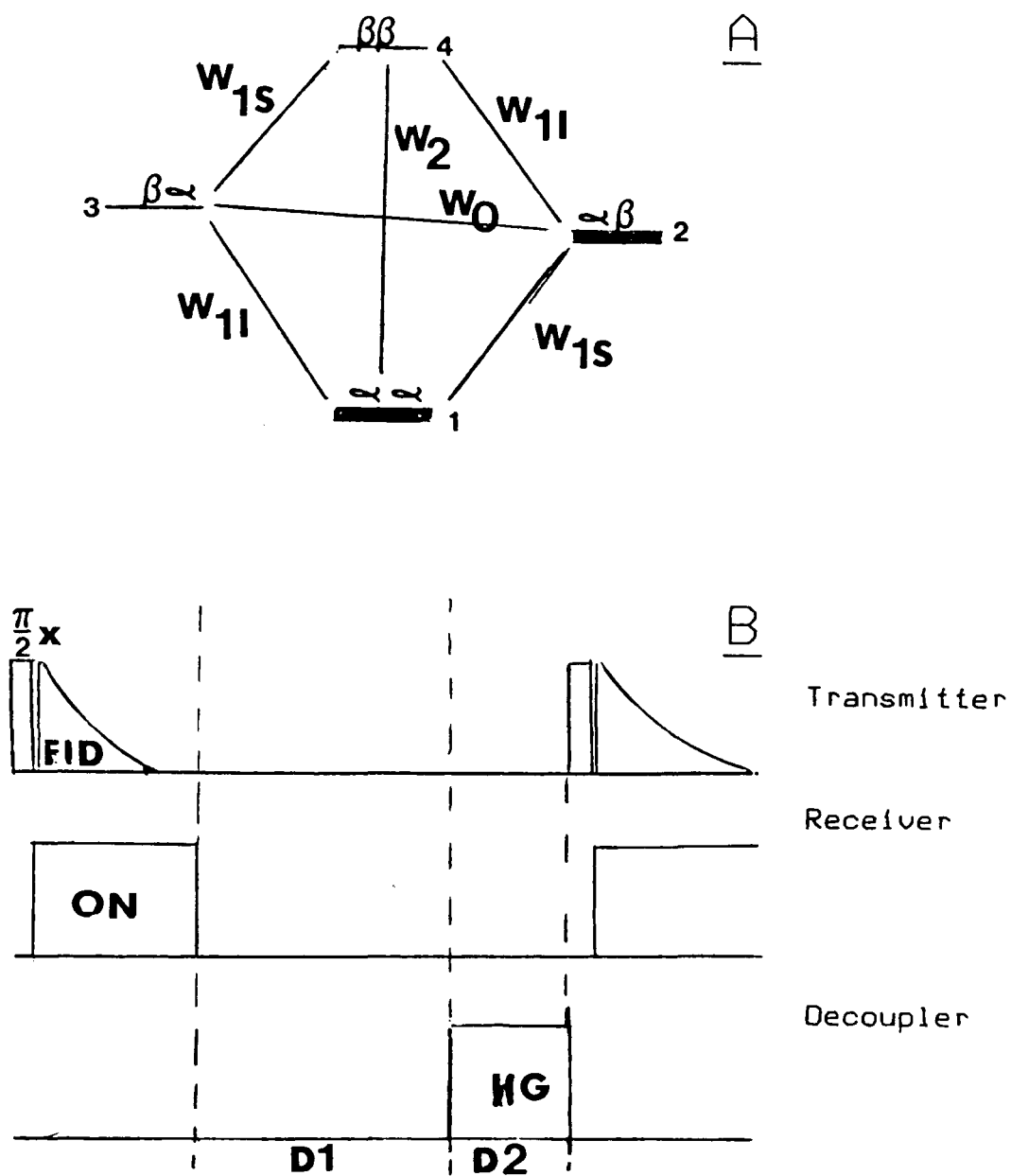


Fig. 8. The Nuclear Overhauser Experiment. A) Energy level diagram for a two spin system, I and S, with one half spins. B) NOE pulse sequence.

decrease. This is because the rapidly alternating  $\alpha/\beta$  states of S allows more opportunity for double and zero quantum transitions, where two nuclei must simultaneously change spins. It may be shown that  $f(S)$ , the fractional increment in the intensity of I due to the saturation of S is given by:

$$f_I(S) = (\delta IS / \rho I) (S_0 / I_0) \quad (48)$$

where  $\delta IS = W2 - W0$  and  $\rho I = 2W_{1I} + W0 + W2$  (Sanders and Merish, 1982).

As a result, a positive or negative NOE depends on whether W2 or W0 is greater. In small molecules with a molecular weight less than 1000,  $\omega T_C$  is usually less than one and W2 effects dominate. The result is a positive NOE. In the fast tumbling limit, with only dipole-dipole relaxation:

$$f_I(S) = (\gamma_S / 2\gamma_I) \quad (49)$$

where  $\gamma$  = the magnetogyro ratio.

Therefore the maximum NOE for the homonuclear proton-proton case, independent of distance, is 50%. It is only because the rate of NOE development depends on internuclear distances in a rigid isotropically rotating molecule does space information occur:

$$\rho_{IS} = \gamma_I^2 \gamma_S^2 \hbar^2 T_C r_{IS}^{-6} \quad (50)$$

where  $r_{IS}$  = distance between nuclei I and S.

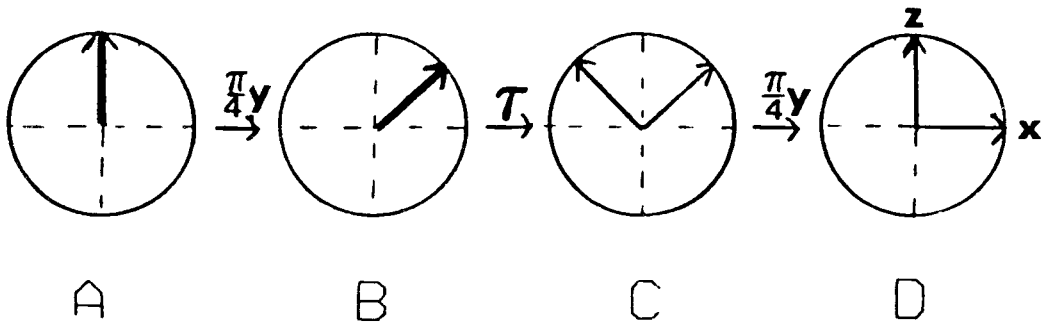
As a result it is possible, under the proper conditions, to see a 2% enhancement from an inter-proton distance of 3.5 Å (Redfield et al., 1981).

A general outline of the pulse sequence used is

presented in Figure 8.  $D_1$  is generally about  $5(T_1)$ . The decoupling is gated on only when the receiver is off (homo-gated decoupling, HG). The difference between this experiment and a spin decoupling experiment is that a long delay is used to allow the molecule to return to equilibrium and the decoupling is applied prior to the  $90^\circ$  pulse, not during it.

#### 2.3.4 Exchangeable Proton Detection

Nucleic acids contain three types of protons that rapidly exchange with water; the imino, amino, and hydroxyl. Of these, the imino and amino are involved in hydrogen bonding in the duplexed state (Figure 4). The occurrence of hydrogen bonding serves to slow down the rate of exchange of these protons with water and often allows for their detection on the NMR time scale. In particular, the imino protons exchange needs to be slowed down by this method to be seen. Because these resonances are also observed further downfield (11-14 ppm range) (Kearns et al., 1971) than any other protons, these are good indicators of duplex formation, its structure, and the environment in the core (Patel and Tonelli, 1974, Hare and Reid, 1982, Fazakerley et al., 1984, Patel et al., 1985). Additionally, the stability of duplexes and their nature in the presence of ligands such as anti-cancer agents or protein may be explored (Patel, 1976,



9. Vector diagram of the 1:1 hard pulse sequence.

Scheck et al., 1983, Hahn et al., 1985).

The problem with observing the exchangeable protons is that the sample concentration is far less than that of the solvent. With oligoribonucleotides, the proton concentration is usually less than 10 mM while the solvent's proton concentration is approximately 110 M. This creates problems in producing a Fourier transformed spectrum because of digitization and dynamic range problems associated with a finite computer word length. The solvent signal quickly overloads the computer. To overcome this obstacle, a number of solvent suppression techniques have been developed. Because a rapidly exchanging system exists, only techniques which limit cross-relaxation, magnetization transfer, or intermolecular interactions between the solvent and solute may be used (Clare et al., 1983). These involve techniques that leave the solvent magnetization along the z-axis when the receiver is turned on. Such methods include the 2-1-4 Redfield pulse (Redfield et al., 1975), the jump and return sequences (Plateau and Guéron, 1982), Hore's 1-3-3-1 pulse (Hore, 1983), the 1:1 hard pulse (Clare et al., 1983), the 1:2:1 sequence (Sklenář and Starčuk, 1982), plus their later variation (Starčuk and Sklenář, 1985). All these techniques offer certain advantages over each other depending on the spectrometer equipment available and the degree of solvent suppression needed. For our purposes the more successful technique was the 1:1 hard pulse sequence developed by Clare

et al. (1983)

The Clore pulse sequence involves two pulses of equal length

$$\theta_{\mathbf{y}} - \mathcal{T} - \theta_{\mathbf{y}} \quad (51)$$

which can be represented by the vector diagrams illustrated in Figure 9.

To acquire the optimal magnetization along the x-y plane, two 45° pulses are generally used. The carrier frequency is placed downfield of the proton frequency of interest. After the first 45° pulse (B) the magnetization of the water is allowed to precess 180°. This is accomplished by a delay  $\mathcal{T}$  equal to  $1/2\Delta\nu$ , where  $\Delta\nu$  is the frequency difference between the solvent and the carrier frequency (C). In the rotating frame of reference the magnetization of the carrier frequency remains stationary and the magnetization close to it rotates only slightly (imino protons of interest). As a result the second 45° pulse rotates this magnetization (the x-component) into the x-y plane. Meanwhile the same 45° pulse rotates the water's magnetization onto the z-axis (D). Because the receiver detects magnetization in the x-y plane the only signals picked up should be solely from the protons of interest. It should be pointed out the signals further from the carrier frequency rotate progressively further away from it during the delay  $\mathcal{T}$ . As a result there will be a smaller x-component of the magnetization projected into the x-y plane

the nearer the signals are to the solvent. This leads to a smaller  $y$ -component for the receiver to pick up. So the intensities of the protons as they appear on the Fourier transformed spectrum will not be directly proportional to the proton concentration. Instead they will be a function of the frequency difference between the carrier frequency and their natural frequency. This must be kept in mind when integrating peaks.

#### 2.3.5.1 Two Dimensional NMR

A one dimensional spectrum generally takes on the following form:

preparation  $\leftrightarrow$  evolution  $\leftrightarrow$  detection

The signal picked up is solely a function of  $t_2$ ;  $S(t_2)$ . If  $t_1$  was varied as well, then the signal would be a function of both  $t_1$  and  $t_2$ ;  $S(t_1, t_2)$ . Because of the two time variables, it is possible to Fourier transform the data twice as a function of two frequency variables,  $F_1$  and  $F_2$  (Benn and Gunther, 1983). As a result the 2D experiment is a series of 1D experiments each with a changing evolution period  $t_1$ .  $F_1$  is then the Fourier transformation of these spectra in the other dimension. The concept is best illustrated via the heteronuclear 2D experiment for a C-H system (Muller et al., 1975) (Figure 10).

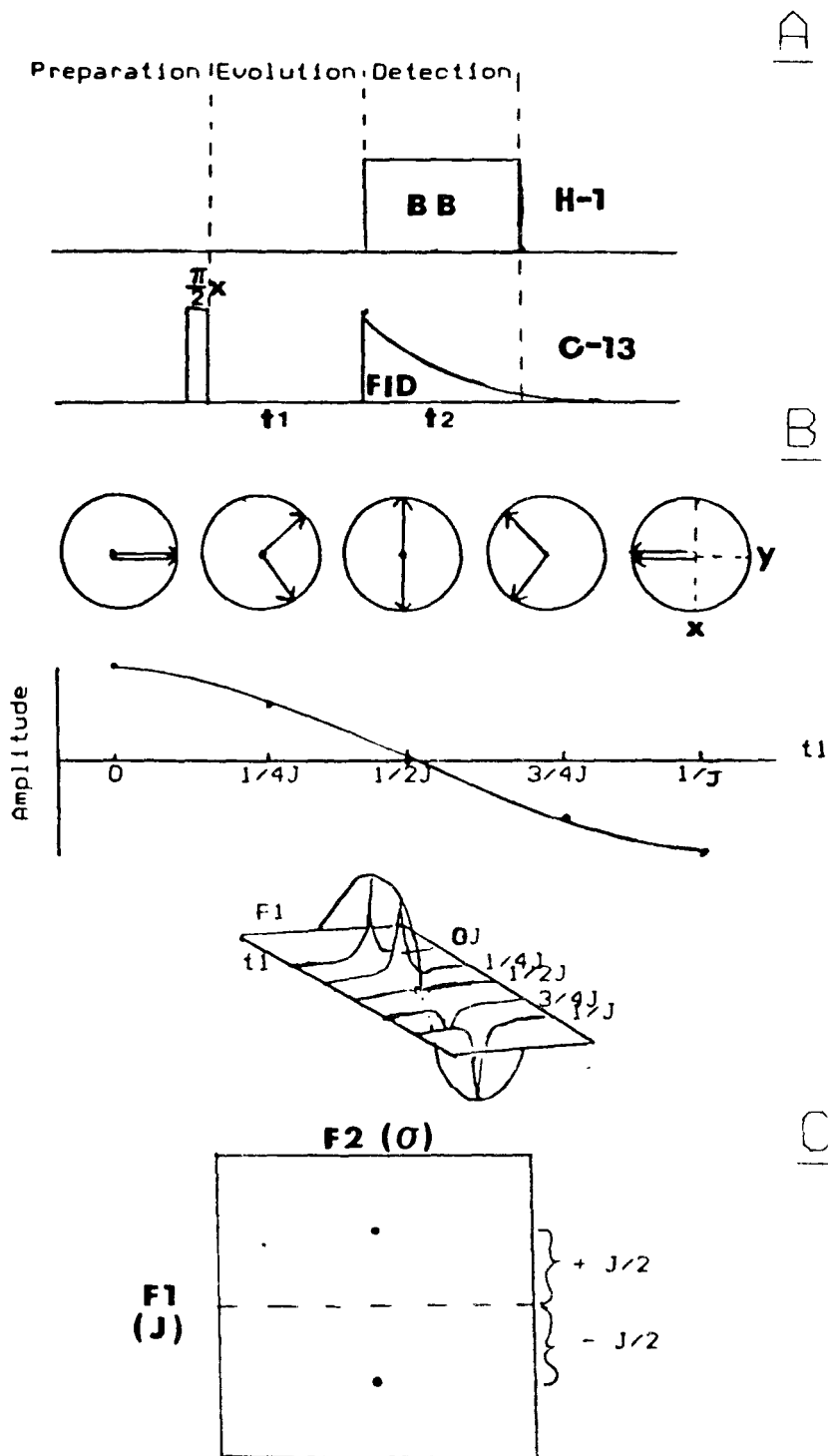


Fig. 10.

A) Schematic pulse sequence for a heteronuclear 2D experiment. B) Vector representation for a C-H system. C) 2D heteronuclear spectrum for C-H.

The  $90^\circ$  pulse tips the C-13 magnetization into the x-y plane. Because C-13 is coupled to H-1, the two vectors will process away from each other a certain distance depending on  $t_1$ . The broadband decoupling (BB) removes the proton coupling and the receiver detects the vector sum of the two coupled vectors, the amplitude of which depends on  $t_1$  (Figure 10B).

The F2 domain contains chemical shift information. The amplitude of these F2 spectra are modulated as a function of  $\cos(\pi J t_1)$  and a Fourier transform produces peaks at  $\pm J/2$  in F1. Hence without acquiring any proton signals, the coupling information of the protons is obtained.

In examining 2D data, 3D stacked plots produce impressive pictures, but the most useful method is to plot 2D slices of these 3D spectra, called contour plots. Such a plot for the previous example would appear as illustrated in Figure 10D.

This is only a simple case. The system becomes more complicated because  $\text{CH}_2$  and  $\text{CH}_3$  amplitudes are modulated by different functions. As a result complicated phase cycling is required for this and all other 2D experiments.

It should be noted that these experiments are limited by computer capabilities and time. This is because a sufficient number of 1D experiments must be carried out to obtain adequate resolution in the F1 domain. As well, the memory of the computer is limited, so instead of conducting

256 F2 experiments at 16 K which would require 4092 K just to store (another 4092 K to process if a square matrix is desired), one usually acquires the F2 spectra in small blocks of 1 or 2 K. Now only 256 or 512 K of storage space is necessary. The effect of this is to decrease the resolution in the F2 domain. Therefore one must balance resolution in F2 and F1 with the storage and processing space available and the time one wishes to spend to acquire and process the data.

Essentially it is possible to transform any one dimensional NMR experiment into a two dimensional experiment by varying the evolution time. Many such experiments exist with acronyms such as SECSY (spin echo correlated spectroscopy) (Bax and Freeman, 1981), COSY (correlated spectroscopy) (Nagayama et al., 1981), NOESY (Nuclear Overhauser Effect spectroscopy) (Macura and Ernst, 1980), and HERPECS (heteronucleus relayed proton correlated spectroscopy) (Delsuc et al., 1984).

In terms of determining proton connectivity through bonds in oligoribonucleotides, the 2D techniques that have proven to be very beneficial are the COSY (Kamur et al., 1979) and relay coherence transfer (RCT) (Bolton, 1982, Bax and Drobny, 1985, Hughes et al., 1985) experiments.

#### 2.6.2.1 Correlated Spectroscopy (COSY)

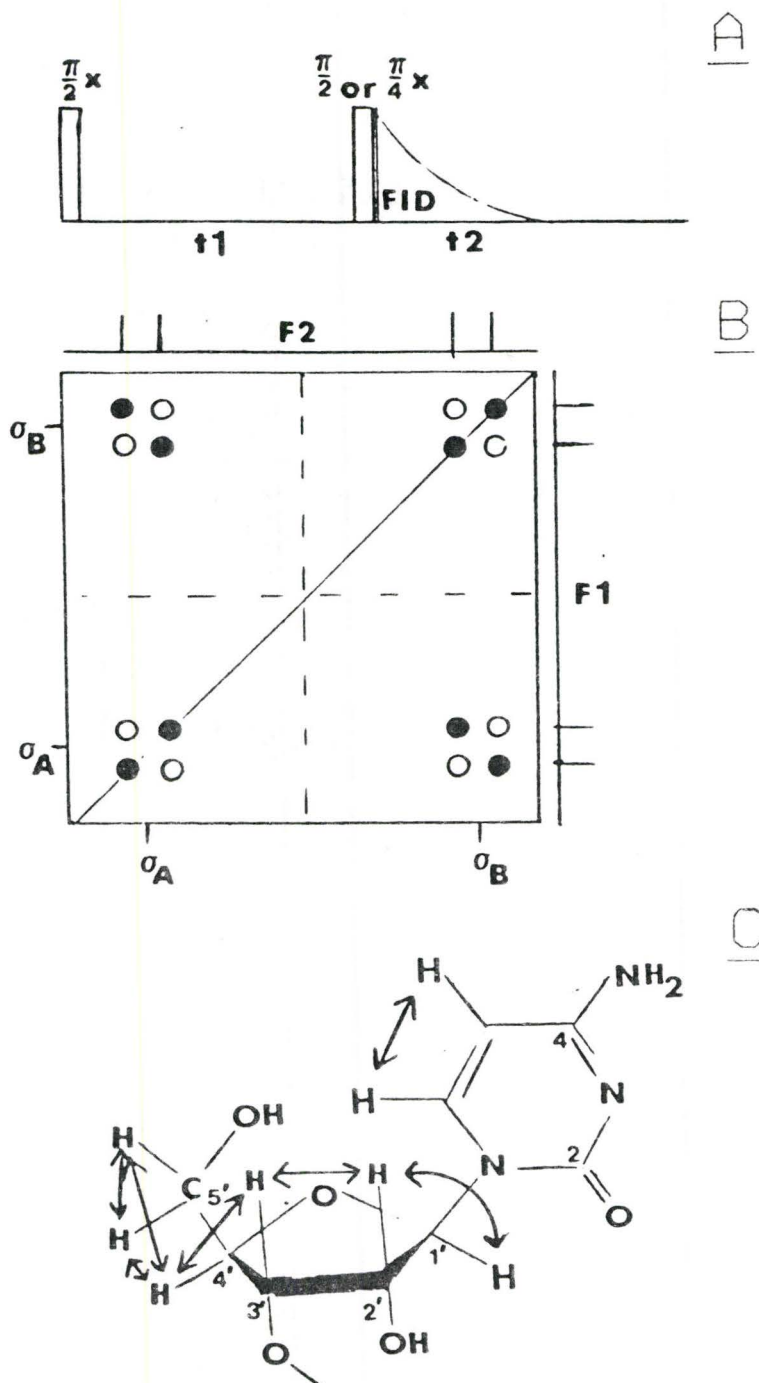


Fig. 11.

The Cosy experiment. A) General pulse sequence. B) 2D COSY spectrum. C) Possible magnetization transfer pathways in a pyrimidine nucleoside.

The general pulse scheme for a COSY experiment is the Jeener sequence illustrated schematically in Figure 11 (Aue et al., 1976).

The first  $90^\circ$  pulse tilts the magnetization into the x-y plane. During the evolution period the individual vectors precess at a rate depending on their frequency and coupling constants. The second  $90^\circ$  pulse is called a mixing pulse and serves to transfer magnetization between coupled spin systems. Thus for a J(A<sub>X</sub>) system where J=0, the result of the 2D experiment would be a single peak on the diagonal. For J not equal to zero,  $\nu_A$  will depend on  $\nu_B$  and peaks will result at the coordinates  $(\delta_A, \delta_B)$  and  $(\delta_B, \delta_A)$ . As a result the COSY experiment produces homonuclear spin correlated spectra with both F1 and F2 domains containing chemical shift information.

A variation of this sequence is to use a  $45^\circ$  mixing pulse instead. This has the effect of reducing the signal intensities of near diagonal peaks. In Figure 11B only the dark circles would appear in such an experiment. For oligoribonucleotides with coupled systems in the ribose region crowded within a small spectral window, such a "cleaning" procedure makes assignments easier.

The advantages of this technique in studying oligonucleotides is that it allows one to assign, theoretically, all the ribose protons to a particular nucleotide, as Figure 11C depicts.

In practice, as the oligoribonucleotide gets longer and chemical shift overlap proliferates, this becomes increasingly more difficult. Even in the worst cases however, at least one can deduce the relative position of the H-2' protons since the H-1' protons are usually well downfield.

### 2.3.5.3 The Relay Coherence Transfer Experiment

A problem with the COSY experiment is the overlap of cross peaks in the ribose region which makes connectivities difficult to follow. One method of circumventing this problem is the relay coherence transfer (RCT) experiment (Bax and Drobny, 1985, Hughes et al, 1985). The simplest explanation of this experiment would be to call it a double COSY which generates a transfer of magnetization from A to C via an intermediate B coupled to both A and C. It involves the following pulse sequence:

$$\boxed{90_{\theta 1}^{\circ} - t_1 - 90_{\theta 2}^{\circ}} - T - 180_{\theta 3}^{\circ} - T - 90_{\theta 3}^{\circ} - Ac \quad (52)$$

The boxed in region is identical to the previous COSY experiment where magnetization from A is transferred to a coupled spin system B via the second  $90^{\circ}$  mixing pulse. The middle  $180^{\circ}$  pulse is inserted to refocus effects due to chemical shift modulations. The third  $90^{\circ}$  pulse now transfers magnetization from spin system B to a coupled spin system C. As a result cross peaks will be observed at  $(\delta_A, \delta_C)$  and  $(\delta_C, \delta_A)$ . The effect is to correlate spin systems not

directly coupled to each other via an intermediate B. Note that normal COSY peaks at  $(\delta_A, \delta_B)$ ,  $(\delta_B, \delta_A)$  and  $(\delta_B, \delta_C)$ ,  $(\delta_C, \delta_B)$  will also be observed due to an incomplete transfer of magnetization of B to C. This transfer is governed by the coupling constant  $J(AB)$  and  $J(BC)$  as given by:

$$\sin(2\pi J(AB)\mathcal{T})\sin(2\pi J(BC)\mathcal{T})e^{-\mathcal{T}/T_2} \quad (53)$$

where  $T_2$  corresponds to the transverse relaxation time of B (Eich et al., 1982, Bax and Drobny, 1985).

Due to the variations of  $J(AB)$  and  $J(BC)$  for all the possible transfer pathways in a sample, an average is taken to determine  $\mathcal{T}$ . As a result, complicated phase cycling must be introduced to minimize the residual COSY peaks (as well as "p-type" signals) whose intensities might otherwise mask RCT signals. Additionally, COSY signals will make assignment more difficult due to the uncertainty of viewing AB or AC connectivity. Consequently it is useful to interpret RCT spectra with COSY spectra present for assistance, even though the cycling systems currently in use are quite successful (Hughes et al., 1985). This is the reason for designating the pulses with subscripts  $\theta_1$ ,  $\theta_2$ , and  $\theta_3$  in Equation (52).

One useful result of an RCT experiment on oligonucleotides is that if the H-3' ribose protons are well resolved and isolated, one is able to take a slice along the F1 axis and obtain a 1D spectrum of all the protons in a particular ribose ring. This is because of the RCT magnetization transfer from H-3' to H-1' and to the H-5'/H-5''

protons along with the COSY type transfer to H-2' and H-4' that is not fully suppressed. Hence in the ideal case, one could extract the 1D spectrum for each of the riboses' ring protons in an oligoribonucleotide from the RCT 2D experiment. In this aspect, residual COSY type magnetic transfer is desirable.

### 3.1.1 EXPERIMENTAL

#### 3.1.1 Deblocking of the Fully Blocked Ribo-oligonucleotide

The general procedure involves three steps (England and Neilson, 1976):

i) removal of the 2,2,2-trichloroethyl blocking group.

ii) removal of the base labile blocking groups trityloxyacetyl (trac) and benzoyl.

iii) removal of the acid labile blocking group tetrahydropyranyl(thp).

#### 3.1.2 Deblocking Procedure

Because deblocking results in the production of an oligonucleotide resembling natural RNA, exposure to nucleases must be prevented. This was accomplished by washing in chromic acid (Manostat Chromerge) all glassware used in the procedure.

A sample of 15-25 mg of the fully blocked compound was deblocked at one time. Such a quantity was weighed out into a vial and dissolved in approximately 1 ml of dry dimethylformamide (J.T. Baker Chemical Co.). Added to this

was a spatula tip of the Zn/Cu couple (ca. 1-5 mg), along with a small bar magnet to stir the parafilm covered solution on a hot plate adjusted to a temperature between 55-60° C. This results in the removal of the 2,2,2-trichloroethyl group (Le Goff, 1964).

To ensure the completion of this reaction tlc was used to follow its course. This involves placing 1 drop of the solution via a capillary tube into a 7 x 70 mm tube. Two to three drops of methylene chloride (Caledon Laboratories, Ltd.) was added and the solution spotted on a scored Silica Gel G 10 x 20 cm tlc plate (Analtech). It was developed in a 1:9 (vol:vol) solution of methanol (J.T. Baker)/methylene chloride. The plate was then sprayed with a 1% acidic ceric sulfate (J.T. Baker) solution in 10% sulfuric acid (J.T. Baker) and then baked at 150-200° C. Oligoribonucleotide with the unremoved 2,2,2-trichloroethyl group will be carried above the baseline by the organic solvents.

Oligoribonucleotide without the group will remain at the baseline due to the -ve charge(s) it has obtained ( $R_f=0$ ). In both cases the spots will be of a yellow/black nature.

The next step was the alkaline treatment to remove the trac and benzoyl groups. Experimentally this was accomplished by adding 2 mls of methanol to the partially deblocked solution followed by 2 mls of concentrated  $\text{NH}_4\text{OH}$  (J.T. Baker). This was tightly bound in parafilm and let to stand at room temperature while being gently stirred.

Upon the passage of 48 hours the solution was filtered and washed 2-3 times with 1N  $\text{NH}_4\text{OH}$ .  $\text{NH}_4^+$  ion chelex-100 (Bio-rad) was then added to the solution and allowed to stir for 1-2 hours. The chelex was filtered off and washed 1-2 times with 1N  $\text{NH}_4\text{OH}$ . This solution was evaporated to dryness, redissolved in 5-10 drops of distilled and de-ionized water, and chromatographed overnight on Whatman #1 paper in a 1:1 (vol:vol) solution of 1M  $\text{NH}_4\text{OAc}$  (Fisher Scientific) and absolute alcohol (Consolidated Alcohols Ltd.).

Upon air drying, the bands were identified with an Ultra-Violet Products, Inc., Transilluminator. Rfs were calculated with the major high Rf band being cut out (Rf ca. .84). The papers were desalted in ethanol for 1 hour, then dried over diethyl ether (BDH Chemicals) for 20 minutes. The oligomers were eluted off the paper with distilled and de-ionized water overnight. At this point the number of optical density units (ODs) present were measured at 260 nm on a Varian Cary 118 Spectrometer.

The sample was then ready for the final step of the deblocking, the removal of the thp group via acid hydrolysis. This involves adjusting the pH of the solution to 2.0 with 2N HCl (Canlab). This was allowed to sit at room temperature for 2 days upon which the pH was brought back up to 7.0 with concentrated  $\text{NH}_4\text{OH}$ . The solution was vacuum dried, descending paper chromatographed on Whatman #1, desalted

twice, and the fully deblocked oligoribonucleotide eluted off the paper with distilled and de-ionized water, as described above. At this stage additional care was taken in handling the papers since now the RNA was susceptible to nucleases. This primarily involved the wearing of gloves (Lite Tex). The number of ODs present were again determined at 260 nm. The samples were then evaporated down and dissolved in a suitable volume of distilled and de-ionized water (20  $\mu$ ls/OD). Upon passage through a Waters coarse filter to remove particulate matter, the samples were ready for HPLC purification.

### 3.2.1 High Performance Liquid Chromatography

All HPLC separations were performed on a Waters Millipore system which included the following: a Model 720 System Controller, a M730 Data Module, a Model 440 Absorbance Detector operating at 254 nm, a M-45 Solvent Delivery System for the aqueous medium, a Model 6000A Solvent Delivery System for the organic component, a WISP 710B to inject the sample and a Pharmacia Fine Chemicals Frac-100 fraction collector. The column used primarily was a Waters Nova Pak C-18, changed to a Waters  $\mu$ Bondapak C-18 towards the end of the separations (due to unacceptable resolution eventually encountered with the first column). The solvents employed were methanol and 0.1 M ammonium acetate (HPLC grade, Fisher Scientific)

TABLE 1  
 HPLC PROGRAM FOR SEPARATING THE  
 FULLY DEBLOCKED CUG ISOMERS

INITIAL	FLOW RATE	% A	% B	% C	CURVE*
initial	1.4	100	0	0	-
30	1.4	96	4	0	5
32	1.0	50	50	0	3
37	1.0	50	50	0	3
40	1.0	100	0	0	3
45	1.4	100	0	0	3

\* INITIAL = time in minutes  
 FLOW RATE = ml/minute  
 CURVE = Waters pre-programmed gradient profiles,  
 numbered 1 - 11, with 6 linear,  
 < 6 = faster initial rate,  
 > 6 = slower initial rate.

TABLE 2  
 HPLC PURIFICATION YIELDS IN OD UNITS  
 (AT 260 nm)

DEBLOCK #	BEFORE HPLC	CUG LOW	CUG HIGH	% CUG LOW RECOVERED	% CUG HIGH RECOVERED
1	308	62	83	20	27
2	162	33	53	20	33
3	268	52	65	19	24
4	260	49	55	19	21*
TOTALS	998	196	256	20	26

\*  $\mu$ Bondapak C-18 column.

adjusted to pH 6.0 with glacial acetic acid (Fisher Scientific Company). Through trial and error a suitable program for the separations was developed for the Novapak column (Table 1).

With the  $\mu$ Bondapak C-18 column a similar program was used except that the flow rate was reduced to 1.3 ml/min for the first 30 minutes and a gradient curve of 7 was applied.

The retention times of the two major peaks on the Novapak column were  $10.1 \pm .2$  and  $16 \pm .2$  minutes, hence the designations CUG low and CUG high for the two isomers respectively. For the  $\mu$ Bondapak column the retention times for the two isomers increased to  $16.5 \pm .3$  and  $21.2 \pm .3$  minutes.

All the material deblocked was purified by either of these two methods. Volumes of up to 200  $\mu$ ls containing no more than 10 ODs of trimer were injected onto the column at a time via the WISP. Manual operation of the fraction collector using a delay of .55 minutes allowed for the collection of the two components. The high and low fractions from a particular deblock were then pooled together, evaporated down, and the optical density measured. Fractions from different deblocks were not pooled until prior confirmation of content via proton NMR. Table 2 lists the various yields expressed in OD units at 260 nm.

### 3.3.1 Enzymatic Digestions

The snake venom (*Crotalus adamanteus* Venom) and Phy M (*P. polycephalum*) phosphodiesterases were purchased from Pharmacia P-L Biochemicals. The spleen phosphodiesterase was acquired from the Worthington Biochemical Corporation.

The Phy M was dissolved into 200  $\mu$ ls of distilled water to yield a concentration of 1 unit/ $\mu$ l. The other enzymes were all made up to the same type of unit concentration with the following appropriate buffers. For snake venom phosphodiesterase this was a 0.1 M Tris buffer (Trizma Base (Reagent Grade), Sigma) made up to pH 8.0 with HCl as described by Wastrodowski (1972). The buffer for the spleen phosphodiesterase consisted of a 75 mM  $K_2HPO_4$  (J.T. Baker Chemical Company) and 25 mM  $(NH_4)_2SO_4$  (Fisher Scientific Company) solution made up to pH 6.0 with 85% phosphoric acid (Fisher Scientific Company) as described by Philippsen and Zachau (1974).

All digestions were carried out in these buffers as well. For Phy M a buffer composed of 20 mM sodium citrate (Merck & Co., Inc.) and 1 mM ethylenediaminetetraacetic acid (EDTA) (BDH Chemicals) made up to pH 5.0 with citric acid (J.T. Baker Chemical Co.) as described by Donis-Keller et al. (1977) was prepared for this purpose. Polypropylene micro-centrifuge tubes (1.5 ml) (Quality Scientific Plastics) washed with a 5% (vol/vol) solution of dimethyldichlorosilane (J.T. Baker Chemical Co.) in carbon

tetrachloride (Caledon Laboratories Ltd.) to prevent nucleotide binding were used for these digestions. Reaction volumes were 200  $\mu$ ls with one unit of enzyme introduced per one OD of oligoribonucleotide. All reactions were temperature controlled in a water bath set at 32 ° C except for Phy M digests that were carried out at 50 ° C. All digests were allowed to proceed overnight (ca. 20 hours) except for Phy M which was halted after four hours. Enzyme deactivation was accomplished by denaturation in boiling water for 2 minutes. Prior to HPLC analysis most of the enzyme was removed by centrifuging the tubes for 5 minutes in an Eppendorf 5414 centrifuge and transferring the supernatant into an injection vessel. The HPLC methodology was identical to the one described above.

For HPLC analysis one OD of oligomer was exposed to the particular enzyme. In digesting larger quantities of oligoribonucleotides for NMR analysis, product separations were performed via Whatman #1 descending paper chromatography as described previously. To aid in the characterization of paper bands or HPLC peaks, various marker samples were run as well.

### 3.4.1 Proton NMR Spectroscopy

All spectra were recorded on a Bruker WM-250

spectrometer except those indicated that were run on a Bruker EM-500 located at Bruker Spectrospin in Milton, Ontario.

Both instruments were operated in the Fourier transform mode with quadrature detection.  $D_2O$  was the field/frequency lock in all cases. Residual HDO suppression was performed on most samples using the following micro-program:

```

1 ZF           ;ZERO MEMORY
2 D1 H6 S1    ;APPLY CW DEC. AT FREQ. D2, POWER DP, DURING D1
3 GO=2 D0     ;GATE DEC. OFF DURING AQ.
4 EXIT        ;EXIT WITH DEC. OFF

```

S1 was generally between 40-45 L and a 1 second delay was used. In most cases a Gaussian multiplication with a GB=.1 and LB=-1 was used before Fourier transformation. In instances of large overlap these parameters were varied to obtain the best trade off between signal to noise and resolution. All spectra recorded on the WM-250 were zero-filled from 16 to 32 K. The EM-500 spectra were all acquired in 32 K.

Most samples were run without salt, in 400 uls of  $D_2O$  (Aldrich) (pD ca. 6.8, Beckman Zeromatic pH meter), in a 5 mm Wilmad 528PP NMR tube. Where indicated, a 1.0 M salt buffer was used consisting of .01 M sodium phosphate buffer (pD ca. 7.2) and 1.0 M NaCl. tert-Butanol-OD (Fisher Scientific Company) was used as an internal reference (1.231 ppm relative to 2,2-dimethyl-2-silapentan-5-sulfonate (DSS)). A

very small amount of EDTA, ca. 0.1 mM, was added to narrow signals otherwise broadened by residual paramagnetic ions.

### 3.4.2 Decoupling Experiments

The Bruker micro-program used was as follows:

```
1 ZE
2 D1 HG O2 S1
3 D2 HD O2 S2
4 GO = 2
5 EXIT
```

The sequence in line 2 was used to suppress the residual HDO signal. Line 3 produced the selective decoupling at a specific frequency O2. Because of the two different irradiating frequencies, a frequency list is required, with the first entry being that of the water. S1 was 42 L and S2 was varied between 25-50 L to selectively decouple only one signal from adjacent signals. The Fourier transformed spectrum was then plotted above a fully coupled spectrum to make detection of decoupling effects easier to observe. It should be noted that the decoupling power would heat the sample, hence the lock frequency would tend to shift slightly. As a result only drastic decoupling effects could readily be detected with any confidence.

The only sample subjected to selective decoupling was CUG high, in 1.0 M salt, to confirm and pinpoint

connectivities suggested from COSY and/or RCT spectra.

### 3.4.3 NOE Experimental Procedure

The following Bruker micro-program was set up to obtain difference NOE spectra:

```
1 ZE
2 D3 O2
3 D1 DO
4 D2 HG
5 GO = 3 DO
6 NM
7 LO TO 2, TIMES: x
8 NM
9 EXIT
```

With the number of scans (NS) set to eight, this program would collect eight FIDs with the decoupler frequency set upon a position of the spectrum with no signal (a control). Then eight FIDs were collected with the decoupler set at the signal of interest. These two sets of FIDs were then subtracted from each other. This was conducted for an X number of times. The Fourier transform of the net FID should yield a positively phased signal at the site of the decoupling and a negatively phased NOE (if it exists) at sites where the signal was enhanced (for positive NOEs, opposite for negative NOEs). D2, the time allowed for the NOEs to develop, was 5.0 seconds. D1 was set at 4.0 seconds.

It was necessary to conduct NOE experiments on both isomers to connect the ribose protons to the proper base.

This involved decoupling the H-8 downfield proton of guanine, and the H-6 protons of cytosine and uridine, with the goal of seeing an NOE to the H-1' ribose proton which is within 3 Å of H-8 or H-6 when in the anti form (Figure 3). Concentrated samples, without salt buffer, were used for all these experiments to shorten the time needed to observe the NOE and to avoid dielectric heating.

#### 3.4.4 The 1:1 Pulse Experiment

Two pulse programs were used to obtain exchangeable proton spectra. The first one was needed to optimize the delay period between the two 45° pulses to allow for maximum return of the solvent magnetization to the z-axis:

```

1 ZE
2 D1
3 (P1 PH1 D2 P2 PH2 VD)
4 GS = 2 PH3
  IV
5 LO TO 2, TIMES: X
6 EXIT

```

```

PH1 = A0 A2
PH2 = A0 A2
PH3 = R0 R2

```

This program allowed one to monitor the FID while manually altering the delay D2 with knob A by entering a value of .0000K for D2 while the program was in operation. Using a receiver gain of 100, this delay was adjusted until a minimal FID was produced.

Once D2 was maximized a program identical to the one

above was used to acquire spectra. This involved altering GS in line 4 to GO. In setting the carrier frequency position and the sweep width, two factors needed to be accounted for. First, the carrier frequency had to be downfield of the imino resonances. Secondly, a data massaging technique used to further eliminate solvent signals before Fourier transformation of the data required the sweep width (SW) to be  $4(\Delta\nu)$ . This is because the data was left shifted four times, then added to the original FID. This serves to produce nulls at:

$$\text{Carrier Frequency} \pm \text{SW}/4 \quad (53)$$

(Roth et al., 1980).

To fulfill both criteria a  $\Delta\nu$  of 3048 Hz was used and a SW of 12,200 Hz. This resulted in a theoretical D2 of  $1/2\Delta\nu = .000164$  seconds. However, because of imperfections in calculating the  $90^\circ$  pulse and the non-perfect additivity of pulses ( $2 \times (45^\circ)$  does not necessarily equal exactly  $90^\circ$ ) the actual delay used, as determined by the above program, was .000157 seconds. It was with these values, together with a  $45^\circ$  pulse of 4.2 micro-seconds, a Gaussian multiplication of the FIDs (normally an exponential multiplication is required, but large sample concentrations eliminated this need), and zero filling from 16 to 32 K, that the exchangeable proton spectra of the two isomers of CUG were obtained. These were all recorded with the trimer dissolved in a 9:1 solution of  $\text{H}_2\text{O} : \text{D}_2\text{O}$  with t-butyl alcohol used as an internal reference.

### 3.4.5 The COSY Experiment

The following Bruker pulse program was used to obtain COSY-45 spectra:

```

1 ZE
2 D1 HG ;RELAXATION, PRE-SATURATION WITH POWER DP
3 P1 PH1 ;90 DEG EXCITATION PULSE
4 D0 ;EVOLUTION OF SHIFTS AND COUPLINGS
5 P2 PH2 ;MIXING PULSE, 90 OR 45 DEG
6 GO=2 D0 ;ACQUIRE FID WITH DEC. GATED OFF
7 MR #1 ;STORE FID
8 IF #1 ;INCREMENT FILE NUMBER
9 IN=1 ;INCREMENT D0 AND LOOP FOR NEXT EXPER.
10 EXIT

PH1=A0 A0 A0 A0 A1 A1 A1 A1
      A2 A2 A2 A2 A3 A3 A3 A3

PH2=A0 A2 A1 A3 A1 A3 A2 A0
      A1 A3 A2 A0 A2 A0 A3 A1

```

The parameters used in all such experiments, except for CUG high dissolved in a 1:1 solution of pyridine:D<sub>2</sub>O, were identical except for the temperature. The number of F2 experiments were 256 collected in 1K. Depending on the time constraints, 64, 72, or 80 scans were acquired for each F2 spectrum. There was no zero filling in F2 but F1 was zero filled from 256 W to 512 W. The 90° pulse used was 8.6 micro-seconds followed by a 4.3 micro-second mixing pulse. A sweep width of 1144 Hz was used with an acquisition time of .447 seconds and a resolution of 2.235 Hz/point. The relaxation delay, D1, was set at 1 second. The residual HDO peak was presaturated for 1.0 seconds at 45 L. All Fourier

transformations were then performed with a sine-bell squared function applied to both dimensions with subsequent symmetrization.

To correlate cross diagonal peaks to a one dimensional spectrum, such a spectrum was acquired using identical F2 parameters as in the 2D experiment except for the use of 8 K.

As noted above, the only variable altered was the temperature. This was done for two reasons. First of all, the best results are obtained when the HDO signal lies in a spectral position removed from sample signals. This could be accomplished because the position of the HDO signal is temperature dependent. Secondly, chemical shifts of the sample also change with temperature. As a result assignments were facilitated by COSY-45 experiments at various temperatures to help monitor these shifts.

The following COSY-45 experiments were performed with an example given in the next chapter: CUG low (5.89 mM), 45.0 and 30.8 ° C, CUG high (7.90 mM), 22.0, 49.8, and 59.7 ° C, CUG high, 1.0 M salt (7.90mM), 60.0 ° C, CUG high in 1:1 pyridine:D<sub>2</sub>O (1.81 mM), 40.1 ° C, and CU>P high (3.90 mM), 50.2 C.

#### 3.4.6 The RCT Experiment

The following micro-program was used with phase cycling as determined by Hughes et al., (1985):

```

1 ZE
2 D1 H6
3 P1 PH1
4 D0
5 P1 PH2
6 D2
7 P2 PH3
8 D2
9 P1 PH3
10 G0=2 PH4 D0
11 WR #1
12 IF #1
13 IN=1
14 EXIT

```

```

PH1=H0
PH2=H0 H0 H2 H2 H0 H0 H2 H2 H1 H1 H3 H3 H1 H1 H3 H3
PH3=H0 H2 H0 H2 H0 H2 H0 H2 H1 H3 H1 H3 H1 H3 H1 H3
PH4=H1 H1 H1 H1 H1 H1 H1 H1 H3 H3 H3 H3 H3 H3 H3 H3

```

A  $T$  value of .046 seconds was used which corresponds to an average  $J$  value of 5.5 Hz ( $T=1/4J$  average). The residual HDO signal was presaturated at 45 L for 2 seconds prior to acquisition (D1). A total of 256 FIDs were collected in 1 K with 60 scans. There was no zero filling in F2, but F1 was zero filled from 256 W to 512 W to produce a 512 x 512 matrix with a resolution of 5.848 Hz/point. The data were processed by a sine bell squared function in both dimensions and the spectra were symmetrized.

The only sample this experiment was performed upon was the CUG high (7.90 mM), no salt solution at 60.1° C. Cross section slices of F1 were taken at various points corresponding to H-3' protons in F2 and compared to the 1D spectrum to help with assignments.

### 3.4.7 P-31 Spectra Acquisition

All P-31 spectra were recorded on a Bruker WM-250 spectrometer tuned to 101.2556472 MHz using the VSPER broadband probe. The following inverse gated decoupling program was used to obtain P-31 proton decoupled spectra:

```
1 ZE
2 D1 BB D0
3 GO=2 BB
4 D1 D0
5 EXIT
```

A pulse width of 28 micro-seconds was employed with a one second delay after FID acquisition. The broadband decoupling power was set at 5 H. Essentially this program involved decoupling the proton resonances after the P-31 90° pulse with the broadband decoupler, followed by a one second delay.

All FIDs, collected in 16 K with a SW of 2500 Hz, were subjected to at least a 1.0 Hz exponential multiplication factor before Fourier transformation and zero filling to 32 K. Variable temperature spectra were produced via a Bruker B-VT1000 variable temperature unit measured to within  $\pm 1^\circ\text{C}$  with an Atkins Digital Thermometer, Scientific E1.6, Series 497. Unfortunately a "P-31 thermometer", such as trimethyl phosphate, was not used to monitor heating due to decoupling. However, because the majority of the spectra were run without a salt buffer, dielectric heating should not

be important. This is because this heating arises primarily from ionic salts present in any buffer (Gorenstein et al., 1982).

### 3.4.8 C-13 Spectra Acquisition

All spectra were recorded on a Bruker WM-250 spectrometer at 62.8960678 MHz operating in the Fourier transform mode. The following power gated pulse sequence was used to minimise dielectric heating:

```

1 ZE           ;ZERO MEMORY
2 D1 BB S1    ;BB DEC. WITH POWER S1 DURING D1
3 D2 S2       ;SWITCH TO POWER S2
4 G0=2 BB     ;90. WITH DEC. POWER S2
5 D2 S1       ;LEAVE DEC. AT POWER S1 FOR NOE
6 EXIT

```

S1 was set at 20 H to allow for NOE generation. S2 was set at 5 H to acquire total proton decoupling. The delay, D1, was set at one second. Samples were dissolved in 100  $\mu$ l D<sub>2</sub>O and placed in a Wilmad microtube. Dioxane was added as a reference (67.4 ppm). Variable temperature spectra were recorded with the use of a Bruker B-VT1000 variable temperature unit. A 90° pulse of 11 micro-seconds was employed and the data was acquired overnight (ca. 8 hours). All data were zero filled from 16 to 32 K and subjected to a Gaussian multiplication to allow for the detection of C-13/P-31 coupling.

## 4.1.1 RESULTS AND DISCUSSION

### 4.1.1.1 Chemical Synthesis of the Trimers

The two trimers studied were prepared previously by Dr. Dirk Alkema (Alkema, 1982). Proton NMR used to confirm the sequence of the fully deblocked oligomer at 70°C indicated that the synthetic route used to produce the trimer resulted in the creation of at least two isomers that had identical Rfs on descending paper chromatography (Rf ca. 0.45). In view of the delicate chemistry of nucleic acid synthesis, such an occurrence has many opportunities to occur.

### 4.1.1.2 Overview of the Phosphotriester Method

A nucleotide has many reactive sites. In joining two nucleotides together via a phosphodiester bond only a single reaction between two of these sites is desired. To eliminate the many side reactions possible the employment of various blocking groups is necessary. These groups must selectively react with a certain site and be selectively removable without altering the natural conformation of the oligomer upon completion. A number of such methods have been

developed which include the phosphodiester, phosphotriester, enzymatic, and combined chemical/enzymatic strategies. Each system has its advantages and disadvantages depending on the sequence length, time constraints, and quantity of product desired. For NMR structural analysis the phosphotriester approach is the best balance of these parameters. A brief summary of the method is given here with a more detailed discussion available elsewhere (Neilson, 1969, Neilson and Werstiuk, 1971, Werstiuk and Neilson, 1972, Neilson et al., 1973, Werstiuk and Neilson, 1973, Neilson and Werstiuk, 1974, Neilson et al., 1975, Werstiuk and Neilson, 1976, England and Neilson 1976, England and Neilson 1977, Gregoire and Neilson, 1978, van Boom and Wreesman, 1984).

The nucleotides are protected as follows:

i) The amino groups of the bases have benzoyl groups attached to them.

ii) The 5' hydroxyl end is blocked with the addition of a base labile trityloxyacetyl group (trac) that is specific for primary alcohols.

iii) The 2' hydroxyl group is blocked with the addition of an acid labile tetrahydropyranyl group (thp). The bulky nature of this compound prevents 3' to 3' phosphodiester bond formation.

iv) A 2,2,2-trichloroethyl group is used to block the third ester site of the phosphate group at the 3' position.

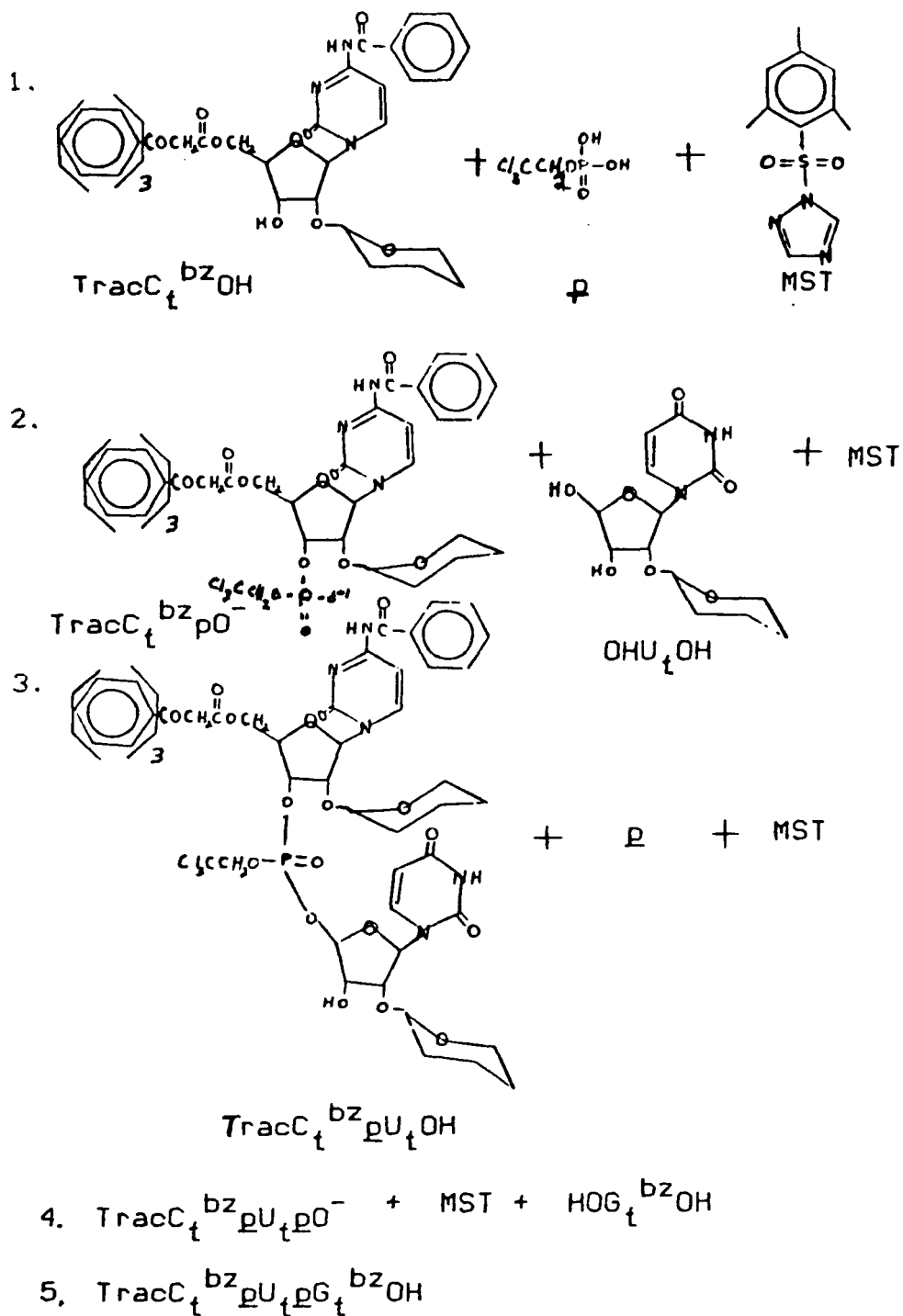


Fig. 12.

Schematic route for the phosphotriester synthesis of CpUpG. First compound in each line represents the product of the previous line.

Nucleotides protected as such are shown in the coupling scheme illustrated in Figure 12 for normal CUG. Synthesis occurs in the 5' to 3' direction, hence the terminal nucleotide has a trac group protecting the 5' end while the incoming nucleotide is free at this position. The 2,2,2-trichloroethyl phosphate group is usually added to the 3' end, in the form of a pyridinium salt, just before a coupling is to be performed. An activating agent, such as mesitylene-1,2,4-triazolide (MST), is required. The reactions are followed on tlc plates and the fully blocked oligomers are crudely purified on silica gel columns with a gradient of methanol in methylene chloride. Greater purification of the completed oligomer is achieved upon deblocking, via paper and HPLC chromatography, as discussed in the Experimental.

All that is required to produce an undesired product is the loss of any of the protecting groups during any stage of the synthesis. Usually a wide variety of such side products are obtained. However, in this instance, the "impurity" was synthesized in amounts equal to the desired product. Advantage was taken of this result, for instead of characterizing only what should be a normal trimer, enough "impurity" existed to allow its characterization as well.

#### 4.2.1 Trimer Proton Assignments

Verification of the base sequences was carried out on all groups of deblocked oligomers by proton NMR at 70°C after HPLC purification. Such a temperature was used to avoid spectral complexity because of self aggregation (double or multi strand) (Ts'o et al., 1969, Martin et al., 1971) and to guard against mixing samples incorrectly together. Such an analysis on both CUG isomers revealed that the nucleotides involved were indeed cytosine, uridine, and guanine. This arose from the observation of the downfield G(H-8) and pyrimidine H-5/H-6 resonances. G(H-8) consisted of a single uncoupled peak in the 8.4 - 7.5 ppm region while U and C were assigned from their  $3J(H5,H6)$  coupling constants. Generally the value for U is 8.1 Hz while C is smaller at 7.6 Hz (Borer et al., 1975).

With this as a basis, it quickly became evident that the difference between the two CUG isomers was in the coupling between nucleotide units. To understand the nature of this unusual linkage and to acquire the most structural information from the spectra, a detailed analysis of the ribose region was required. Such an analysis dictates correct proton assignments and such a feat was accomplished through the use of decoupling, NOE, COSY, and RCT experiments as described in Chapter 2.

#### 4.2.2 CUG Low Proton Assignments

This isomer's base content was verified by the downfield resonances. At 70.4°C the 5.89 mM sample has a single resonance at 8.00 ppm. This was assigned to G(H-8). Slightly upfield existed two well defined doublets centered at 7.86 and 7.79 ppm. These were assigned to C and U respectively from the characteristic coupling constants of 7.64 and 8.13 Hz they possessed.

From here it was possible to extract the H-5 resonances in the 6.1 - 5.3 ppm region from the H-1' signals also located there. This was accomplished by the finding of doublets with similar coupling constants at 6.02 ppm ( $J=7.61$  Hz) (C) and 5.83 ppm ( $J=8.14$  Hz) (U). The three H-1' proton doublets were then assigned to the six remaining resonances. In this case it was beneficial to examine a lower temperature spectrum where the signals were more dispersed, then follow this back to the 70°C spectrum. The results were proton signals located at 5.88, 5.87, and 5.83 ppm with couplings to H-2' protons of 5.61, 5.39, and 3.81 Hz respectively.

To assign these protons to a ribose ring required the use of COSY-45 experiments. Such spectra were acquired at 45.0 and 30.8°C. The 30.8°C spectrum is reproduced in Figure 13 along with connectivity pathways. Overlap exists and some magnetization transfers are weak. Analysis in relation to the 45.0°C COSY spectra, where the different position of the water resonance allows verification of some of these weak transfers, enables one to follow each ribose from H-1' to

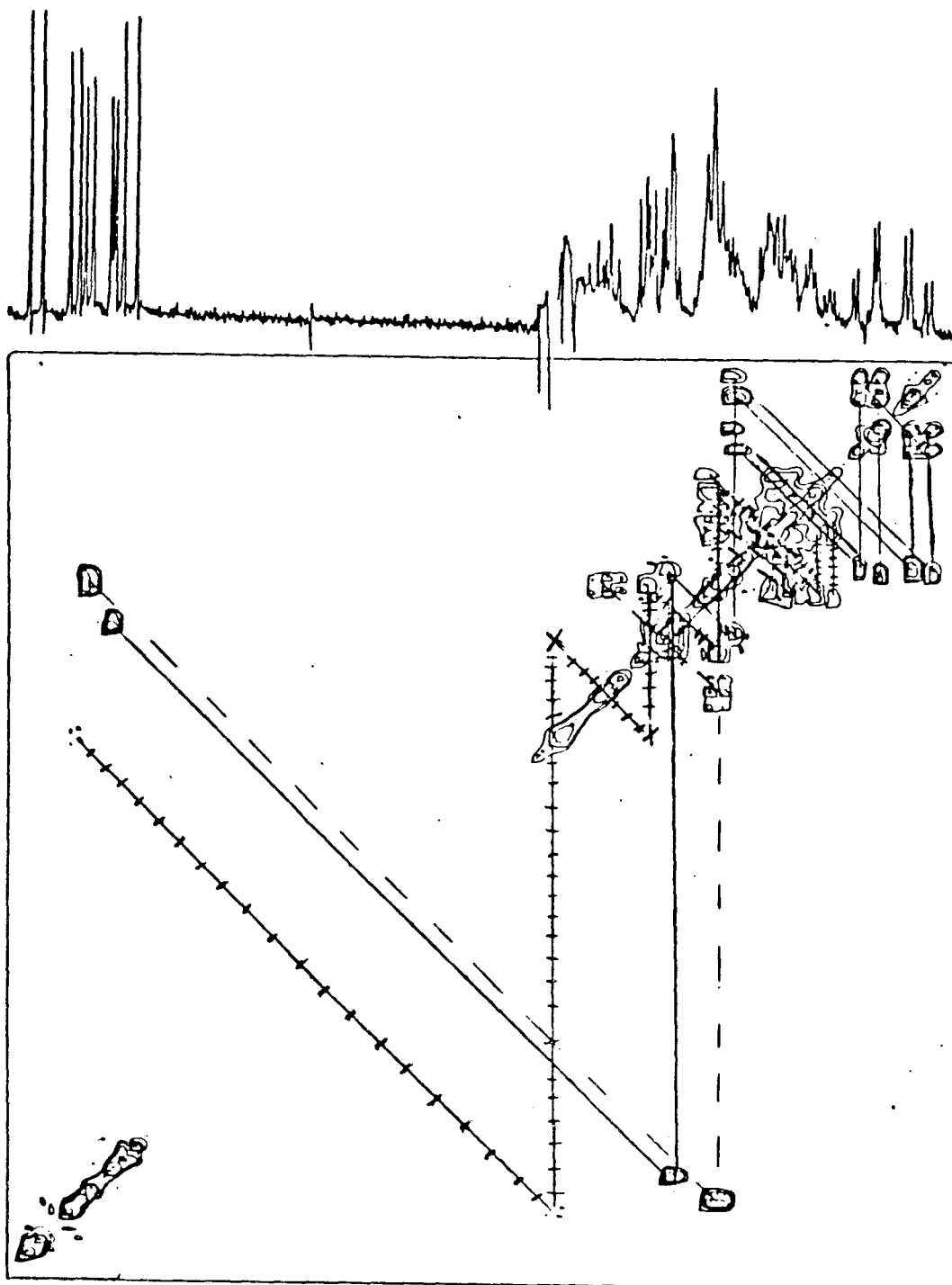


Fig. 13.

2D contour plot of a COSY-45 experiment  
 on CUG low, 5.89 mM, at 30.8°C.  
 (—)=C, (---)=U, (-·-·)=G

H-5". The two x positions marked on Figure 13 represent a magnetization transfer not seen at all at 30.8°C but present at 45.0°C.

Labelling of the ribose rings to specific bases was facilitated by characteristic "handles" each sugar possessed. The most obvious was the presence upfield of the H-5'/H-5" resonances at a carbon 5' position not participating in a phosphodiester bond. These resonances were of a typical ABM system, M corresponding to H-4', with no phosphorus coupling (Guittet et al., 1984). This was assigned to Cp and the coupling through to H-1' was traceable and is represented by an unbroken line in Figure 13.

The other two bases were assigned to ribose rings by clues left by the H-3' protons. Of the three such protons present, only one, the terminal G, had a 3' hydroxyl group instead of an ester linkage to a phosphorus. Hence this proton should be the only H-3' that existed as a quartet due to H-2' and H-4' couplings. The other two are ideally octets due to an additional coupling to phosphorus. Such a proton was exposed by the COSY-45 spectrum in Figure 13 and is labelled with (~~---~~) lines. Through the process of elimination the other H-3' proton, present as an octet, was assigned to U (----).

It is essential that the magnetization pathways deduced from the COSY spectra are correctly assigned to the proper base. Such a verification was obtained by the

confirmation of the H-1' assignments from three different sources. Two other groups studying this identical trimer independently designated the protons in the same chemical shift order (Lee and Tinoco Jr., 1980, and Alkema, 1982). Also, this data compares favourably to theoretical numbers obtained from Bell et al. parameters for predicting H-1' chemical shifts (1985). A comparison of these values is given in Table 3.

Additional confirmation of these assignments were furnished by an NOE experiment. This involved irradiating both H-6 protons coincidentally and observing NOEs for the two upfield H-1' protons at 50°C.

It was possible to assign most of the proton resonances except for the H-4' protons of U and G from 70.4 to 5.6°C. Coupling constants were taken as an average of all appropriate lines visible and, under the assumption of an approximate first order spectrum, expressed as a standard deviation. The resolution of the spectra was .12 Hz/point therefore any standard deviations less than ±.2 Hz is not real. Standard deviation calculations therefore served as a measure of the error in assignments when signal overlap was a problem. Generally, the standard deviation increased as the temperature decreased due to signal line broadening and greater overlap. A 500 MHz spectrum at 47.7 and 30.0°C confirmed these assignments. Additionally, the resonances

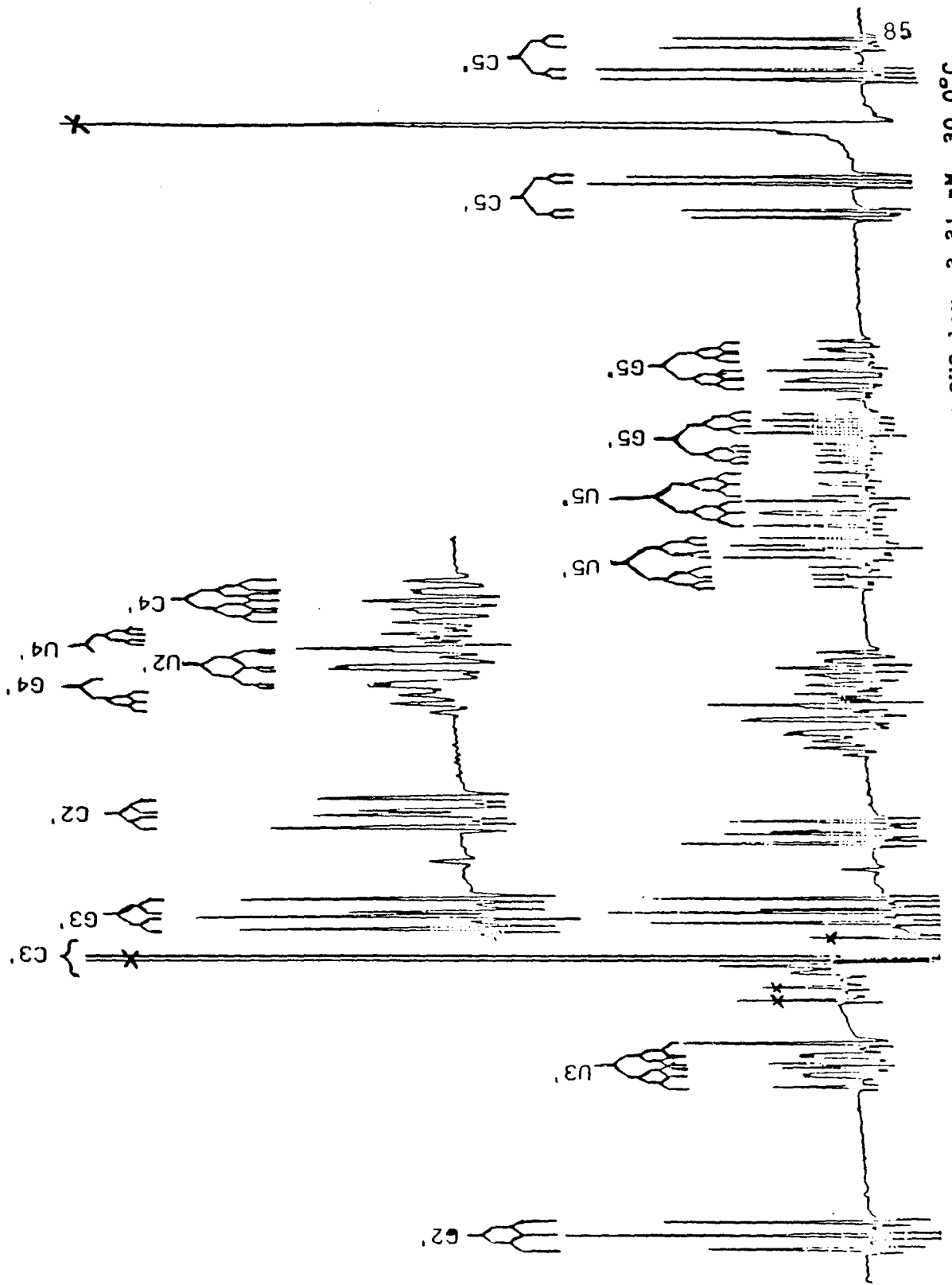


Fig. 14. 500 MHz spectrum of the ribose region of CUG low, 3.31 mM, 30.0°C.

TABLE 3

CUG LOW H-1' CHEMICAL SHIFT COMPARISONS IN ppm

BASE	LEE <sup>a</sup>	ALKEMA <sup>b</sup>	PARAMETERS <sup>c</sup>	EXPERIMENT <sup>d</sup>
C	5.758	5.865	5.866	5.831
U	5.834	5.865	5.891	5.873
G	5.891	5.888	5.896	5.879

a Lee and Tinoco, 1980. 20°C, 1 - 5 mM, salt ?.

b Alkema, 1982. 70°C, 1 - 10 mM, 1 M salt.

c Bell et al., 1985. 1 M salt, 70°C.

d 70.4°C, 5.89 mM, no salt.

TABLE 4

CHEMICAL SHIFTS OF CUG LOW, 5.89 mM,  
NO SALT, AT FOUR DIFFERENT TEMPERATURES\*

PROTON	70.4	50.1	30.2	10.0
C H-6	7.857	7.881	7.907	7.940
C H-5	6.023	6.001	5.967	5.923
C H-1'	5.831	5.797	5.780	5.734
C H-2'	4.386	4.395	4.412	4.439
C H-3'	4.498	4.475	4.447	4.395
C H-4'	?	4.263	4.268	4.276
C H-5'	3.910	3.922	3.937	3.961
C H-5"	3.809	3.812	3.816	3.824
U H-6	7.785	7.794	7.804	7.818
U H-5	5.830	5.794	5.739	5.661
U H-1'	5.873	5.858	5.838	5.807
U H-2'	?	4.320	4.311	4.307
U H-3'	4.604	4.592	4.578	4.565
U H-4'	?	?	?	?
U H-5'	4.192	?	4.202	4.218
U H-5"	4.148	?	4.146	4.139
G H-8	8.003	8.016	8.031	8.045
G H-1'	5.879	5.878	5.873	5.864
G H-2'	4.731	4.723	?	4.671
G H-3'	4.471	4.473	4.473	4.471
G H-4'	?	?	?	?
G H-5'	4.124	4.129	4.147	4.191
G H-5"	4.061	4.058	4.061	4.071

\* 250 MHz spectrum. H-5'/H-5" calculated from the following equation for AB systems:  

$$\Delta\delta = \frac{\sqrt{(1-3)^2 - (1-2)^2}}{2} = \frac{\sqrt{(2-4)^2 - (3-4)^2}}{2}$$
 where 1,2,3,4 are the observed resonances (Pasto and Johnson, 1969).

TABLE 5  
 FIRST ORDER COUPLING CONSTANTS  
 OBSERVED FOR CUG LOW (3.31 mM)  
 IN NO SALT AT 47.7°C\*

J/BASE	C	U	G
5-6	7.88 ± .01	8.15 ± .01	-
1'-2'	3.6 ± .5	5.4 ± .06	5.38 ± .06
2'-3'	5.09 ± .06	4.75 ± .08	4.2 ± .2
2'-P	?	< 1	-
3'-4'	?	4.75 ± .08	4.064
3'-P	?	7.83 ± .02	-
4'-5'	2.75 ± .06	2.99 ± .02	2.59 ± .08
4'-5"	3.86 ± .08	4.8 ± .1	3.4 ± .02
4'-P	?	1.7 ± .2	-
5'-P	-	4.75 ± .2	4.85 ± .09
5"-P	-	4.8 ± .1	4.0 ± .1
5'-5"	-12.92 ± .04	-11.60 ± .06	-11.9 ± .3

\* from 500 MHz spectrum. All couplings in Hz with a standard deviation based on all the observable values. No standard deviation indicates only one observed value. Real error is ±.2 Hz for all values.

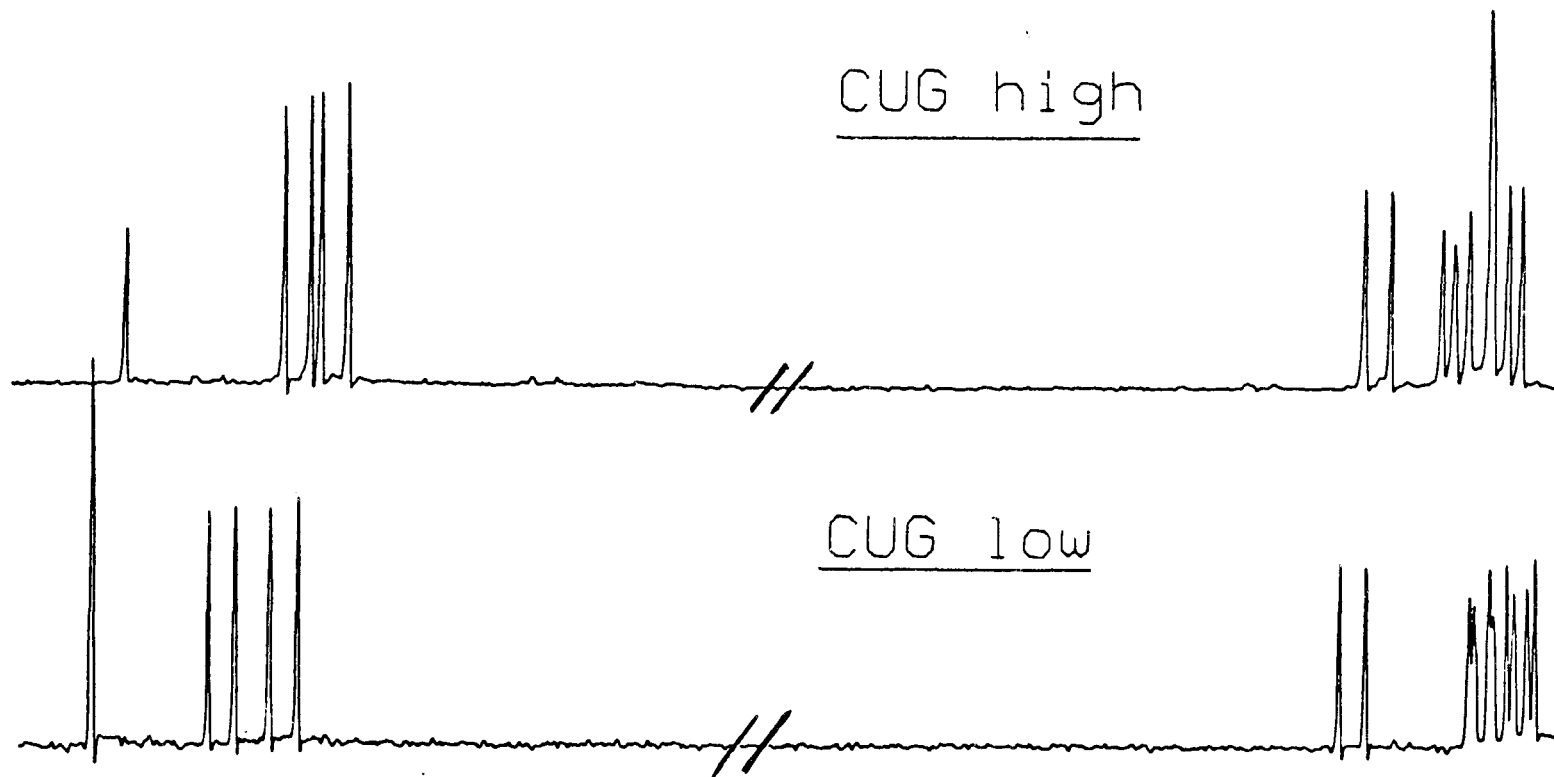


Fig. 15.

Comparison of the downfield proton  
spectral region of CUG high and low  
at 70°C.

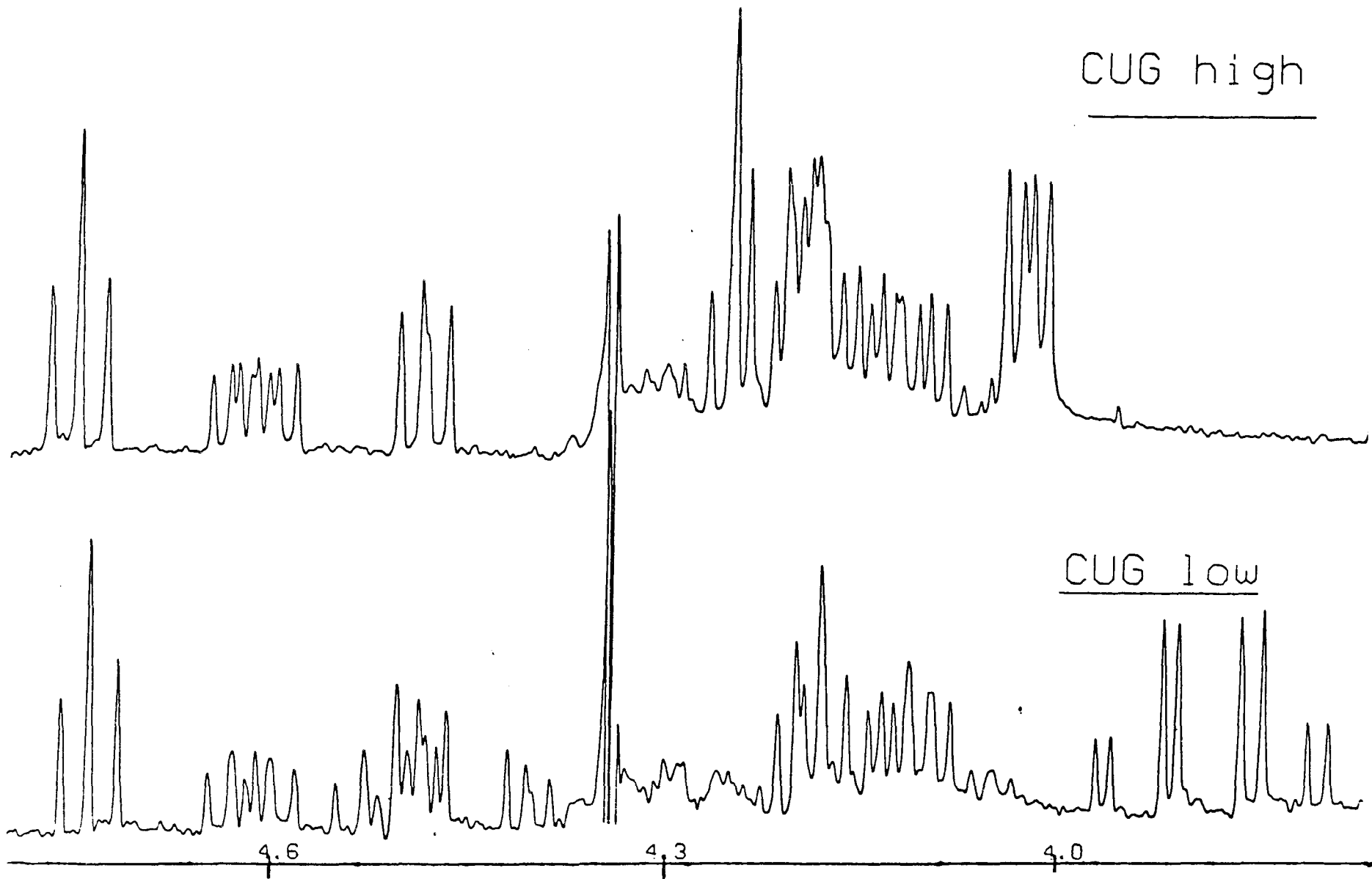


Fig. 16.

Comparison of the upfield ribose  
proton spectral region of CUG  
high and low at 70°C.

due to U and G H-4' became apparent at the higher field. The 47.7°C spectrum is displayed in Figure 14 along with the assignments.

From this information it became apparent that the CUG low isomer was the normally linked 3'-5' molecule. However, a quick view of the proton spectra of the two isomers at 70°C led one to conclude that something was drastically different between the two (Figures 15 and 16). It would be possible to compare the biologically normal trimer with the unusually linked one only after its proton assignment.

#### 4.2.3 CUG High Proton Assignment

The downfield proton assignment was quite facile with the single resonance of the 7.90 mM sample at 7.97 ppm being assigned to G(H-8) (68.5°C). The other four resonances in this group were assigned to C(H-6) (7.78 ppm) and U(H-6) (7.73 ppm) by the size of their coupling constants (7.55 (C) and 8.09 (U) Hz). From this information H-5 resonances could be extracted from the next set of signals between 6.1 and 5.3 ppm by finding similar coupling constants (6.00 (C) and 5.86 ppm (U)). The other five resonances were then assigned as H-1' doublets centered at 5.92, 5.88, and 5.86 ppm (one H-5 and H-1' signal overlapped).

Further resonance assignments became more difficult, even with the use of COSY-45 experiments, because most of the

ribose resonances were crowded within less than .35 ppm. However, four major proton resonances did appear outside this region. The most obvious, as is visible in Figure 16, was the downfield shift of the most upfield H-5'/H-5" resonances of the CUG low isomer (ca. .15 ppm). This apparent quartet evolved with temperature lowering into an ABMX system characteristic of the usual H-5'/H-5" protons coupled to each other (A and B), H-4' (M) and phosphorus (X). The appearance of two other sets of H-5'/H-5" phosphorus coupled protons, made more distinct at 500 MHz, indicated that all the 5' carbons were coupled to a phosphorus. However, the phosphorus spectra dictated the presence of only two phosphorus atoms in the isomer. The explanation of these observations was the presence of a 5'-5' link between two of the nucleotides.

In addition to this H-5'/H-5" region, three other well isolated resonances were observed. Two of them were triplets, at 4.74 and 4.47 ppm. From COSY-45 spectra the downfield resonance was identified as an H-2' proton and displayed magnetization transfer to the upfield triplet which therefore was an H-3' proton. The remaining resonance was an octet assigned to an H-3' proton. Its appearance was due to H-2', H-3' and P-31 coupling. It was coupled to an H-2' proton located on the downfield side of the clustered .35 ppm region between 4.35 and 4.00 ppm. This left one pair of H-2' and H-3' protons to be observed. This was where the major

further verify that all the 5' carbons were linked via ester bonds to phosphorus.

The existence of four 2' and 3' free hydroxy groups belonging to the same ribose ring was obtained by dissolving the CUG high isomer in a 1:1 solution of pyridine:D<sub>2</sub>O (1.81 mM). A COSY-45 spectrum of this solution at 40.1°C, displayed in Figure 19, revealed the presence of only one H-3' proton with an octet shape. The other two, as revealed by cross peaks from H-2' to H-3', were a tall triplet and quartet. While the actual peaks assigned to H-3' at 4.58 ppm could possibly have been H-5'/H-5" protons instead, since they appeared to be clustered in this region, this still served to prove that the H-2' had a connectivity to an H-3' not seen previously in 100% D<sub>2</sub>O. This indicated that the ribose ring was still intact and had not opened between the 2' and 3' carbons.

One unfortunate aspect of this molecule is that no "handle", such as a well defined upfield non-phosphorus coupled H-5'/H-5" region, exists to assign the ribose ring to a base. To acquire such a relation, difference NOE experiments were conducted. Figure 17 illustrates the result of irradiating G(H-8) and the positive NOE seen at the upfield most H-1' doublet at 50°C. Further experiments carried out while irradiating the H-6 protons selectively at ambient temperature revealed the downfield most H-1' to be bound to C and the middle doublet to be part of the U

assignment problem occurred because while the COSY-45 spectra led one to an H-2' proton at about 4.23 ppm, no cross peak to an H-3' proton was observed. Furthermore, at all temperatures, three to four major peaks appeared in this region without any readily discernable or consistent pattern. Integration suggested the presence of two protons in this region. A similar pattern emerged when the isomer was placed in 1 M salt, as well as in the dimer CU>P obtained in an enzymatic digest of the trimer. The conclusion drawn from these observations was that an AB system existed between the H-2' and H-3' protons, the chemical shifts of which were nearly identical. This was given further support with the recreation of similar signal patterns by computer simulations (Bruker PANIC program and Wiberg and Nist, 1962). The unfortunate result was that the chemical shifts of the H-2' and H-3' protons of one ribose would not be clearly definable with respect to their variable temperature behaviour.

Note that even at 500 MHz, spectra obtained at 70.0, 47.7 and 30.0°C led to no further insights into differentiating the H-2' and H-3' protons' chemical shifts. These spectra did partially reveal lines due to H-4' protons, but the overlap was such that it was not possible to obtain much chemical shift or coupling information about them. The major benefit of the 500 MHz spectra was the spreading out of the H-5'/H-5" regions which allowed for an easier interpretation of the 250 MHz spectra. This served to

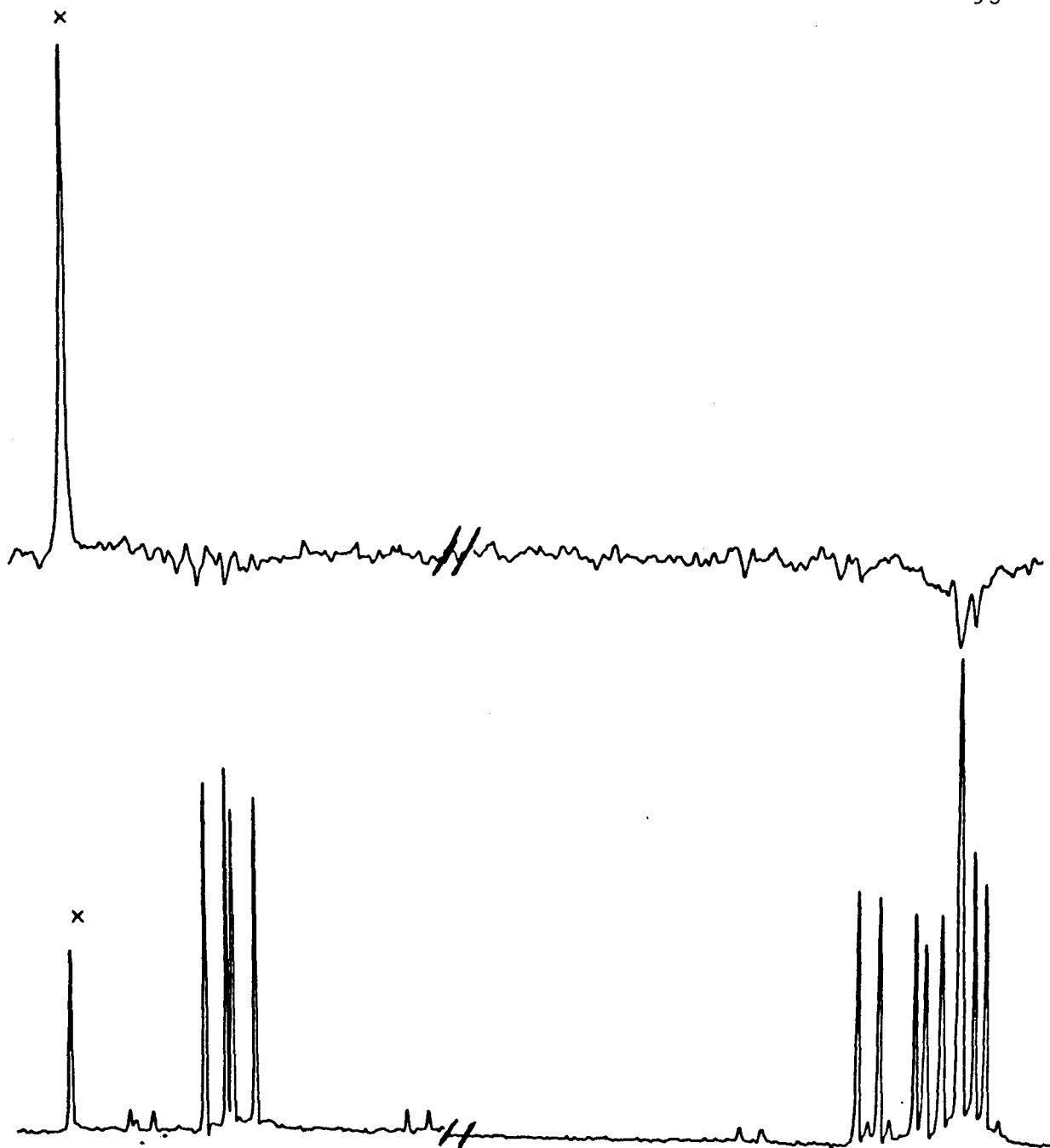


Fig. 17.

Difference NOE experiment involving the irradiation of G(H-8) at site x. The bottom spectrum is unperturbed. The top spectrum is the result of the NOE difference experiment, collected with 160 scans at 50°C.

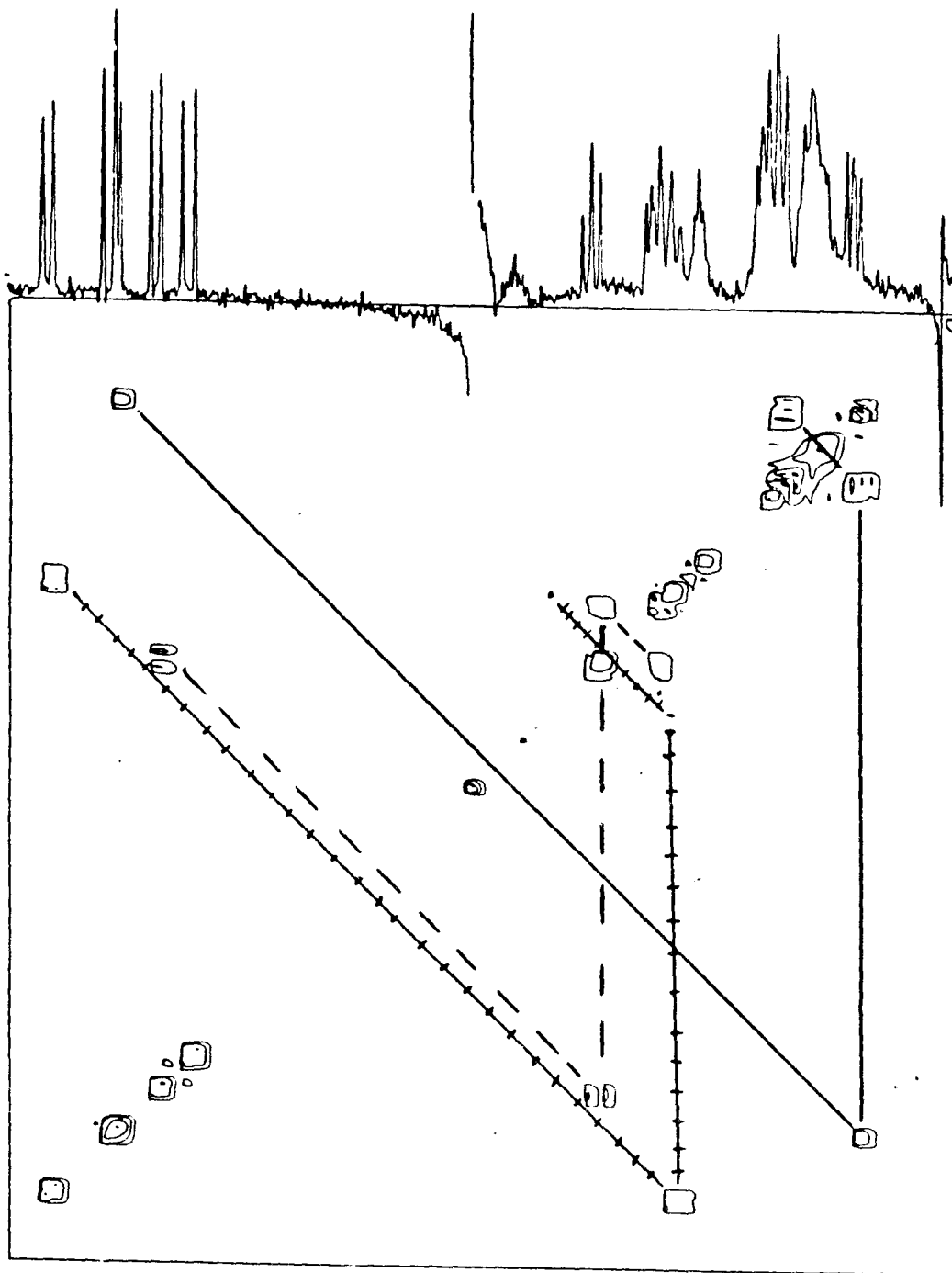


Fig. 19. 2D contour plot of CUG high, 1.81 mM, in a 1:1 solution of D<sub>2</sub>O:pyridine.

nucleotide. This allowed for the assignment of the other ribose protons from COSY-45 and RCT spectra.

An RCT spectrum is reproduced in Figure 18.a and proved to be the most useful of the 2D techniques in following magnetization transfers between protons of this molecule. Fortunately, two of the H-3' protons were in isolated spectral positions, therefore it was possible to take slices at these spots and possess essentially a 1D spectrum of the individual ribose protons for a particular ring. Examples of this technique are given in Figure 18.b where all the connectivities are shown for the H-3' protons at 4.48 and 4.60 ppm (59.4°C). An important result was that it linked the most upfield H-5'/H-5" protons to the H-3' octet unambiguously. From COSY-45 spectra such a conclusion was not as obvious. On the basis of the NOE experiments that labelled the H-1' protons, this ring system was assigned to U.

Similar treatment enabled the assignment of the ring system for G, although the resonances appeared broader because the H-3' proton at 4.60 ppm was close to the HDO signal. However, it did narrow the area which contained the H-4' resonances of this system. More importantly, it pointed out the H-5'/H-5" protons for this nucleotide as being the most downfield of the three systems.

The remaining signals were assigned to C by elimination. As additional proof, a F2 slice taken at the

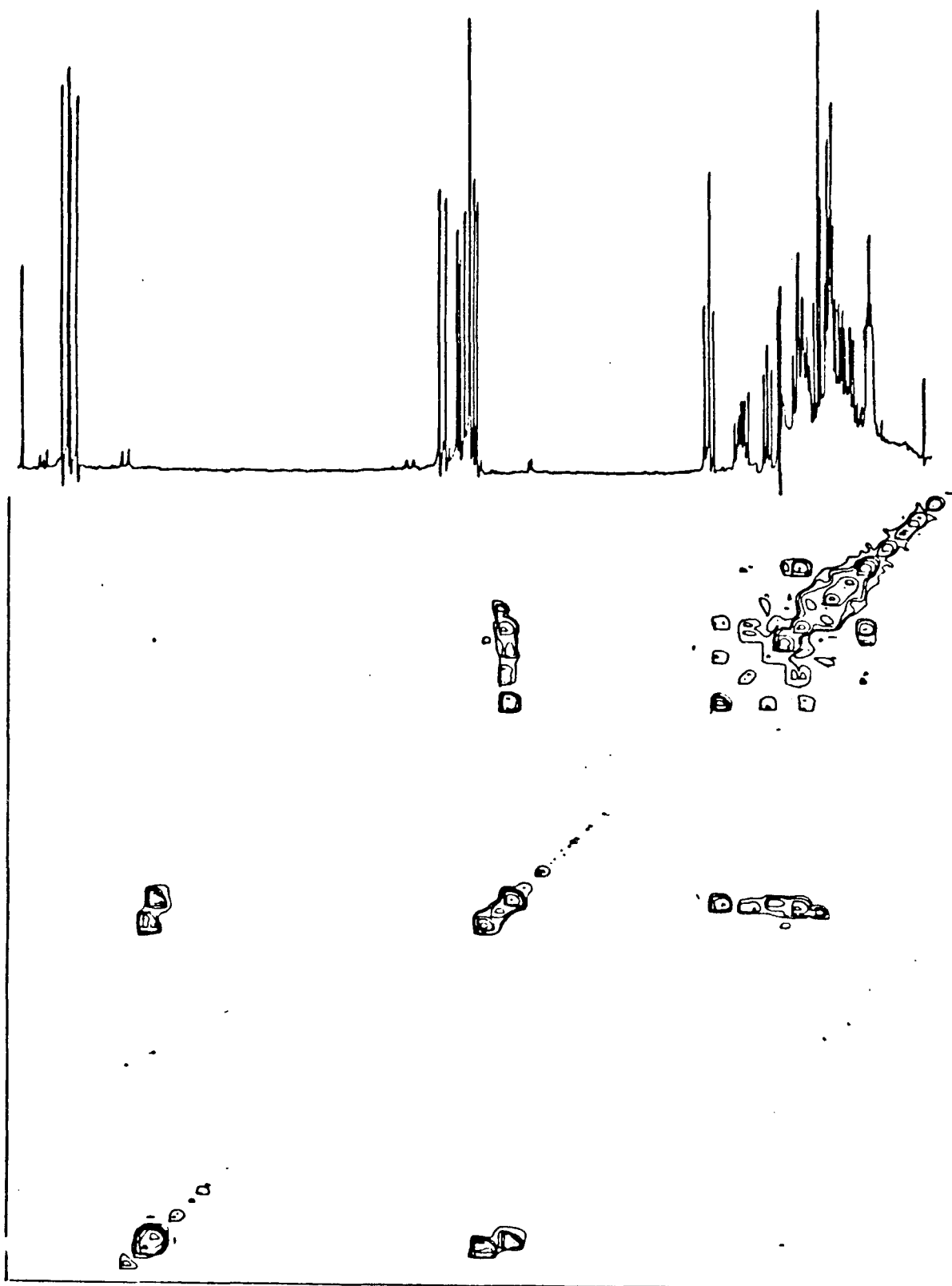


Fig. 18.a 2D contour plot of the RCT experiment on CUG high, 7.90 mM, at 60.1°C.

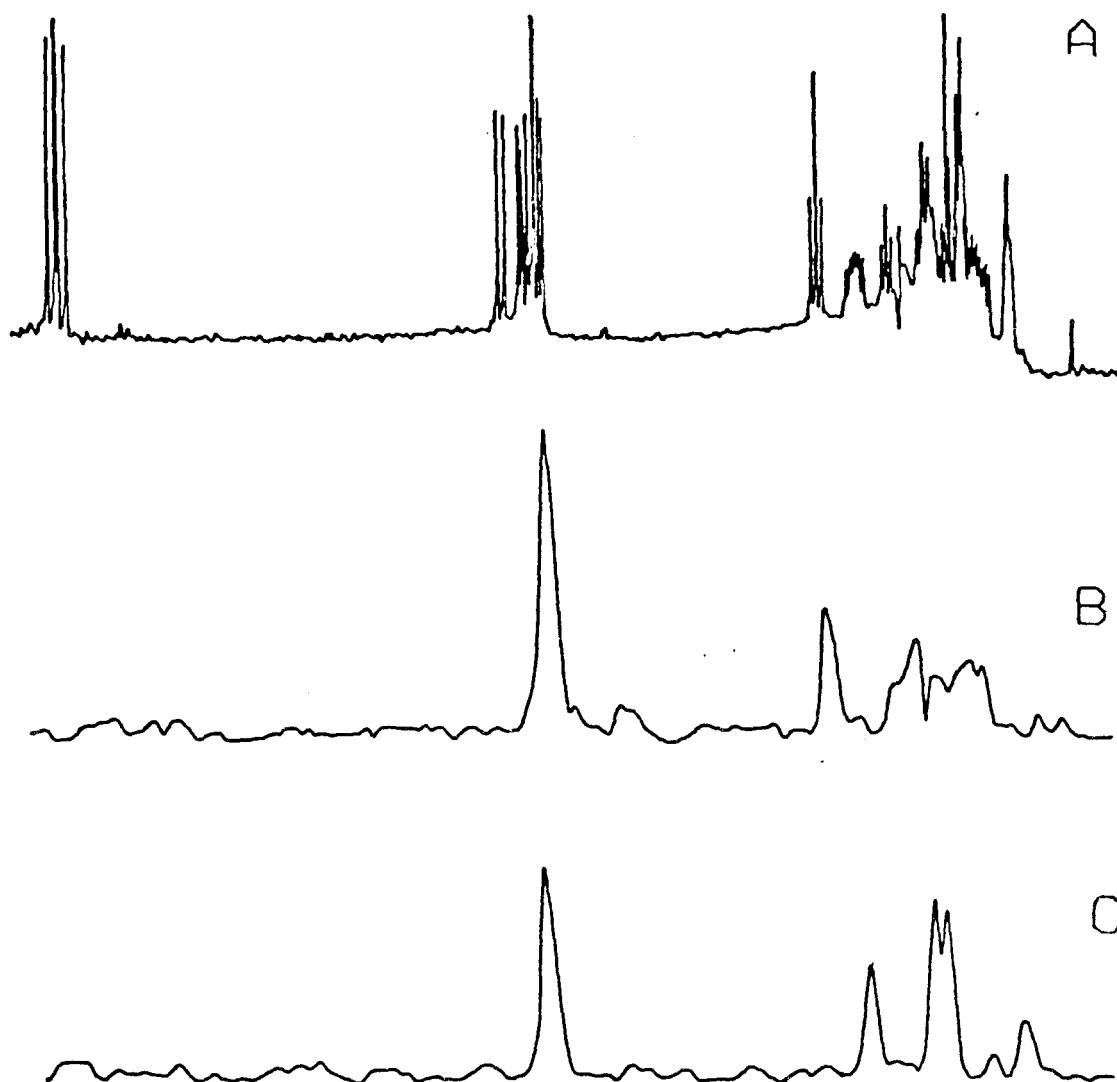


Fig. 18.b Comparison of F1 slices of the RCT experiment to a full proton spectrum at 60°C.  
A) Normal proton spectrum of CUG high (7.90 mM).  
B) F1 slice at 4.599 ppm assigned to G.  
C) F1 slice at 4.475 ppm assigned to U.

TABLE 6

CHEMICAL SHIFTS OF CUG HIGH, 7.90 mM,  
NO SALT, AT FOUR DIFFERENT TEMPERATURES\*

PROTON	68.5	50.1	30.2	10.0
C H-6	7.775	7.770	7.765	7.763
C H-5	5.999	5.986	5.967	5.959
C H-1'	5.918	5.915	5.911	5.909
C H-2'	?	?	?	?
C H-3'	?	?	?	?
C H-4'	?	?	?	?
C H-5'	4.136	4.135	4.132	4.129
C H-5"	4.067	4.065	4.062	4.062
U H-6	7.732	7.731	7.728	7.727
U H-5	5.853	5.845	5.832	5.815
U H-1'	5.883	5.875	5.862	5.850
U H-2'	?	4.321	4.306	4.291
U H-3'	4.606	4.593	4.578	4.563
U H-4'	?	?	?	?
U H-5'	?	3.996	3.980	3.965
U H-5"	?	3.858	3.908	3.848
G H-8	7.971	7.972	7.965	7.952
G H-1'	5.861	5.852	5.839	5.821
G H-2'	4.743	4.755	4.770	4.792
G H-3'	4.473	4.478	4.486	4.498
G H-4'	?	?	?	?
G H-5'	?	?	?	?
G H-5"	?	?	?	?

\* 250 MHz spectrum. H-5'/H-5" calculated from the following equation for AB systems:  

$$\Delta\delta = \frac{\sqrt{(1-3)^2 - (1-2)^2}}{2} = \frac{\sqrt{(2-4)^2 - (3-4)^2}}{2}$$
 where 1,2,3,4 are the observed resonances.  
 (Pasto and Johnson, 1969).

TABLE 7  
 FIRST ORDER COUPLING CONSTANTS  
 OBSERVED FOR CUG HIGH (7.90 mM)  
 IN 1 M SALT AT 47.7°C\*

J/BASE	C	U	G
5-6	7.55 ± .01	8.13 ± .01	-
1'-2'	3.558	5.942	5.25 ± .08
2'-3'	?	5.34 ± .02	5.2 ± .1
2'-P	?	1.22	-
3'-4'	?	3.65 ± .03	4.7 ± .1
3'-P	-	7.81 ± .01	-
4'-5'	2.6 ± .1	3.31 ± .05	2.8 ± .2
4'-5"	3.42 ± .05	2.5 ± .1	4.93 ± .01
5'-P	4.60 ± .07	5.0 ± .2	4.7 ± .2
5"-P	4.22 ± .02	4.84 ± .07	6.50 ± .01
5'-5"	-11.73 ± .04	-11.9	-11.5 ± .2

\* from 500 MHz spectrum. All couplings in Hz with a standard deviation based on all the observed values. No standard deviation indicates only one observed value. Real error is ±.2 Hz for all values.

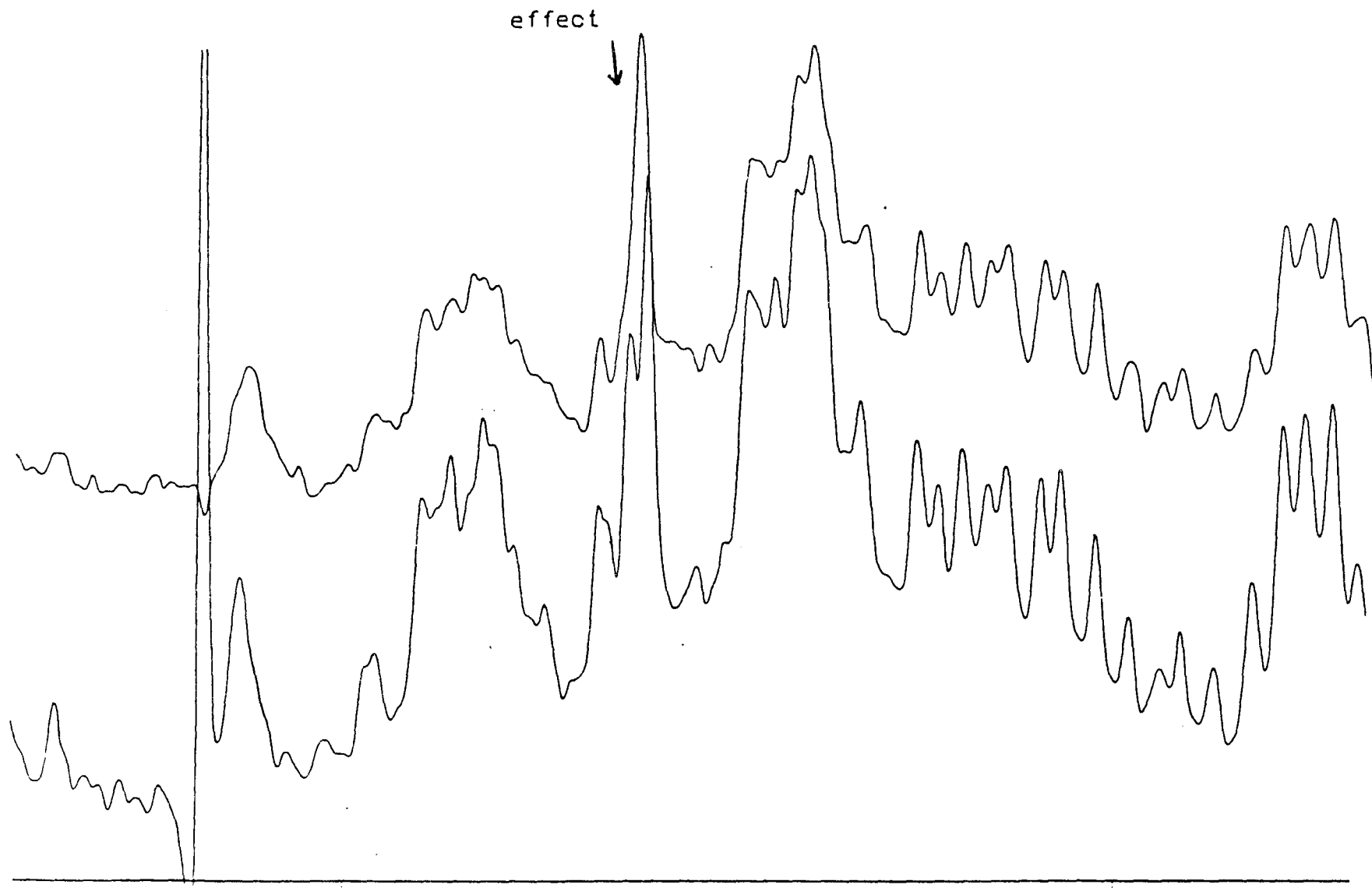


Fig. 20.

Example of a decoupling experiment involving the irradiation of the C H-1<sup>102</sup> proton of CUG low. Bottom spectrum is fully coupled, top one is the result of the double resonance experiment.

middle of the coincident H-2'/H-3' proton region exposed three additional peaks. One was to the most downfield H-1' proton, labelled by a NOE experiment to C. The other was just upfield of the slice region, designated H-4'. The third signal was centered in the middle of the remaining H-5'/H-5'' region. Hence from one experiment the ribose protons were all assigned to narrow spectral regions. Such an accomplishment was not possible from the COSY-45 experiments because of extreme overlap. While it was still not possible to acquire actual coupling constants and precise chemical shifts for the H-4' protons, at least their general vicinity was revealed.

To reinforce the assignments made by COSY-45 and RCT experiments, a number of decoupling experiments were conducted. Because of sample heating during irradiation, which resulted in field/frequency shifts, the resolution was poor. This is evident in the example in Figure 20, which shows the effect of saturating the most downfield H-1' doublet assigned to C. The greatest difference was the collapse of the peak at x, but other "rounding" of signals occurred. It did show, as the RCT and COSY-45 experiments, that a proton coupled to H-1' existed within this region.

Attempts to decouple protons other than H-1' in the ribose region were further complicated by the difficulty in selectively saturating one proton when there existed many others nearby. This was an especially difficult problem with

the CUG high isomer because ten of the fifteen ribose protons, other than the H-1's, were confined to a .35 ppm region. As a result the decoupling experiments did not add any new insights into coupling connectivities, but they did confirm assignments made with other techniques.

#### 4.2.4 Trimer Exchangeable Proton Spectra

With the two CUG isomers no duplex formation should occur, and did not appear to occur experimentally. However, out of curiosity, the exchangeable proton spectra of these isomers were acquired between  $-3.4 - 24.6^{\circ}\text{C}$  as described in the Experimental. The expected result was to observe identical spectra from the imino protons of U and G, with similar amino resonances from C and G. The spectra, as displayed in Figure 21 at  $-3.4^{\circ}\text{C}$ , indicated quite a substantial difference.

With regards to the imino protons, both the U and G resonances appeared to be coincident in both CUG isomers, except at  $-3.4^{\circ}\text{C}$  in the CUG high isomer, where two peaks at 11.27 and 11.17 ppm were visible. This compared closely to the one large resonance seen at 11.30 ppm at this temperature in the CUG low isomer. Their upfield position was indicative of no double bond character. Both these signals broadened as the temperature was increased, with the CUG low imino protons broadening out at a slightly slower rate. In both CUG

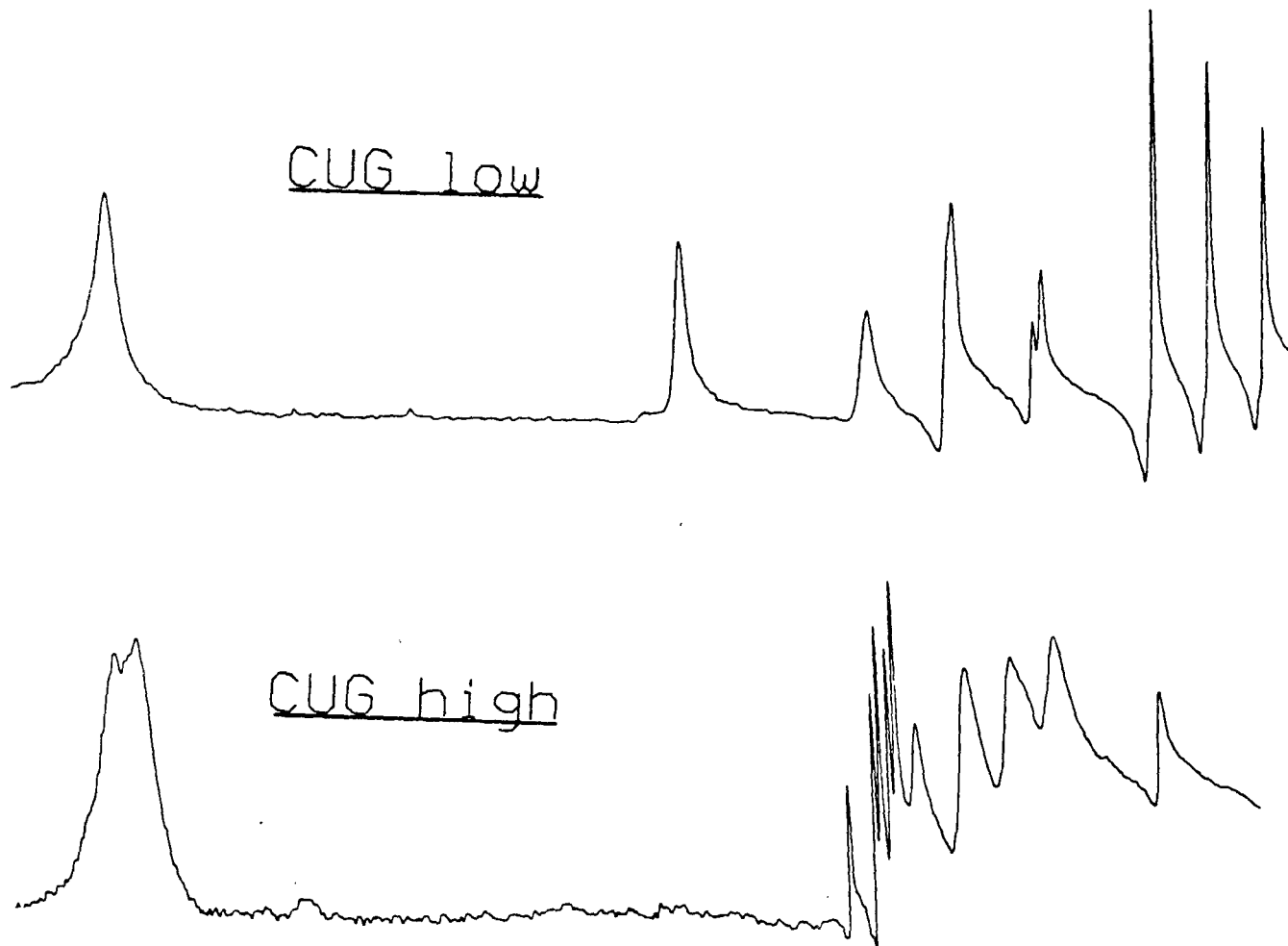


Fig. 21.

Exchangeable proton spectra of CUG high and low at  $-3.4^{\circ}\text{C}$ . Note that they are not both plotted on the same scale.

isomers they moved upfield, towards the water resonance, with increasing temperature.

Unexpected results were encountered in the amino and  $\text{NH}_4^+$  resonances. Ammonium ions are easy to detect because of their trademark 1:1:1 triplet pattern with a characteristic coupling constant of 52 Hz (Fazakerley et al., 1984). The triplet in the high isomer began to broaden out at  $8.8^\circ\text{C}$  and appeared as one lump at  $17.6^\circ\text{C}$ . This contrasted sharply to CUG low where these resonances were still sharp lines at  $24.6^\circ\text{C}$ . Evidently the ammonium ions in the low isomer were not exchanging with water as rapidly as those in the high isomer. This may be due to the different type of phosphodiester linkage which meant the ion/RNA complex was different. In the 5'-5' isomer the ionic phosphate may be more exposed to solvent because of a longer ribose to ribose link (one additional C4'-C5' bond). At low temperatures it settles into a protective position that makes exchange slow. However at higher temperatures the extra rotational freedom it has may expose it to more solvent.

Another major difference was in the amino protons. Two resonances were visible in the high isomer at 7.39 and 6.49 ppm ( $-3.4^\circ\text{C}$ ). The downfield signal broadened completely by  $17.6^\circ\text{C}$  while the upfield signal still remained sharp at  $24.6^\circ\text{C}$ . Although it was difficult to assess accurately, the upfield resonance appeared to possibly contain two protons.

In the low isomer two signals also appeared but at

9.15 and 8.46 ppm ( $-3.4^{\circ}\text{C}$ ). The downfield resonance appeared to contain two proton signals. Both resonances broadened out by  $24.6^{\circ}\text{C}$  but the downfield one was more intense.

The one definite conclusion about this observation was that the amino signals of the CUG low isomer were more downfield than those of the high isomer. This indicated that the amino protons of the high isomer were more over the plane of the adjacent base or the G was in the syn position where it would be more likely to feel deshielding effects from the ribose oxygens and the phosphorus backbone. This will be useful information in interpreting the variable temperature plots in later sections.

Of the four amino protons, only three appeared to be observed in each isomer. One explanation would be that one of the amino groups had protons that rotated rapidly enough to feel identical environments, while another explanation would be that one amino group had one proton protected while the other was exchanging too rapidly with the water to be observed. However, the more likely explanation was that both resonances were due to two protons, except one exchanged faster with water and therefore was less intense.

It was also possible to speculate on the assignment of the amino resonances from the behaviour of the ammonium ion resonances. It was suggested that the 5'-5' link allowed for a faster solvent exchange for these protons in the CUG high isomer. Since the C amino group was more closely

associated with this linkage one might have inferred that the signal broadening out first in the high isomer was due to these protons. This could have been because this ion was more able to catalyse this exchange or this base did not stack well and the amino group was more exposed to solvent. By elimination, this would have meant the other signal was due to G, its presence at 24.6°C indicating it was more stable.

#### 4.3.1 Enzymatic Analysis

When dealing with the structural determination of large molecules a simple method for easier structural assessment is to break it down into fragments. This has been done previously for tRNA sequencing (Holly et al., 1965) and later for ribosomes (Sanger et al., 1967). In terms of assigning the NMR spectra of oligo-RNA, the method of sequential analysis has been used (Borer et al., 1975, Alkema et al., 1982). The latter method involves assigning sequentially the monomer, dimer, trimer, etc., using the previous molecule as a reference. Such a technique was deemed necessary to confirm the structure of the CUG high isomer. However a slightly different approach had to be used because a 5'-5' linked dimer was not available. Its acquisition necessitated the sequential destruction of the trimer.

The most specific method for hydrolysing the

phosphodiester bond connecting nucleotide units together is various endo- and exo-nucleases. The most widely used exonucleases are snake venom and spleen phosphodiesterases.

Snake venom phosphodiesterase cleaves off one nucleotide at a time starting at a free 3' hydroxyl end (Razzell and Khorana, 1959). For example, such a digestion of normal CUG would produce the fragments illustrated in Figure 22A.

Spleen phosphodiesterase does the same thing but starts at the other end of the molecule. It needs a free 5' hydroxyl end to cleave off one nucleotide sequentially (Razzell and Khorana, 1961). The product of the complete digestion of normal CUG would be Cp, Up, plus G.

By deactivating the enzyme midway through a digestion it is possible to obtain fragments of various lengths. Such a technique was used by Holley et al (1965) to sequence the first tRNA.

A number of endoribonucleases exist that recognize a specific base or sequence in the middle of the oligomer. One such enzyme is Phy M which recognizes guanine residues and cuts it at the 5' hydroxyl side (Hiramaru et al., 1969, Donis-Keller et al., 1977). Its action on normal CUG will produce two fragments as illustrated in Figure 22B.

All these enzymes leave a phosphate group at the 5' or 3' end of the molecule. With Phy M stable 2'-3' cyclic

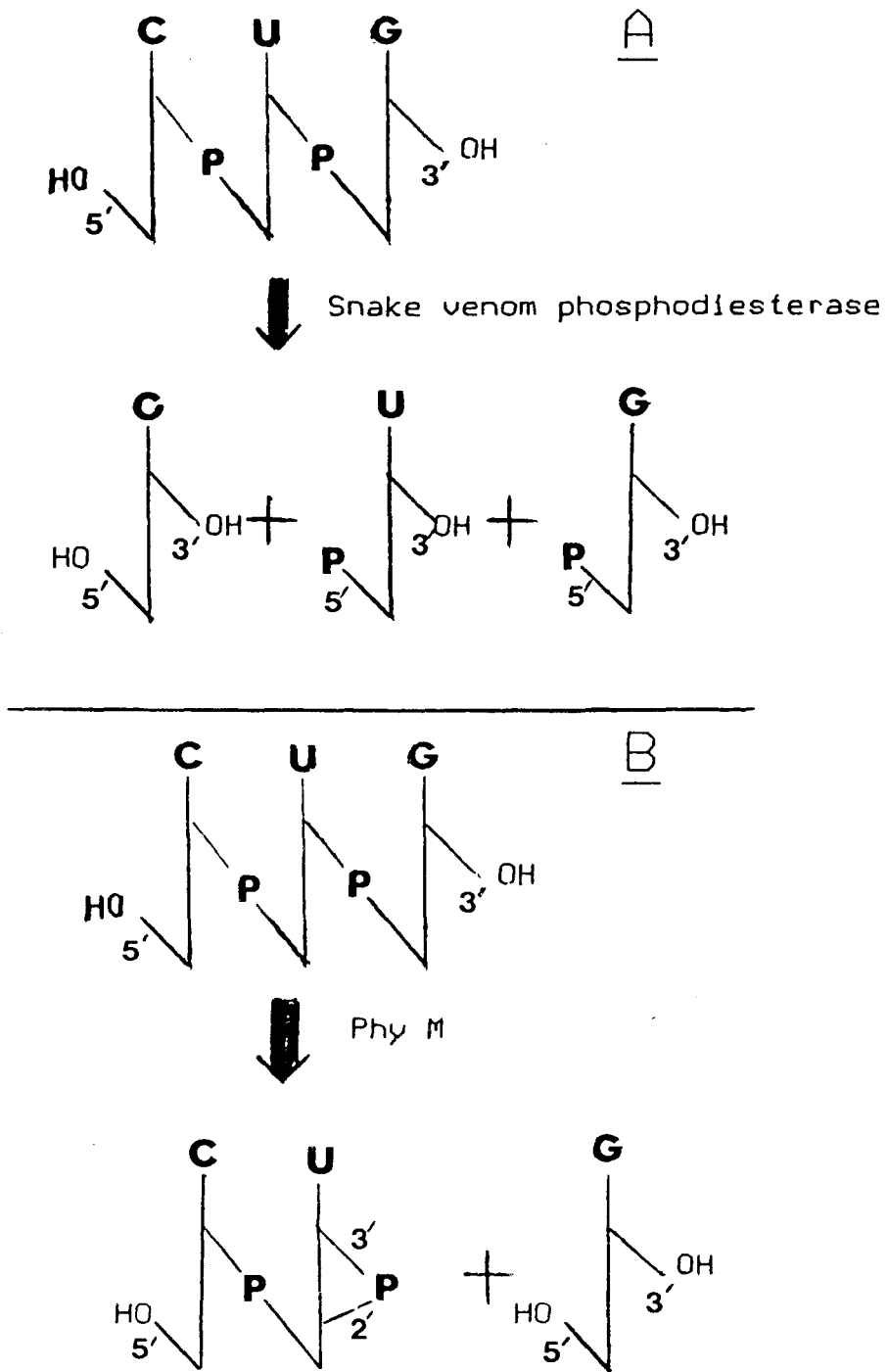


Fig. 22. Enzymatic digestion products of CUG low:  
 A) Snake venom phosphodiesterase. B)  
 Phy M.

phosphates are produced upon cleavage.

Another useful aspect of these enzymes in structural determination is that their action, or lack of it, confirms the presence or absence of certain structural features in a molecule. For example, spleen phosphodiesterase needs a free 5' hydroxyl group. A phosphate group replacement at this position would prevent hydrolysis. It is this feature that was utilized to verify the existence of the 5'-5' link in the CUG high isomer.

#### 4.3.2 The Enzymatic Results

The first approach was to treat the two trimers with exonucleases to determine the existence of free 3' and 5' hydroxyl ends. Treatment of both isomers as described above resulted in the total digestion of the CUG low isomer into monomers with both snake venom and spleen phosphodiesterases. This would be expected for a normally linked molecule with free 5' and 3' hydroxyl ends. Treatment of the CUG high isomer resulted in its total digestion with snake venom phosphodiesterase. Therefore at least one free 3' hydroxyl end existed. More revealing was the fact that this isomer was not touched by spleen phosphodiesterase. Since the normally linked trimer reacted under identical conditions, the possibility of the sequence being too short to bind to the protein to be cleaved can be ruled out (even though dimers

TABLE 8  
PHY M DIGESTION PRODUCTS  
AS ELUTED BY DESCENDING PAPER CHROMATOGRAPHY\*

SAMPLE	BAND #1	BAND #2
CUG high	.68	.48
CUG low	.69	.38
G	.67	-

\* Rf values on Whatman #1,  
1:1 mixture of  
methanol:1M ammonium acetate,  
with 1 OD sample sizes.

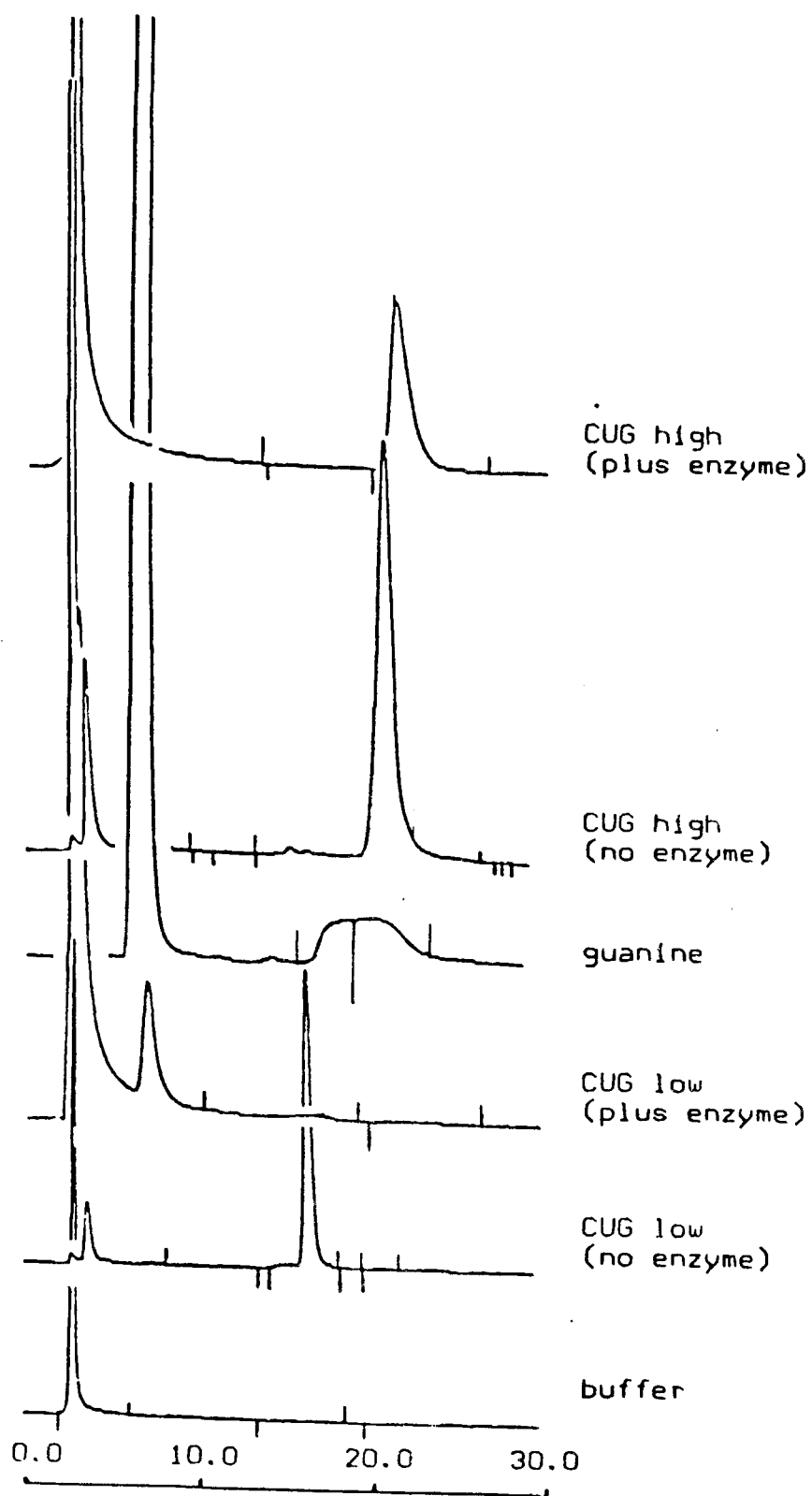


Fig. 23.

HPLC chromatograms of various spleen phosphodiesterase digests (1 OD samples).

were known to be long enough to react (Razzell and Khorana, 1961)). Hence the CUG high molecule did not possess a free 5' hydroxyl end, substantiating the NMR data.

A large quantity of the CUG isomers were digested with Phy M to remove the Gs and acquire enough sample for NMR analysis. Descending paper chromatography, as described for the deblocking procedure, was used to follow the course of the reactions. One OD digests of the CUG high isomer revealed bands with Rfs of .68 and .48. The low isomer had two bands with Rfs of .69 and .38. Meanwhile G by itself travelled with a Rf of .67. These results are summarised in Table 8 and suggested a single cleavage of only one phosphodiester bond. It appeared that the high Rf band was the G and the low Rf bands were the dimers. To verify this conclusion NMR analysis was required.

Such an analysis required treating 50 ODs of both isomers with Phy M and separating the products on Whatman #1 papers as described for the one OD samples. For the high isomer, 16.5 ODs of the high Rf fraction were collected as compared to 12.8 ODs for the low fraction. With the low isomer digest, 10.0 ODs were recovered for both Rf fractions. Although these samples were small, their parent trimers were isolated in a very pure form with HPLC, therefore proton NMR spectra were obtainable.

#### 4.4.1 Dimer Proton Assignment

The NMR analysis of both high Rf fractions from the two Phy M digests revealed that they both were indeed Gs. Similar analysis of the two low fractions confirmed the presence of dimer sequences. This was deduced from the downfield aromatic region. Both contained two doublets with coupling constants characteristic of C and U. The spectra of these two dimers differ substantially in the downfield region as the comparison in Figure 24 reveals. Evidently they behaved differently in solution.

Unfortunately the quantity of dimer present did not enable the acquisition of well resolved spectra of the complete ribose regions. A few features were well outside the major cluster of ribose protons to enable some assignment. The first were markedly downfield H-2' and H-3' protons in both dimers. Their lowfield position and their coupling pattern and size dictated that they were due to a cyclicized 2'/3' phosphate at U. This is supported by the data in Table 9 which compared all the possible coupling constants present to those for cyclic uridine monophosphate (cUMP) obtained from the literature (Lapper and Smith, 1973).

These numbers are very similar and in most cases the quoted results are within experimental error of the experimental results. Note that the cUMP is thirty times more concentrated and in a different salt form than the dimers and therefore greater discrepancies might have been

TABLE 9  
 COMPARISON OF THE COUPLING CONSTANTS, IN Hz,  
 OF THE 2' AND 3' PROTONS  
 OF 2'-3' CYCLIC U  
 WITH THOSE PRESENT IN THE PHY M DIMERS

COUPLING	U*	CU>P HIGH <sup>a</sup>	CU>P LOW <sup>b</sup>
1'-2'	3.0	2.7 + .1	2.90 + .01
2'-3'	6.9	7.0 + .1	6.8 + .2
3'-4'	5.5	5.3 + .3	4.91 + .08
2'-P	6.9	7.08 + .03	7.0 + .2
3'-P	11.5	11.22 + .01	11.5 + .2

\* Ba<sup>+</sup> form, .15 M (Lapper and Smith, 1973).

a NH<sub>4</sub><sup>+</sup> form, 3.90 mM.

b NH<sub>4</sub><sup>+</sup> form, 2.38 mM.

CU>P low



CU>P high



Fig. 24.

250 MHz comparison of the lowfield proton spectra of CU>P high and low at 60.6°C.

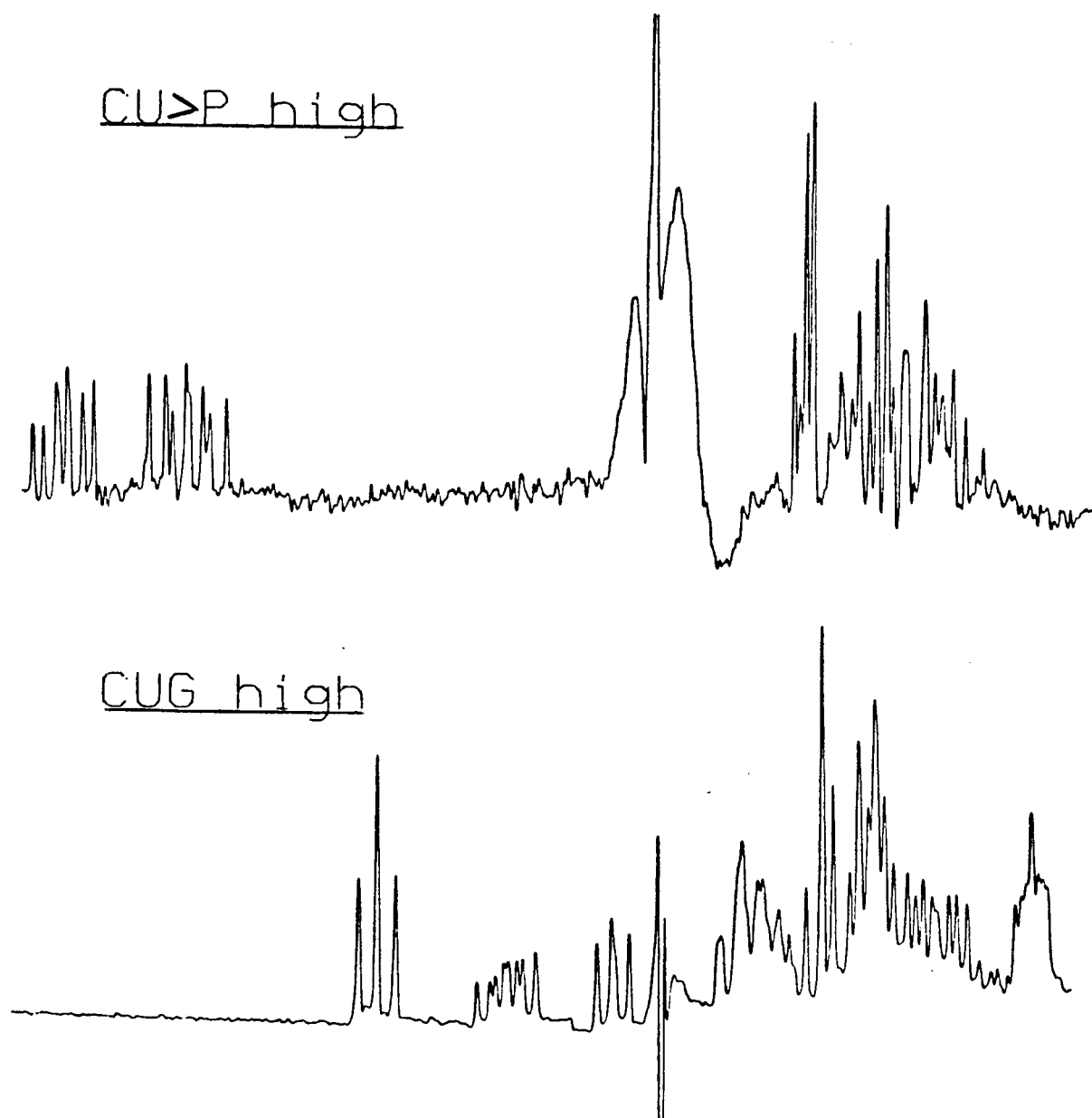


Fig. 25.

250 MHz comparison of the upfield ribose proton region of CUG high with CU>P high at 60°C.

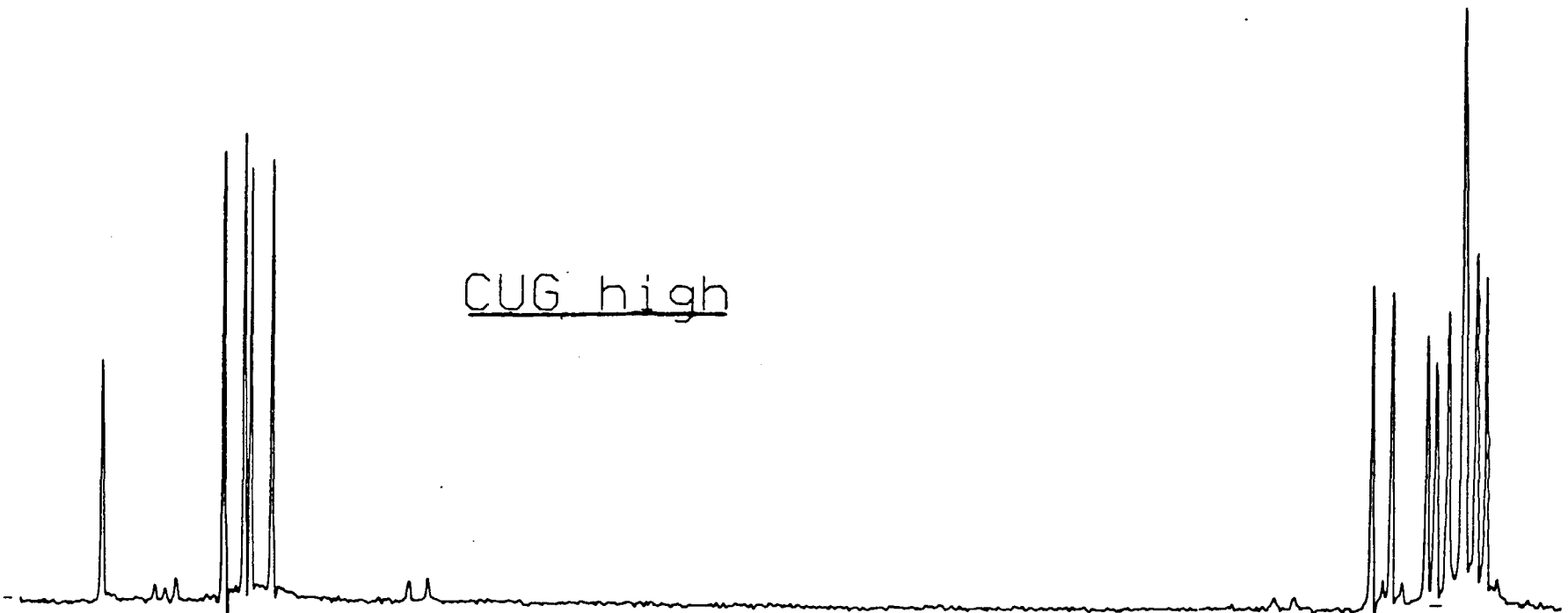
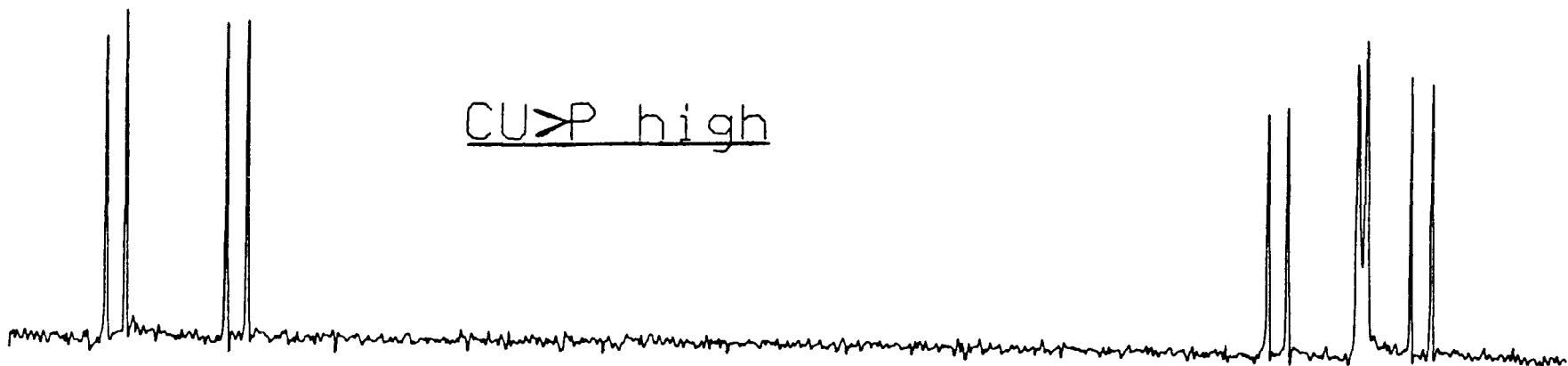


Fig. 26.

250 MHz comparison of the lowfield proton spectra of CUG high and CU>P high at 60°C.

119

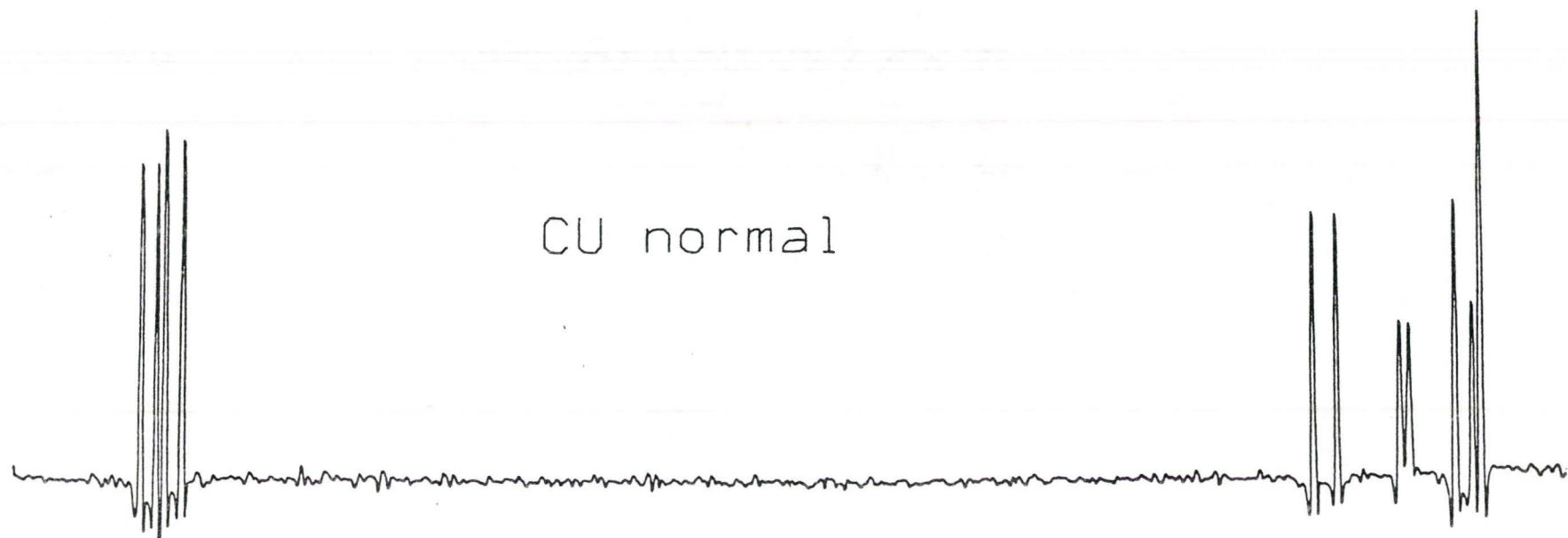
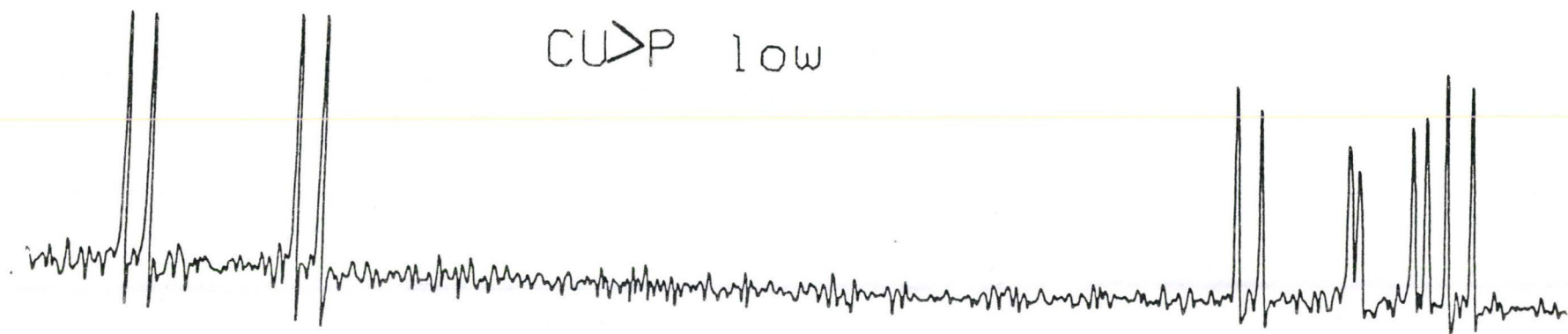


Fig. 27.

250 MHz comparison of the lowfield proton spectra of 3'-5' linked CpU with CU>P low at 30.0°C.

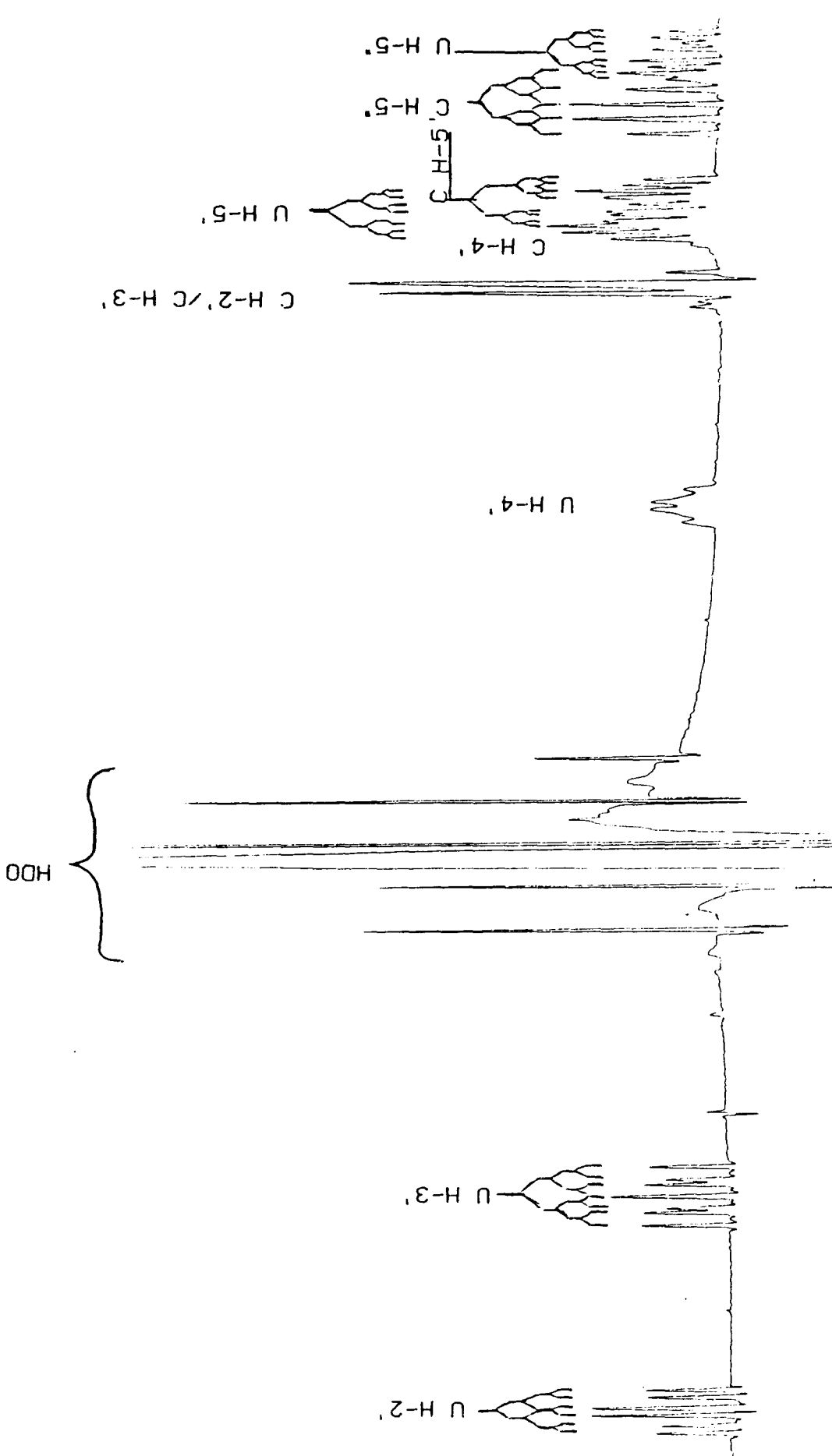


Fig. 28. 500 MHz proton spectrum of the ribose region of CU>P high at 30.0°C.

expected. As a result the dimers will be labelled as CU>P to delineate a 2'/3' cyclic phosphate, with a high or low title following it to denote the parent trimer.

Another readily visible aspect of the dimer spectra was the presence of a free 5' hydroxyl end in the CU>P low molecule. This was established on the same basis its presence was established for the trimers, upfield and with no phosphorus coupling.

In the CU>P high isomer the major similarity with the parent trimer was in the region containing C 2' and 3' protons with a near identical chemical shift. This is evident in Figure 25 which compares CU>P high with CUG high at about 60°C. Apparently the feature that resulted in the C 2' and 3' protons' chemical shifts laying upon each other in the CUG high isomer have been carried over to the dimer. However, it is still not possible to acquire any information on their exact chemical shifts or coupling constants because they still perturb each other greatly.

Proton assignment of the 250 and 500 MHz spectra was based on U containing a cyclic 2'/3' phosphate. A COSY-45 spectrum was obtained at 250 MHz in an attempt to follow the ribose ring magnetization transfers. Unfortunately, due to the small amount of sample and time constraints, the resolution was not satisfactory. Hence the assignment of the H-5'/H-5" protons rest mainly on the appearance of a well resolved H-4' proton which was connected to U(H-3') via the

COSY experiment. This was connected to the upfield most set of H-5'/H-5" resonances due to better agreement of the coupling constants. The assignments are illustrated in Figure 28 for CU>P high at 30.0°C and at 500 MHz.

It should be pointed out that the spectra at 500 MHz reveals two sets of H-5'/H-5" protons in an ABMX pattern. Hence the 5'-5' linkage is still intact in the dimer after the Phy M digest.

Note that 500 MHz spectra of the CU>P high dimer was obtained at 70.0 and at 47.7°C as well in the hope of more fully spreading out the C H-2'/H-3' region. This proved unsuccessful but information on some of the other protons were obtained. To enable comparisons, spectra of CU>P low and normally linked CpU were obtained in this temperature range as well to compare trends observed in the proton chemical shifts readily visible. Such an endeavor would hopefully provide insights into the solution behaviour of these dimers which might help in the interpretation of the trimer data. Additionally it would enable one to compare the effect of a 3' terminal G on the 5'-5' linked dimer.

#### 4.5.1 Phosphorus NMR

The backbone of oligoribonucleotides consist of phosphodiester linkages. In cells, it is this backbone that is most exposed to the environment in double helical DNA. As

a result it has been inferred that the shape of this outer region, determined by specific DNA sequences, may play a vital role in DNA/enzyme recognition (Griffen et al., 1973, Scheek et al., 1983, Clore et al., 1984, Hall et al., 1984). Fortunately this "spine" is composed of the nucleus phosphorus-31 (P-31) that has a spin of 1/2 and is 100% naturally abundant. Therefore it is possible to use NMR to study the behaviour of nucleic acids in solution by monitoring P-31 resonances (Patel, 1976, Gorenstein et al., 1982, Gorenstein, 1984, Cheng et al., 1984, Ott and Eckstein, 1985).

P-31 NMR is useful because it is a sensitive monitor of the torsion angles about itself,  $\alpha$  and  $\zeta$ , in the diester form, and the O-P-O bond angle. Such a conclusion has been reached on both theoretical (Gorenstein and Kar, 1975, Pradd et al., 1979) and experimental grounds (Gorenstein et al., 1976, Gueron and Shulman, 1975). These findings suggested that the P-31 chemical shift should move upfield when going from the -ap to the -sc orientation. This is the case when an oligoribonucleotide goes from the random coil to the duplexed or base stacked state. As a result "helix (base stacking)-coil" transitions may be followed over temperature by monitoring the P-31 chemical shift (Gorenstein, 1976, Haasnoot and Altona, 1979). Furthermore, no protons are involved in the torsion angles  $\alpha$  and  $\zeta$  (Section 1.3.3.6). Therefore this becomes an important method for acquiring

information on these angles which appear to donate the most flexibility to the nucleic acid backbone (Arnott and Hukins, 1969).

#### 4.5.2 Phosphorus Referencing and Assignments

One of the problems associated with P-31 NMR spectroscopy is the suitable referencing of the spectra. This arises because there is no suitable reference compound that can be added to the sample, the chemical shift of which is not temperature dependent. Normally, in proton spectroscopy, a reference such as t-butyl alcohol, tetramethylsilane (TMS) or 2,2-dimethyl-2-silapentane-5-sulfonate (DSS) is used where the resonance frequency has no significant intrinsic temperature coefficient. For aqueous solutions any changes that might occur are the result of changes in the deuterium D<sub>2</sub>O lock frequency that occur with temperature. By following the change of the HDO signal versus any of the above signals with temperature, it is possible to monitor the way in which the D<sub>2</sub>O lock frequency will change with temperature. Such an experiment was conducted by Coddington and Bell (1983). A straight line was obtained at 250.13 MHz that spanned more than 200 Hz with a slope of  $\pm 2.56 \text{ Hz}/^\circ\text{C}$ . At the P-31 frequency this corresponded to  $+1.035 \text{ Hz}/^\circ\text{C}$ . With this value one is able to eliminate the chemical shift change of the

deuterium lock frequency from the P-31 chemical shift by applying this correction factor to the sample set at one particular temperature and reference signal. Now P-31 chemical shift differences with temperature are due solely to environmental changes and not changes due to the movement of the field/frequency deuterium lock signal.

The two most often used references in the literature appear to be 85% or 15% phosphoric acid in D<sub>2</sub>O at room temperature or at 30°C. The standard of choice was the 15% phosphoric acid in D<sub>2</sub>O/H<sub>2</sub>O at 30°C because: i) readily available commercial phosphoric acid was 85% in H<sub>2</sub>O and ii) 30°C was more specific than room temperature. This resulted in the use of a spectral reference frequency (SR) of 25825.380 Hz for all spectra at all temperatures. Then to all the acquired spectra 1.035 Hz per °C was added or subtracted from the observed chemical shifts depending on whether the temperature was above or below 30°C. It is these corrected data that are plotted in Figure 29.

A second problem involved in P-31 spectroscopy of oligonucleotides was the assignment of the resonances to a particular dimer unit. Various techniques have been employed to attain such assignments:

i) Synthesis of oligomer with O-17 directly bound to the phosphorus at a particular site (Joseph and Bolton, 1984, Petersheim et al., 1984, Shah et al., 1984, Gorenstein et al., 1984). Because of its fast relaxation rate, the O-17 induces

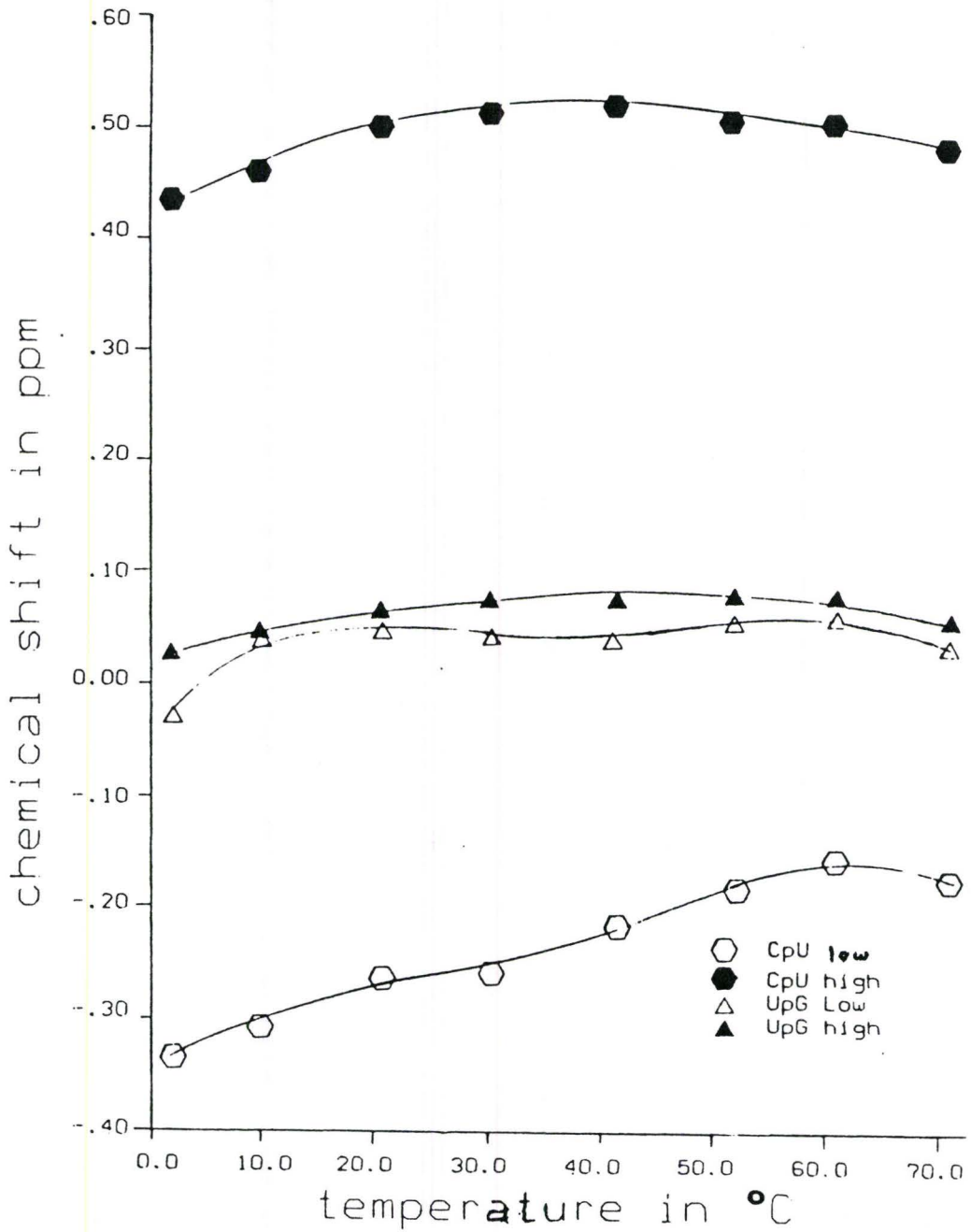


Fig. 29.

Variable temperature plots of the temperature corrected phosphorus spectra for CUG high and low.

scalar relaxation of the second kind and broadens out the phosphorus signal it is bound to. However, pure O-17 H<sub>2</sub>O is difficult to obtain, because a certain percentage of O-18 is usually present and this has the effect of producing an upfield isotope shift. Thus O-18 can be alternatively added to one site, and in most cases a combination of O-17 and O-18 is used to label more than one phosphorus in a sequence.

Although this technique appears very useful in identifying phosphorus signals to a particular dimer unit, it does have its drawbacks. Primarily, oxygen isotopes add additional expenses to the synthesis. In the case of the CUG isomers under study, the molecules were already synthesised, with one being a side product. Therefore isotope labelling would have meant new synthesis.

ii) Decoupling one phosphorus signal at a time and observing the proton spectrum (Cheng et al., 1982, Cheng et al., 1984). If the ribose proton spectrum is completely assigned, one can identify the sequence position of the phosphorus from the H-5'/H-5" and H-3" protons which lose their phosphorus coupling.

The problem with this technique is that it requires a proton probe that specifically decouples phosphorus, or the use of additional equipment to modify signals produced by the usual P-31 detection/H-1 decoupler probes.

iii) Two-dimensional heteronuclear chemical shift spectroscopy (Pardi et al., 1983, Lai et al., 1984, Lown and

Hanstock, 1985). The principle is similar to a COSY experiment except polarization transfer now occurs between heteronuclei. Cross peaks are produced at positions where the proton spectrum, F1, cross correlates with coupled phosphorus signals in F2. To make use of the technique the ribose proton spectrum needs to be assigned. This method was attempted on a WM-250 spectrometer but, most likely due to either improper  $90^\circ$  and  $180^\circ$  H-1 and P-31 pulse calibrations and/or, instrumental variations in successive pulses, both techniques proved fruitless.

iv) The use of a double resonance, selective decoupling experiment (Gronenborn et al., 1983). This is possible if the ribose proton spectrum is assigned and the H-3' phosphorus coupled protons are sufficiently resolved and separated. Decoupling is accomplished with a continuous wave (CW) centered upon an H-3' phosphorus coupled proton. The decoupling power is then adjusted until the observation of one phosphorus signal becoming sharper than the other(s). This signal is now more effectively decoupled than the other phosphorus signal(s) because the decoupling field is centered specifically upon one coupled proton.

The above was the method of choice to assign the phosphorus signals of the CUG low isomer as described in the Experimental. The spectra of these experiments are displayed in Figure 30 for the low isomer (3.31 mM, no salt) at  $30^\circ\text{C}$ . Figure 30A is the broadband decoupled spectra. Figure 30C is

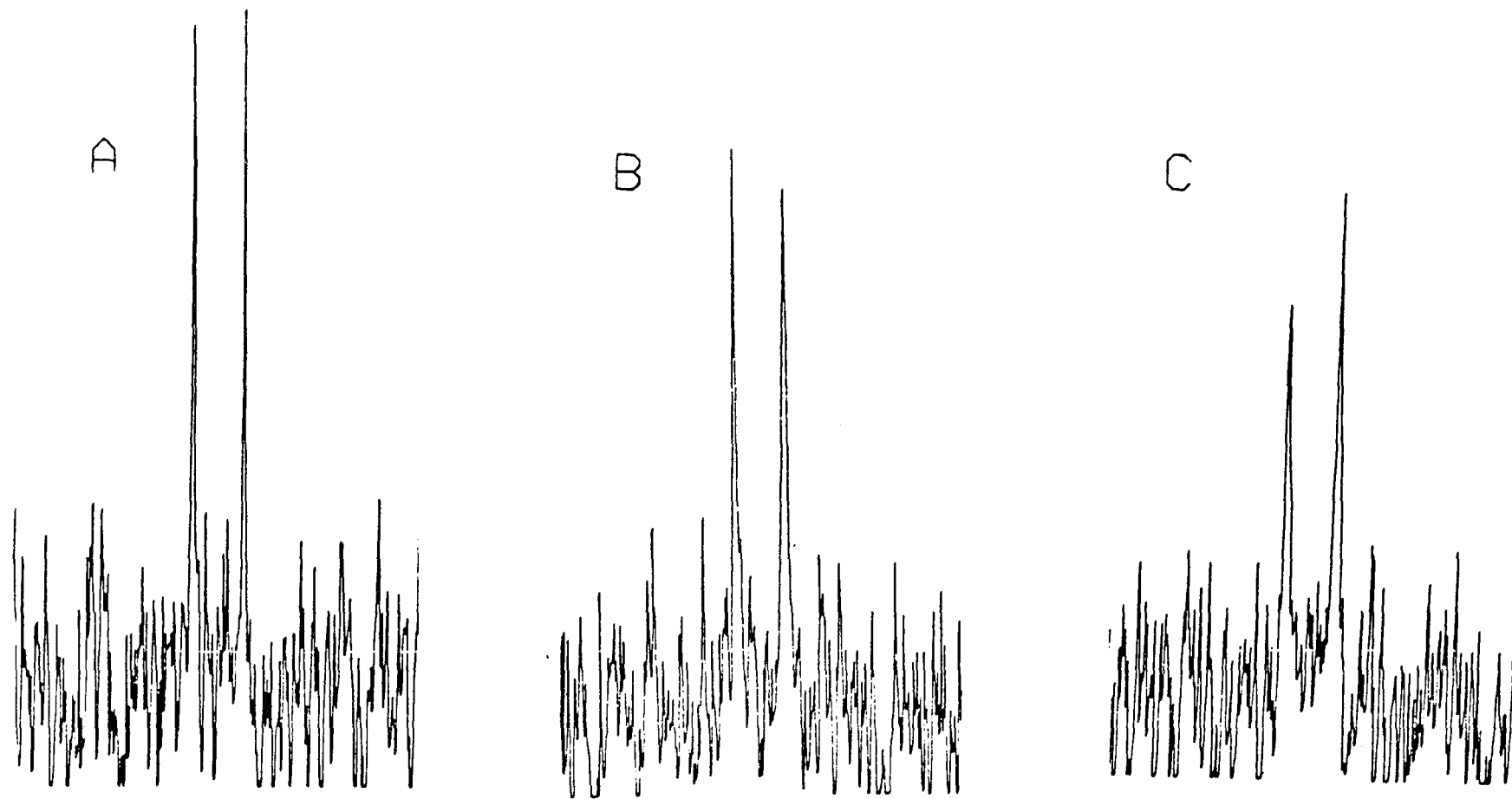


Fig. 30.

Spectra obtained in selective CW decoupling experiments to assign the CUG low phosphorus signals. A) BB decoupled spectrum. B) CW irradiation at U H-3' (4632.794 Hz). C) CW irradiation at C H-3' (4596.122 Hz).

the result of applying CW irradiation of 25 H upon C H-3' centered at 4596.122 Hz. Obviously the upfield signal was more intense hence this was assigned to CpU. Figure 30B is the result of 22 H irradiation upon U H-3' at 4632.794 Hz. In this instance the opposite effect occurred with the downfield signal appearing more intense. This confirmed the first assignment because the process of elimination required this signal to be UpG.

Figure 29 is the variable temperature plot of the temperature corrected chemical shift data for both CUG isomers. From the assignment of the signals of the low isomer it was possible to infer assignments for the two high isomer signals. The one coincident upon the UpG signal of the low isomer should have been due to the same isomer unit. Conversely the other signal, shifted radically downfield, was assigned to the 5'-5' linked CpU unit. With these assignments it was then possible to interpret the variable temperature graph.

The obvious observation was that the UpG resonances both followed similar paths. Both moved only slightly upfield with decreasing temperature, indicating mild base stacking. This observation indicated that the UpG unit behaved similarly in both isomers, at least with regards to the phosphodiester backbone orientation.

With regards to the CpU low signal, an obvious upfield trend was seen from 60 to 0°C. This corresponded to

an upfield transition of .17 ppm which contrasted sharply to the .03 ppm shift seen for CpU high over the same temperature range. This suggested that the C and the U were stacking better than the U and the G in the low isomer. In the high isomer the reverse appeared to be true. This was in accord with proton data, which will be interpreted more fully later, that suggested the low isomer stacked from the 5' end while the high isomer stacked from the 3' position.

Another feature was the large difference in chemical shifts of the CpU resonances in both isomers. CpU high was .67 ppm downfield of the signal of the low isomer at 61°C. Evidently both phosphorus atoms were in very different chemical environments as would be expected with a different linkage. The 5'-5' phosphodiester bond appeared more deshielded than the biologically normal 3'-5' linked dimer unit. Even so, an upfield trend was seen from 40 - 2°C which suggested some form of order was occurring about the dual  $\alpha$  torsion angles as they adopted more of an -ap conformation about the riboses.

#### 2.6.1 Carbon-13 Spectroscopy

To obtain details on the orientation of an oligonucleotide, it is useful to possess the carbon-13 (C-13) spectra of such compounds (Gronenborn et al., 1983, Lankhorst et al., 1985). It is from C-13/P-31 coupling constants that

information on the torsion angle  $\epsilon$  can be obtained (Sec. 1.3.3.5). The problem is to obtain enough oligomer to obtain a C-13 spectrum. Further, if one desires to accurately assign the carbons via a 2D heteronuclear chemical shift correlation experiment (Mandsley et al., 1977, Budenhausen and Freeman, 1977), then one needs yet more sample to conduct the experiment in a reasonable period of time. As a result assignment is made by comparing the spectra of the trimers to those of monomers and dimers (Gronenborn et al., 1977). In the case of the two separate isomers under study an additional advantage rests in comparing the two isomers. This is because the nature of the phosphodiester bond confers certain recognizable features to the carbon-13 signals.

The primary feature of phosphorus is its ability to split a C-13 signal due to the possession of a 1/2 spin nuclear quantum number. In the two isomers, the CpU bond differs in terms of the carbons linked to phosphorus. In the high isomer this was 5'-5', in the low isomer 3'-5'. Up to three bond coupling was observable if the molecule was oriented properly. The coupling or non-coupling features of the carbon signals would therefore have labelled it to the first nucleotide C. This was because in the high isomer, C C-2' should have been a singlet since it was five bonds away from the nearest phosphorus. In the low isomer it should have existed as a doublet because it was only three bonds away and would then feel the effect of phosphorus.

Comparison of the spectra in Figures 31 and 32 bear this out and these were used to assign the 74.30 ppm single resonance (55°C) to C in the high isomer because it was split in the low isomer (74.47 ppm, 22°C).

Similar arguments, together with another feature of the effect of phosphorus, was used to assign C C-3' (as well as C-5's). This is the downfield shift of approximately 3 ppm seen in dimers that phosphorus induces upon a carbon involved in the phosphodiester bond (Alderfer and Ts'o, 1977).

Such an effect is evident in Figure 32 where the signal at 71.07 ppm in the high isomer disappeared in the low isomer spectrum (Figure 31). This signal was a singlet and upfield approximately 3 ppm from the middle of the nearest region containing other similar signals. Also, there was another singlet slightly upfield of it that appeared in both spectra at 70.09 (high) and 69.97 (low) ppm. The latter signal was assigned to G C-3' which meant the former at 71.09 ppm (high) was C C-3'.

Three of the six C-2' and C-3' signals were now identified. Assignment of the other signals were made by using knowledge of the effect of changing temperature on the chemical shifts of these carbons. C-2's were invariant with temperature while C-3's shifted by up to .8 ppm over 100°C (Gronenborn et al., 1983). Such a change was noticed for the unassigned doublet centered at 73.75 ppm in the high isomer

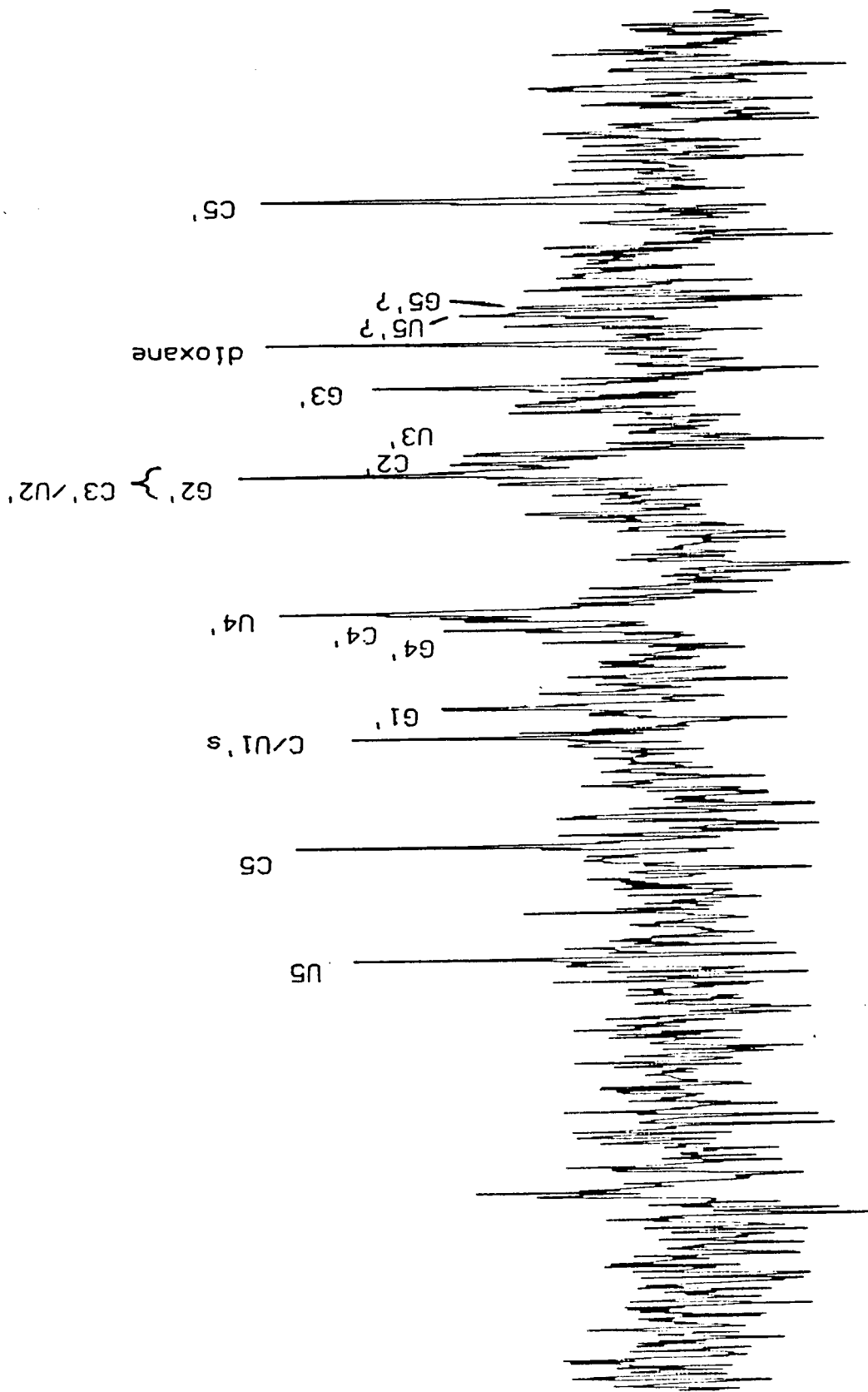


Fig. 31. Carbon-13 spectrum of the ribose region of CUG low, 50.6 mM, at 22°C.

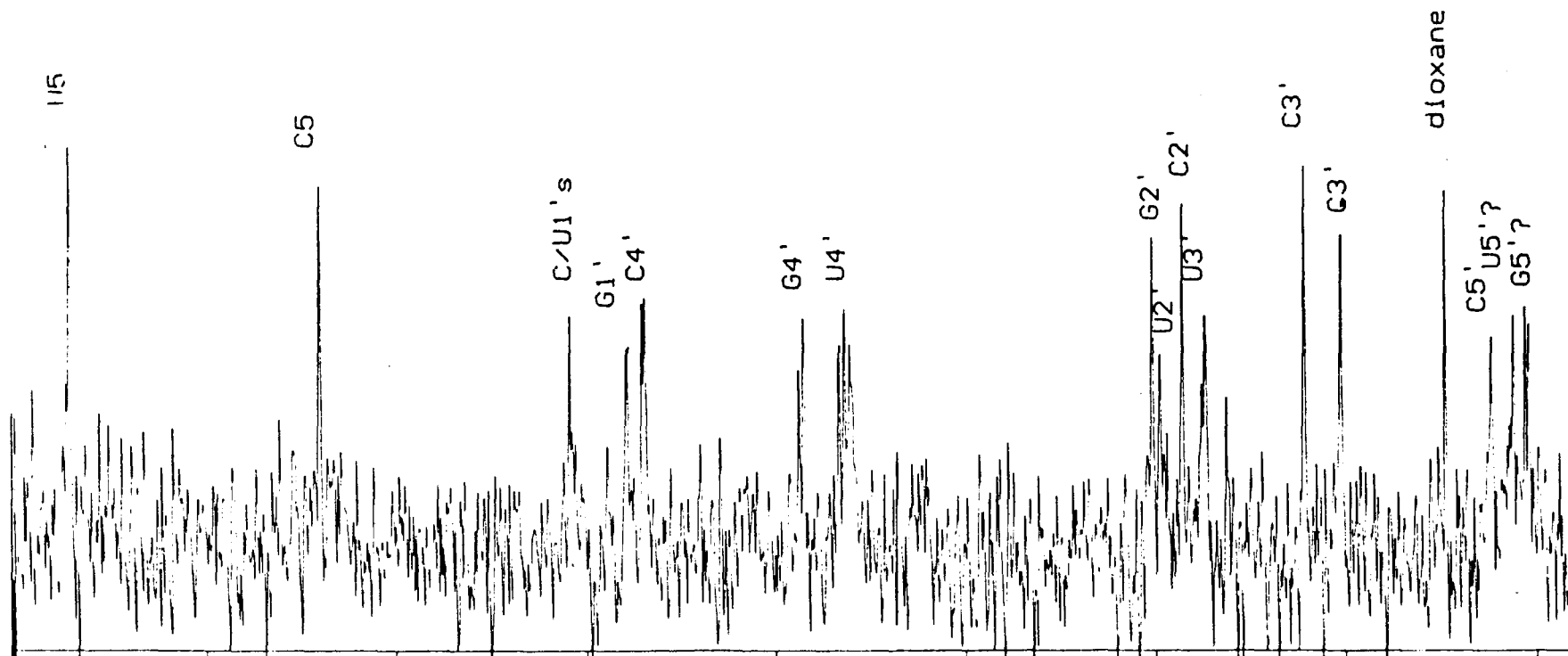


Fig. 32.

Carbon-13 spectrum of the ribose region  
of CUG high, 65.4 mM, at 55 C.

at 55°C and the broader doublet seen at 73.87 ppm in the 22°C spectrum. This was a difference of .12 ppm over 33°C which was the largest shift of any of the carbons as yet unassigned. Therefore, this signal was assigned to U C-3'. A doublet appearing at 73.82 ppm in the low isomer was additionally assigned on the basis of the high isomer assignment since its chemical shift was similar. This would be expected since both carbons were involved in a 3'-5' phosphodiester bond.

The remaining two C-2' were assigned on the basis that U should be a doublet and G a singlet in both isomers. This singlet was seen at 75.08 ppm (high) and 75.06 ppm (low) and assigned to G in both isomers. In the high isomer only a doublet centered at 74.84 ppm remained unassigned and therefore, by elimination, was assigned to U C-2'.

Note that two carbon signals were unassignable in the low isomer, U C-2' and C C-3'. Both should have appeared as doublets and must have been located within the relatively broad region centered at 75.1 ppm.

The C-5's appear furthest upfield of any of the nucleotide carbons (Jones et al., 1970). In assigning these signals use was made of the phosphorus deshielding effect on carbon. Free hydroxyl 5' carbons appear upfield of carbons involved in a phosphodiester bond. As a result the sharp signal most upfield at 58.93 ppm in the low isomer could only have been due to C C-5'. The problem, however, was that the

other two C-5's were split and did not appear above the noise level. Various data massaging techniques did show maximum signal intensities centered at 65.64 and 65.23 ppm. This roughly corresponded to better resolved signals in the high isomer spectrum at 65.60 and 65.25 ppm at 55°C (these signals were poorly resolved at 22°C). Of these, two appeared as wide singlets while only one was clearly split. Since these apparent singlets were not twice the intensity of the definitely split C-5', the phosphorus coupling of these carbons must then be less than 5.7 Hz as observed for the doublet at 65.60 ppm (high).

It was not possible to unambiguously assign the U and G C-5's. However a few comments may be made about the features of these resonances.

Firstly, the presence of three signals within .96 ppm of each other in the high isomer and all coupled to phosphorus indicated that each C-5' was bonded via an ester link to a phosphorus atom. This offered further support for the 5'-5' link assignment. Secondly, a free 5' hydroxyl bonded carbon usually appears about 3 ppm upfield of the normally linked carbons involved in phosphodiester bonds in dimers. In the few C-13 spectra of RNA trimers available, the only one containing traditional bases is 4 ppm upfield from the nearest C-5' carbon (UUC) (Gronenborn et al., 1983). In the CUG low isomer, the C C-5' was 6.3 ppm away from the nearest C-5'. If one assumed the peaks at about 65.6 and

65.2 ppm were from the same C-5' nucleotides (which was a reasonable assumption considering the UpG parts were the same), then the 66.16 ppm high isomer peak belonged to C C-5'. This represented a change of 7.2 ppm in going from the free hydroxyl to the phosphodiester linked form which increased the difference even more. The trend appeared to be that in the trimer, the free C-5' signal was further upfield than the corresponding signal in the dimer which was further upfield than the one in monomers. This observation appeared to arise not from the downfield carbons moving further downfield, but due to the upfield C-5's moving further upfield, as the data in Table 10 indicates. Perhaps the upfield shift is a reflection of a more sterically hindered carbon in the trimers than in the dimers or monomers (Wehrli and Wirthlin, 1976). This would be in accord with Sundaralingam's "rigid" nucleotide model that denotes more rigidity to nucleotides as the sequence length increases (1973).

Downfield of the C-2'/C-3' region lay the signals due to C-4'. In both isomers two doublets should have been observed (C and G) plus a quartet (U). This was the case with doublets centered at 84.22 and 83.20 ppm in the low isomer and 84.33 and 88.51 ppm in the high isomer. Coupling constants were extractable from these signals. The quartet appeared as a triplet in both isomers (two apparently identical couplings) at 83.19 (high) and 83.49 (low) ppm.

TABLE 10  
C-5' CHEMICAL SHIFTS IN ppm\*

SEQUENCE			
UUG <sup>a</sup>	62.4 U (1)	66.5 U (2)	66.5 C (3)
CUG (LOW) <sup>c</sup>	58.9 C	65.3 (U/G?)	65.6 (U/G?)
CUG (HIGH) <sup>b</sup>	66.2 C	65.3 (U/G?)	65.6 (U/G?)
C <sup>d</sup>	63.2 C	—	—

\* relative to dioxane at 67.40 ppm.

a Gronenborn et al., 1983. 0°C.

b 22°C.

c 55°C.

d Hruska and Blonski, 1982. 27°C.

The major difference between the two sets of C-4' signals was the 88.51 ppm doublet in the high isomer and the doublet at 83.20 ppm in the low isomer. These signals may be assigned to C where the orientation of the ribose relative to the remaining UpG unit changed drastically. Therefore by elimination the other set of doublets was assigned to G.

At 22°C the difference between the C-4' chemical shifts of the low and high isomers were -5.44 (C), +.39 (U) and -.06 (G) ppm. This reflected G C-4' being in relatively the same environment in both isomers with U experiencing some change due to its nearer proximity to the reoriented ribose in the 5'-5' isomer.

The signals due to C-1' could not be unambiguously assigned. In both isomers two signals existed practically on top of each other at about 90.4 ppm. An additional signal existed in both isomers at 88.81 (high) and 88.77 (low) ppm (22°C). Since the G C-1' of the monomer is slightly upfield of the C-1' of pyrimidine analogues (Dorman and Roberts, 1970), it could be inferred that this upfield signal belonged to G.

The only other signals that were assignable were the C-5s because of a difference of 6 ppm in their chemical shifts (Dorman and Roberts, 1970). The values for the heterobases were almost identical in both isomers. This was a consequence of the poorer sensitivity of carbons to base-stacking anisotropic effects and the small amount of

TABLE 11  
 CARBON-13 CHEMICAL SHIFTS (ppm)  
 AND PHOSPHORUS-31 COUPLING CONSTANTS (Hz)

CARBON	TEMP. °C	C	U	G
C-5' H	55	66.16 (-)	65.60 ( 5.7)	65.25 (5.7)
H	22	-	-	65.15 (4.9)
L	22	58.93	65.64 (8.9)	65.23 (-)
C-4' H	55	88.51 (4.5)	83.19 (2(8.9))	84.33 (7.3)
H	22	88.64 (9.9)	83.10 (2(9.1))	84.27 (8.7)
L	22	83.20 ( $\cong$ 9)	84.49 (2(10.5))	84.22 ( $\cong$ 10)
C-3' H	55	71.07	73.75 (5.1)	70.09
H	22	71.02	73.87 (5.9)	69.92
L	22	?	73.82 ( $\cong$ 9.5)	69.97
C-2' H	55	74.30	74.94 ( $\cong$ 10)	75.08
H	22	74.21	74.84 (6.6)	75.04
L	22	74.47 ( $\cong$ 7.9)	?	75.06
C-1' H	55	90.44 (C?)	90.36 (U?)	88.96
H	22	90.51 (C?)	90.39 (C?)	88.81
L	22	90.53 (U?)	90.53 (C?)	88.77
C-5 H	55	96.93	103.54	-
H	22	97.03	103.53	-
L	22	97.06	103 50	-

stacking that was occurring over this temperature range.

#### 4.7.1 Solution Behaviour

With these carbon assignments and coupling constants, tabulated in Table 11, it was possible to use various Karplus styled equations in combination with the proton and phosphorus data to make more definite statements about the preferred conformation of the two isomers in solution.

#### 4.7.2 Trimer Base Region

Figures 33 and 34 are variable temperature plots comparing the behaviour of the H-8, H-6, and H-5 protons of both isomers. The H-6 and H-8 protons of the low isomer shift to low field with decreasing temperature. In the high isomer, an upfield trend is seen. Because H-6 and H-8 are close to the phosphodiester backbone and near the ribose ring oxygen in the anti form, they feel the diamagnetic anisotropy of these groups when orientated appropriately (Lee and Tinoco, 1980). Hence any shielding arising from base-stacking may be overpowered by the phosphorus and/or oxygen deshielding.

The trend is in contrast to that seen for H-5, which moves upfield in both isomers. Generally these protons are considered to be the more reliable indicators of base

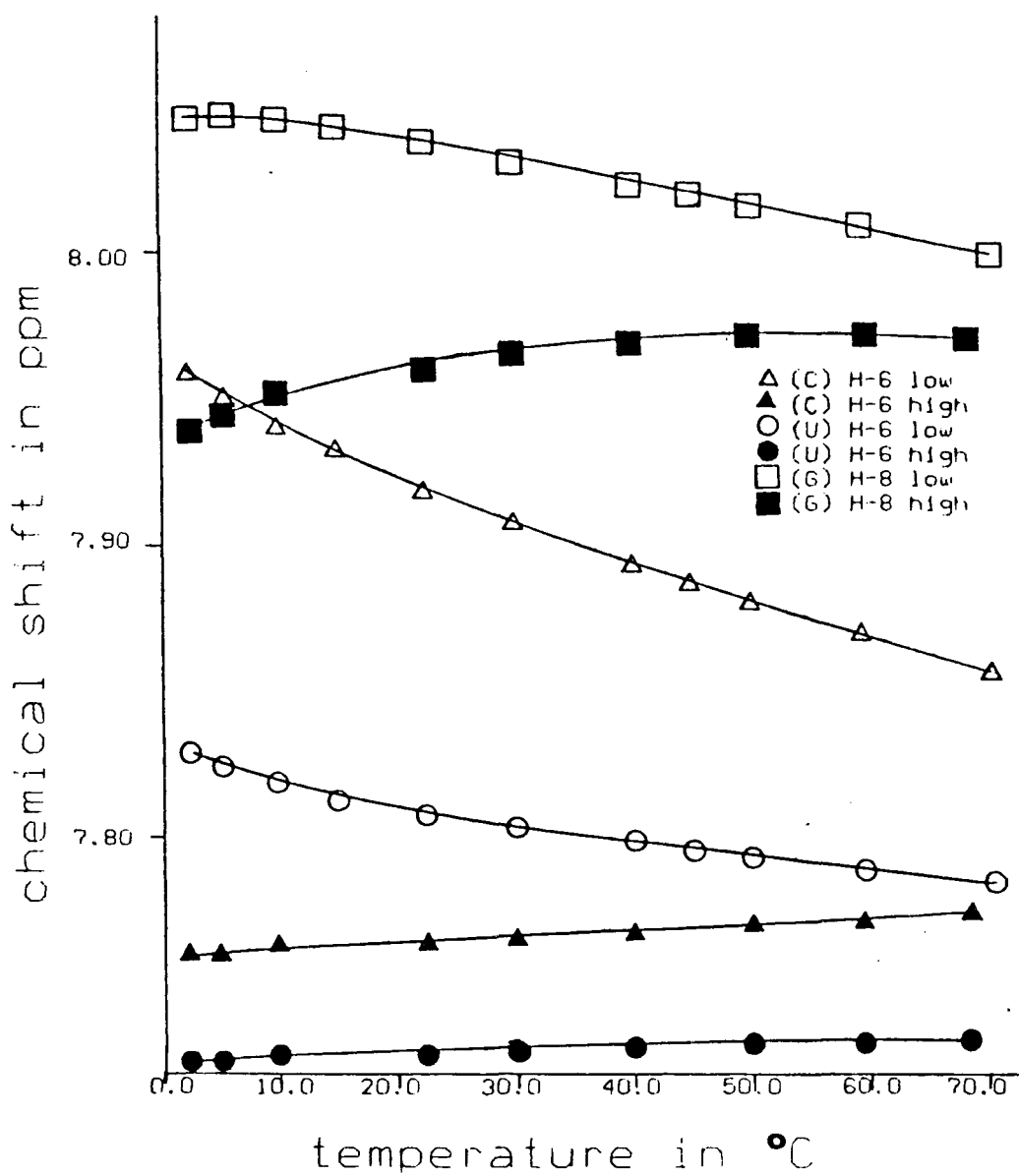


Fig. 33. Variable temperature plots comparing the H-8 and H-6 protons of CUG high and low.

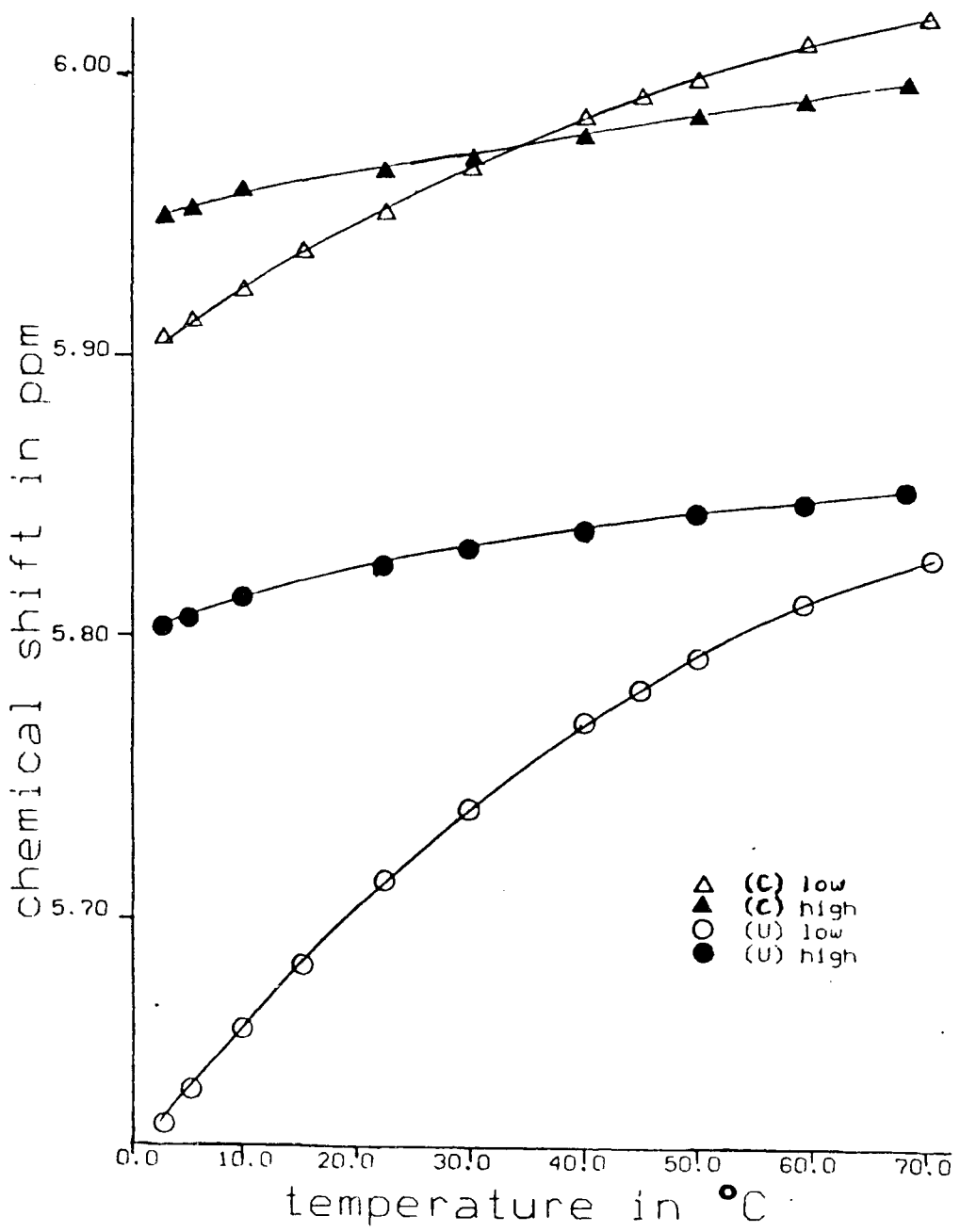


Fig. 34. Variable temperature plots comparing the H-5 protons of CUG high and low.

TABLE 12  
 AROMATIC AND H-1' CHEMICAL SHIFT  
 DIFFERENCES OVER TEMPERATURE  
 FOR CUG HIGH<sup>a</sup> AND LOW<sup>b</sup> IN ppm\*

PROTON	HIGH	LOW
G H-8	+0.0268	-0.0416
C H-5	+0.0462	+0.1116
U H-5	+0.0454	+0.1907
C H-6	+0.0150	-0.0939
U H-6	+0.0082	-0.0390
C H-1'	+0.0126	+0.1116
U H-1'	+0.0397	+0.0763
G H-1'	+0.0483	+0.0189

a no salt, 7.90 mM, 68.5 to 5.6°C.

b no salt, 5.89 mM, 70.4 to 5.6°C.

\* positive values indicate upfield shift  
 in going from high to low temperature.

stacking behaviour (Lee and Tinoco, 1980). With this in mind, note the greater ability of C to stack in the low isomer as indicated by the greater upfield shift of .112 ppm in comparison to .046 ppm in the high isomer (Table 12). The better stacking in the low isomer is further seen in the U H-5 protons which show an upfield shift of .191 ppm in comparison to the .045 ppm movement in the high compound. The shielding effect in the low isomer of U is roughly twice that seen in C, as would be expected, since it would feel magnetic anisotropy shielding effects from the base above and below it. Its weak presence in U H-5 in the high isomer suggests that base-stacking above and below it is not as appreciable.

This information, in view of the H-6/H-8 data, suggest that the low isomer is in a predominant  $\chi$  anti conformation. It is because of its anti conformation that downfield shifts in H-6 and H-8 are produced in the low isomer (overriding phosphate and ring oxygen effects). Also, base-stacking interactions appear in the anti form in A-RNA hence this form in the single helix should also be more favourable. The opposite shift for these protons does not necessitate that the high isomers' bases exist more in the syn form. This would explain the upfield shifts, but perhaps a better explanation involves the presence of the additional C4' - C5' bond in the CpU part. This would allow the phosphorus to be pushed out slightly more from the center of

base stacking, hence its magnetic anisotropic deshielding effect would not be as powerful. The upfield shift of the G H-8 proton may then be due to distortions in the UpG backbone carried down by the 5'-5' linkage. However, the G H-8 behaviour is probably due to it existing more in the  $\chi$  syn form. This is more plausible for G because the energy barrier between syn and anti is smallest for purines. Additionally, for the syn form to exist, the ribose must be in an 2' endo (S) conformation (de Leeuw et al., 1980). This conclusion has been reached on X-ray crystallographic studies of purine nucleosides which correlate the anti form with 3'-endo (N), while the 2' endo form is an almost equal mixture of syn and anti. For G the amount of 3'-endo is calculated to be nearly identical in both isomers at 44% (high) and 46% (low) (47.7°C). Hence the criteria and precedence for more syn character exists.

#### 4.7.3 Trimer H-1' Proton Regions

Figure 35 is a variable temperature plot of the H-1' protons of both isomers. H-1' is another good indicator of base-stacking (Lee and Tinoco, 1980). All protons move upfield with decreasing temperature, indicative of shielding trends associated with base-stacking. In the low isomer, the proton at the 5' end moves upfield the most, the terminal 3' G proton the least (Table 12) This is in contrast to the

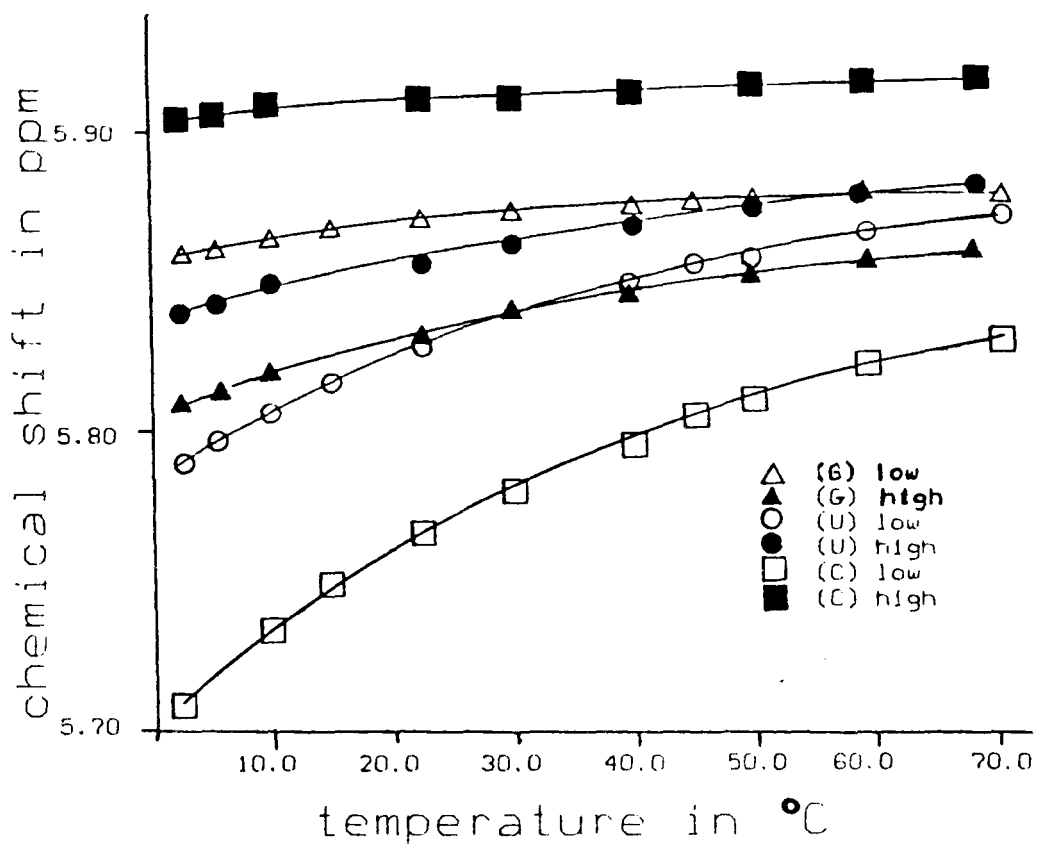


Fig. 35. Variable temperature plots comparing the anomeric H-1' protons of CUG high and low.

high isomer which displays an opposite behaviour. The result for the low isomer is unusual because generally the 5' base H-1' proton displays the least upfield shift when stacking occurs since it is situated right over top of the molecule. A substantial part of this upfield motion may therefore be due to changes in the glycosidic torsion angle  $\chi$ . A plot of  $3J(H1',H2')$  versus chemical shift (Figure 36) suggests a linear relationship until a value of about 2.3 Hz is reached. Because  $3J(H1',H2')$  is an indicator of the percent S character in the ribose, it appears that the chemical shift effect up to this point is  $\chi$  dependent. This is because more N character means more anti character (de Leeuw et al., 1980). However, more anti character should result in the keto group being placed closer to the H-1' proton. This would deshield it and produce an opposite effect. The contradiction is explicable when one considers that even at high temperatures C is predominately in the N form (approximately 60%). This would indicate that a change is occurring in the anti position itself, shifting slowly away from the proton. This continues down to 20°C, at 2.3 Hz, where more complicated behaviour takes place as suggested by the non-linear pattern past this point.

In terms of relative chemical shifts, the greatest difference is between C H-1's, where the high isomer is downfield of the low one. Obviously its chemical environment has been altered radically. It may be due to a larger

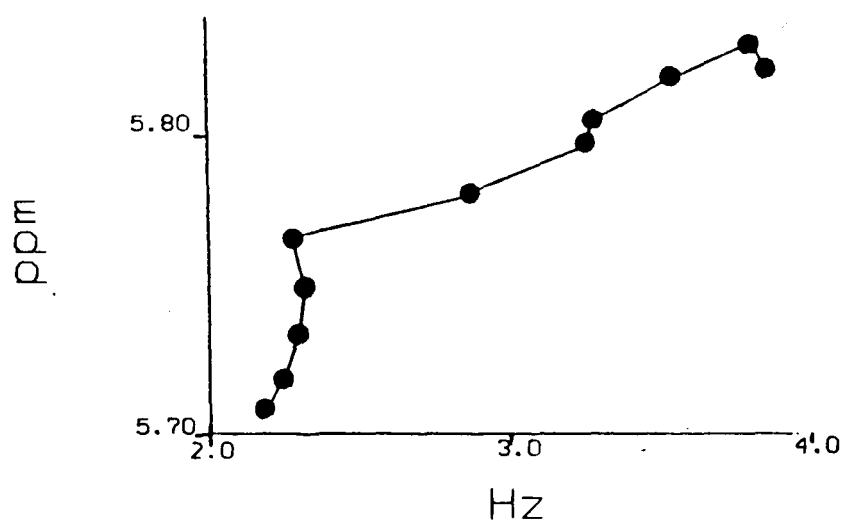


Fig. 36. Plot of the chemical shift of the C-H-1' proton of CUG low versus its  $3J(H1', H2')$  coupling constant.

interbase distance in the 5'-5' link resulting in less shielding from the lower base, a twisting of the ribose about the phosphodiester bond such that this proton is more outwardly exposed, or a combination of these two explanations.

Both U H-1's behave more similarly, with their chemical shifts being more identical at all temperatures than any of the other base H-1's. However the high isomer moves less upfield than the low one, possibly due to a weaker anisotropic influence from C.

The G H-1' in the low isomer is downfield of the high isomer. The difference is not nearly as dramatic as for C, but the presence of this effect indicates that the 5'-5' phosphodiester link one base removed is having an effect on the terminal base. Furthermore, this is the only H-1' proton, the chemical shift movement of which, is greater in the high isomer than in the low. This could be indicating that the UpG part in the high isomer is acting more on its own with regards to base-stacking. That is, in the low compound the CpU part preferably stacks first, but in the high isomer, it is the UpG portion where the bases are interacting first.

#### 4.7.4.1 Dimer Behaviour

At this point it would be appropriate to study the

information obtained on the dimers and determine if trends seen here extend into the trimers. Variable temperature plots are produced in Figures 37, 38, and 39 between 30 and 70°C. While these do not go to as low a temperature as the trimers, they are indicative of trends. The unfortunate aspect of these comparisons is that the CpU was in salt (1 M) while the cyclic dimers were not. This should not effect the shape of the curves however, but perhaps only alter their position (Cantor and Schimmel, 1980). This is because salt increases the  $T_m$  of base-stacking or duplexation. Such behaviour is a result of the salt making hydrophobic interactions more favourable at low salt concentrations. This appears to have resulted in upfield movement of all the chemical shifts of the base and H-1' protons of the CUG trimers except for G H-1', whose curve moved downfield in salt. Figure 40 compares some protons to give an idea of the trends. Also, because duplex formation is not occurring in any of these molecules, especially in this temperature range, the salt/no salt difference is made less important. This is because the hydrophobic region in a base stacking oligoribonucleotide will not be as large as the region that would exist in a double helix.

All the dimer spectra were obtained at a pD of about 7.0. It was later discovered that the phosphate groups of trimers only contain one negative charge at this pD but monomers and dimers are similarly charged at a pD of 5.5

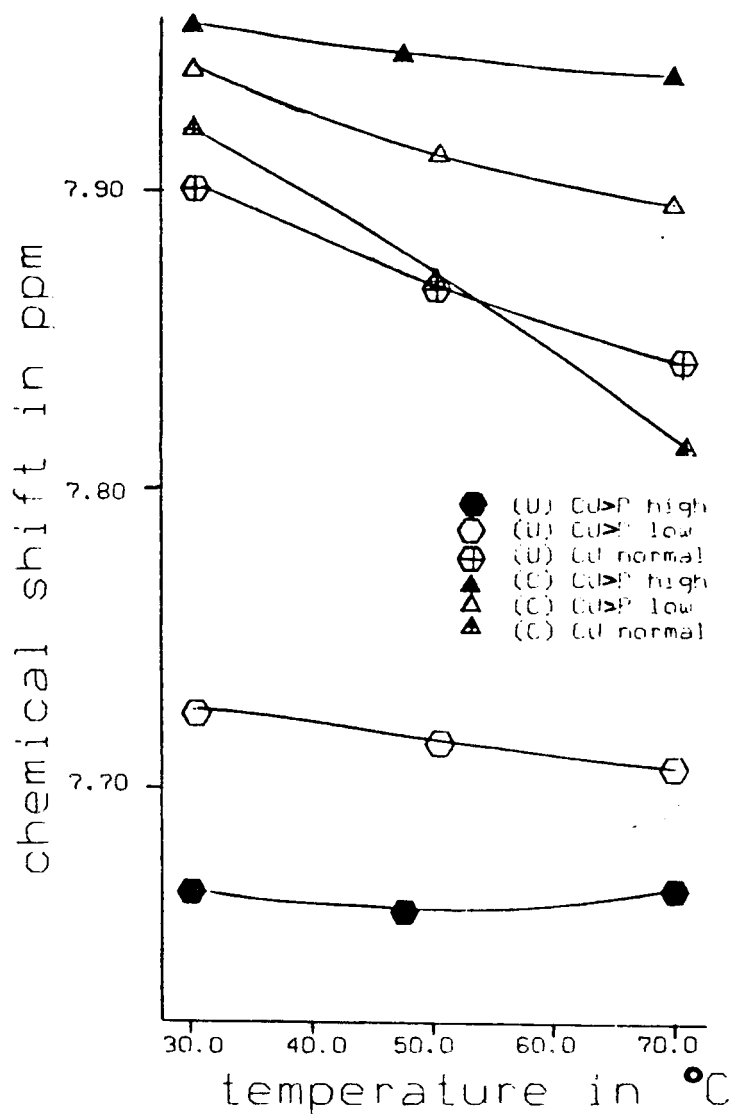


Fig. 37. Variable temperature plots comparing the H-6 protons of CU>P high, CU>P low and CpU (3'-5').

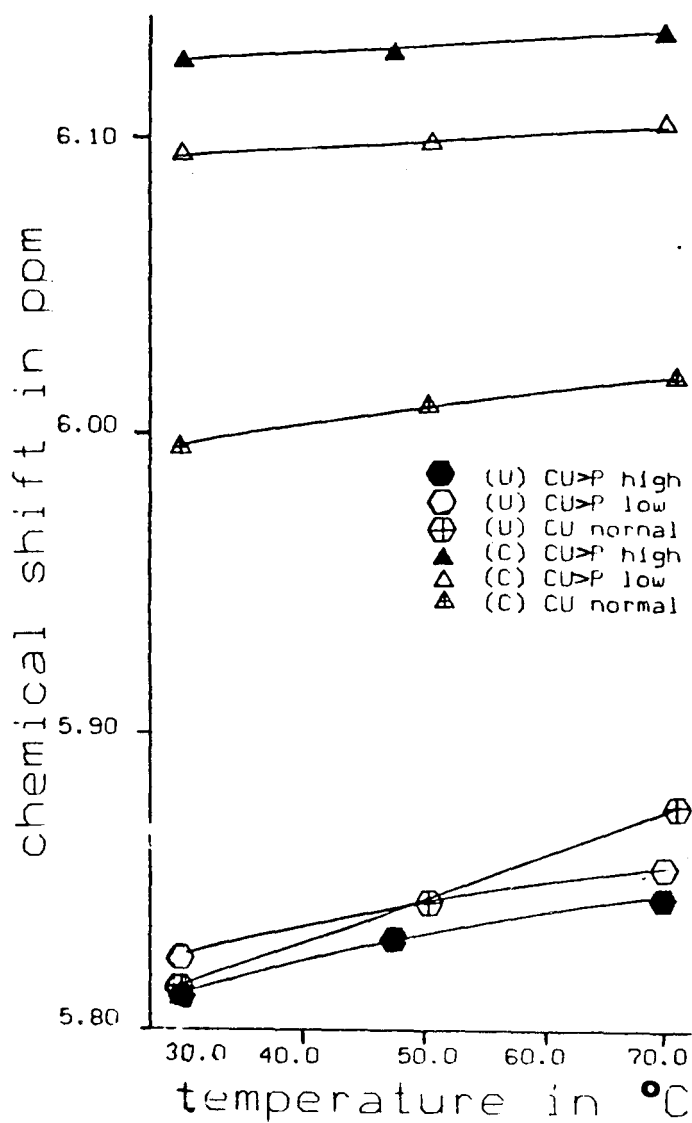


Fig. 38. Variable temperature plots comparing the H-5 protons of CU>P high, CU>P low and CpU (3'-5').

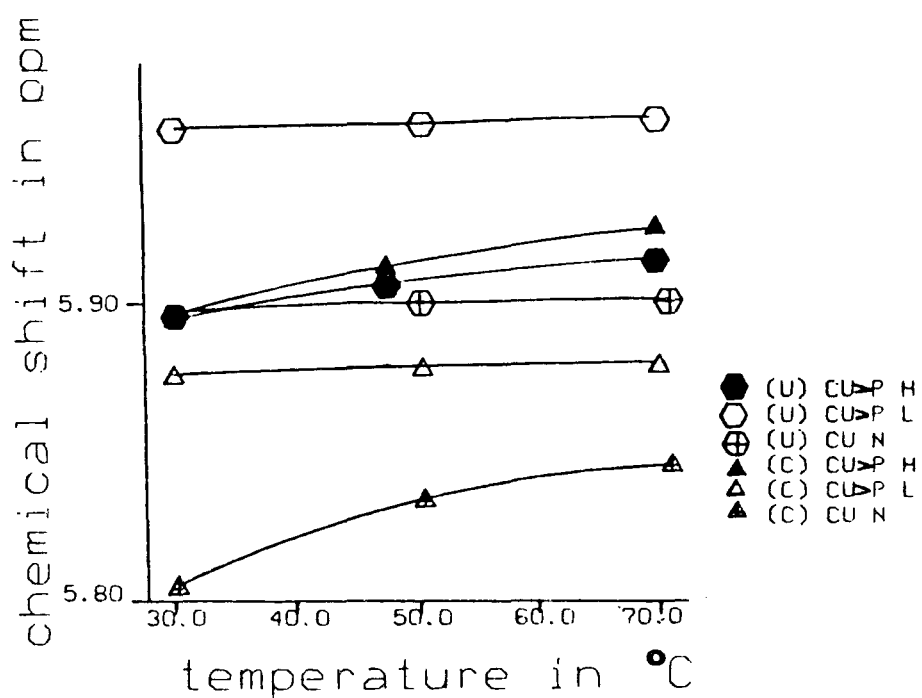


Fig. 39. Variable temperature plots comparing the H-1' protons of CU>P high, CU>P low, and CpU (3'-5').

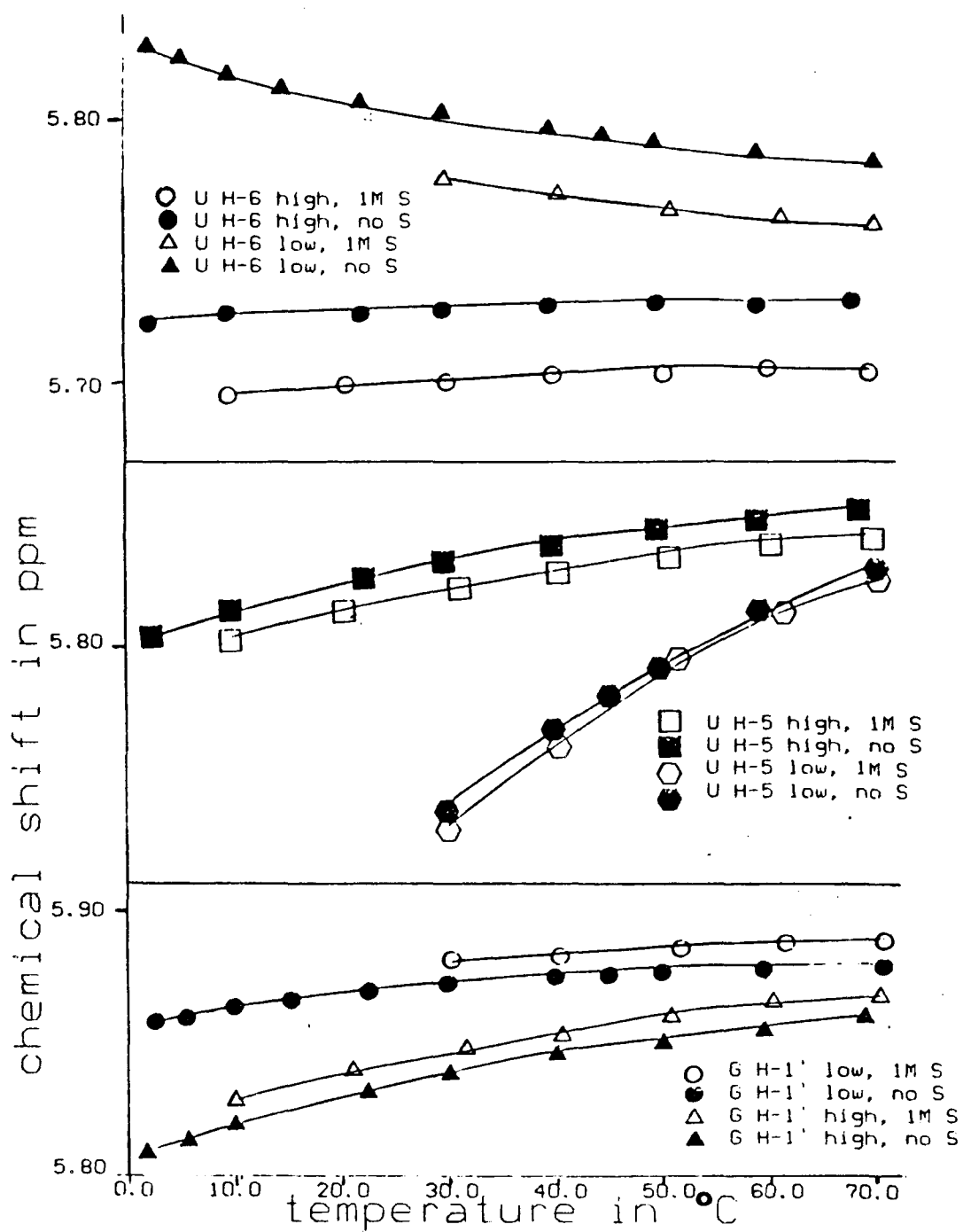


Fig. 40.

Variable temperature plots comparing the effect of salt on selective protons of CUG high and low.

(Cheng et al., 1980). Therefore these dimers have less of a charge upon their phosphodiester backbone than the trimers and this could effect the behaviour of these molecules. However, all the dimers are similarly charged, therefore the comparison of trends between them is still viable. It is when comparing these trends to the trimers that care will have to be taken because the results will not be quantitative and differences seen may be under or over expressed.

#### 4.7.4.2 Aromatic Region

The chemical shifts of all the H-6 protons move downfield with decreasing temperature (Figure 37). In the trimers, the high isomer was the exception, moving upfield. This difference is likely due to the 2'-3' cyclic phosphate on the U ribose which probably contributes additional magnetic anisotropic deshielding effects to these protons since it is closer to the two bases.

The downfield trends in this temperature range are only marginal for CU>P high. By contrast the CU>P low isomer moves downfield more significantly, while the normal dimer moves yet more drastically. The order of downfield movement in the dimers is consistent with the trimers; CU normal > CU>P low > CU>P high, compared to CUG low > CUG high.

Both U H-6 protons move marginally with temperature. This is consistent with effects seen by others in cyclic

monomers (Gerald and Williams, 1978). This was interpreted via lanthanide ion probes to mean that the base was in a syn position. That the U H-6s are upfield markedly from the normal dimer is additional proof for this occurrence. In the syn position the H-6 will be away from the center of the ribose ring, not feeling the effects of oxygen and phosphorus deshielding. This contrasts to the C H-6s in both CU>P dimers, where the resonances are downfield of those of the normal dimer at high temperature. Such an effect must be a result of this proton being influenced by the cyclic phosphate group on the adjacent ribose.

The H-5 protons of the dimers all show upfield chemical shifts with decreasing temperature as the trimers did. Of these, the Cs' movements are the smallest, probably due to the poor ring current effects of U (Geissner-Prettre, et al., 1976, Everett et al., 1980).

The U H-5 protons all have similar chemical shifts while the C H-5 protons are more variable. This suggests that the cyclic C H-5s are feeling the effect of the cyclic phosphate more so than the U H-5s. This is because they can swing over top this group while the U H-5s are locked away from it by the glycosidic bond holding it in the syn position.

#### 4.7.4.3 H-1' Region

Figure 39 compares the H-1' chemical shifts of all three dimers with temperature. All move upfield with decreasing temperature, but some do so more distinctively than others. It is this feature that offers significant insights about the nature of the 5'-5' dimer.

In the normal isomer only the C H-1' proton moves decisively upfield, the U H-1' moves marginally. This is odd because the 5' nucleotide usually is shifted upfield the least during stacking. However this is the same trend as seen in the similarly linked CUG trimer, hence the same events, related to the glycosidic torsion angle, might be occurring.

With regards to the CU>P low dimer, neither H-1' moves significantly. Since the U in the normal CpU did not move much, similar behaviour might be expected here. The absence of movement in the C H-1' then must be due to the cyclic 2'-3' phosphate. Its effect could be due to deshielding or induced changes in the manner of stacking which result in H-1' not moving upfield much. It could also mean that stacking in the cyclic dimer is inhibited by the cyclic phosphate.

In the CU>P high dimer both H-1's move upfield. Their chemical shifts are nearly identical and they coalesce at 30.0°C. This slight chemical shift difference is only observable at 500 MHz. Such behaviour is nearly identical to that seen by Kondo et al. (1970) with their 5'-5' linked ApA.

This observation was interpreted to mean that both H-1's were orientated towards each other, in between the bases. In the ApA molecule a two fold axis of symmetry involving a plane parallel to both bases and bisecting the phosphorus was suggested. Such a molecule would have to be right-handed because a left handed molecule would have flipped the protons away from the center and not have produced the shielding trend with decreasing temperature. In the CU>P 5'-5' dimer a true C<sub>2v</sub> symmetry group does not exist, as indicated by marginally different chemical shifts for both H-1' protons. This would be expected since different bases are involved plus one ribose possesses a cyclic phosphate.

Base/base stacking may not be as inhibited in this 5'-5' molecule as it may be in the CU>P low dimer by the cyclic phosphate group because another C4'-C5' bond exists that allows the phosphates to assume a lower energy position where they would avoid each other.

The important feature is the manner in which the C/U ribose rings appear to orient themselves in the 5'-5' CU>P dimer. This can be used as a starting point to describe the CpU part in the CUG high molecule. The different behaviour that occurs will be due to perturbations caused by having a G attached to the 3' end of U instead of a cyclic phosphate.

#### 4.8.1 The Phosphodiester Backbone

TABLE 13

CUG HIGH<sup>a</sup> AND LOW<sup>b</sup> TORSION ANGLE COMPARISON AT 47.7°C

ANGLE	C	U	G
N (HIGH) <sup>c</sup>	65%	41%	44%
N (LOW) <sup>c</sup>	65%	46%	46%
$\gamma_{+sc}$ (HIGH) <sup>d</sup>	78%(15/08)	71%(09/20)	60%(27/12)
$\gamma_{+sc}$ (LOW) <sup>d</sup>	69%(20/11)	59%(29/12)	74%(16/10)
$\beta_{ap}$ (HIGH) <sup>e</sup>	74%	73%	60%
$\beta_{ap}$ (LOW) <sup>e</sup>	-	74%	77%
$\epsilon_{ap}$ (HIGH) <sup>f, h</sup>	-	63%	-
$\epsilon_{ap}$ (LOW) <sup>f, g</sup>	53%	62%	-

a no salt, 7.90 mM.

b no salt, 3.31 mM.

c Equation 3.

d Equations 8 - 10, (ap/-sc).

e Equations 14, at 22 C.

f Equation 22.

g assuming  $(3J(C2',P3') + 3J(C4',P3'))$  same as for C, at 22°C.

h at 55°C.

While all the ribose protons in both trimers were not fully assigned, all the H-5'/H-5" protons were, plus most of the 2' and 3' protons. This information can be used with the coupling constants obtained from both proton and C-13 spectra to obtain more detailed insights into the behaviour of these two molecules. This involves the use of "Karplus styled" empirical equations described in the Introduction. These results are given in Table 13. It should be noted that only a first order approximation of the coupling constants were used in such calculations. This is because the equations used are empirical and the use of more refined second order values in only first order equations would not make the results obtained sufficiently more precise. Furthermore, the equations most often used narrow the number of conformations that can exist over a 360° range into a few preferred conformations. The basis for these simplifications is well supported, but these approximations introduce an uncertainty to the results. More precise equations exist to determine better values for the average torsion angle, but they still are empirical and they still are an average. Hence no second order values for coupling constants were obtained and the values used were an average of all the first order values extracted from the spectra.

From these empirical calculations upon the two isomers at approximately 50°C, a number of interesting features appear. Firstly, the O5'-C5'  $\beta$  torsion angle in

both isomers is almost identical at 73 - 77% ap in all cases. This is in agreement with the "rigid" nucleotide concept (Sundaralingam, 1973) and is true even for the 5'-5' linkage. This is an important observation when taken into account of the  $\gamma$  population (C5'-C4').

All nucleotides show a  $\gamma_{+sc}$  preference, in accord with the "rigid" nucleotide concept (Sundaralingam, 1973). However, the behaviour of both isomers is different. In the high isomer the 5'-5' linked nucleotides C and U are both over 70% populated in this conformation, with C > U. G is least populated at 60%. In the low molecule the population distributions are all greater than 59%, but now the order is G > C > U. The striking feature is that the CpU 5'-5' linked dimer unit appears to prefer this orientation more so than the 3'-5' linked counterpart. The preference for this C5'-C4' orientation dictates a zig-zag phosphodiester backbone when viewed with the  $\beta_{ap}$  population preference. Such a feature makes base/base overlap less favourable because this would straighten the internucleotide backbone, increasing the distance between the two bases. This would explain the poorer base stacking abilities of the CpU part in the high isomer as suggested by the U and C H-5 and H-1' protons and the phosphorus data. So, even though an additional bond exists in the 5'-5' linked dimer, the molecule still settles into a preferred position, not randomly flipping about, in line with the "rigid" nucleotide

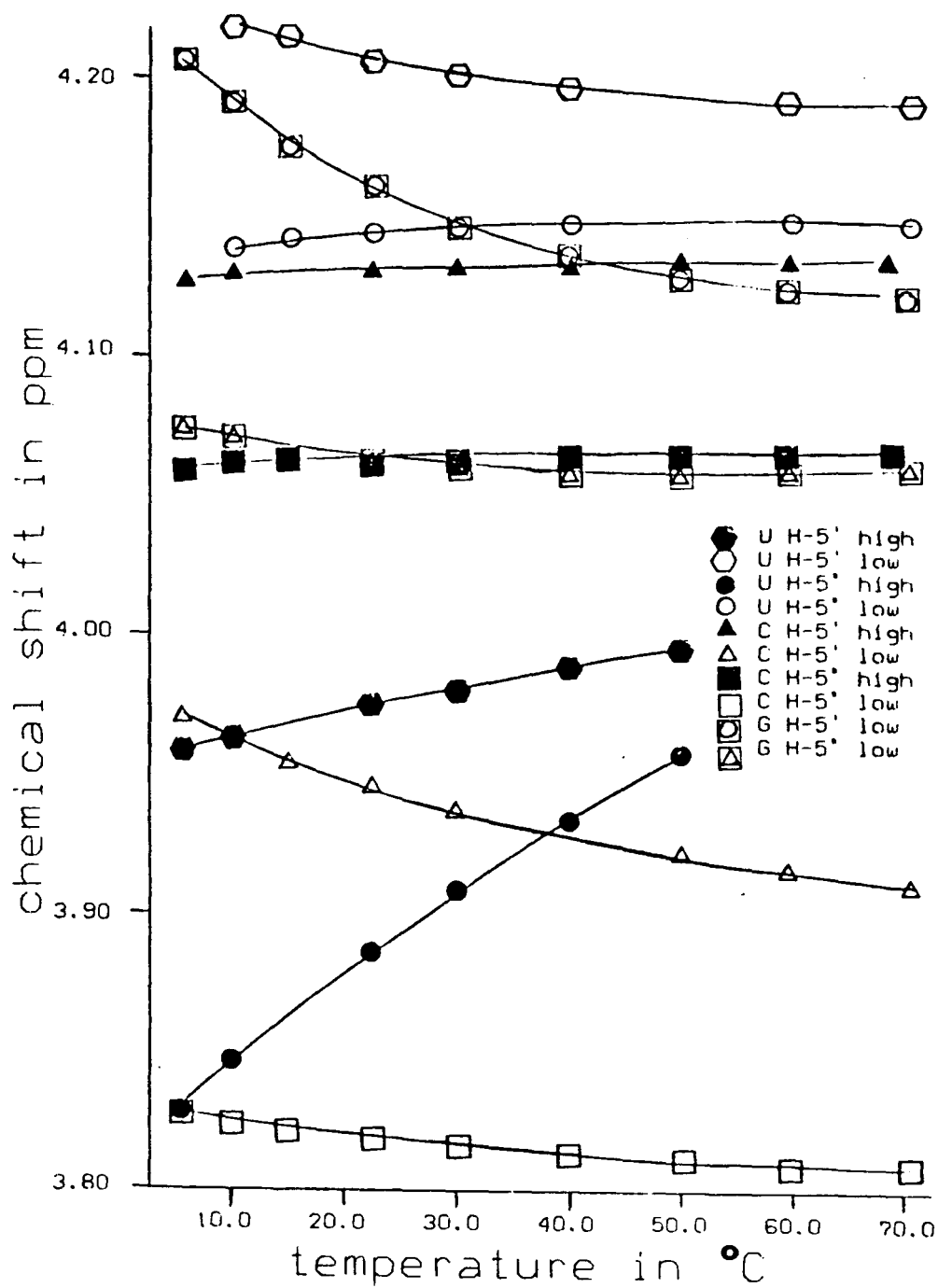


Fig. 41. Variable temperature plots comparing the H-5'/H-5" protons of CUG high and low.

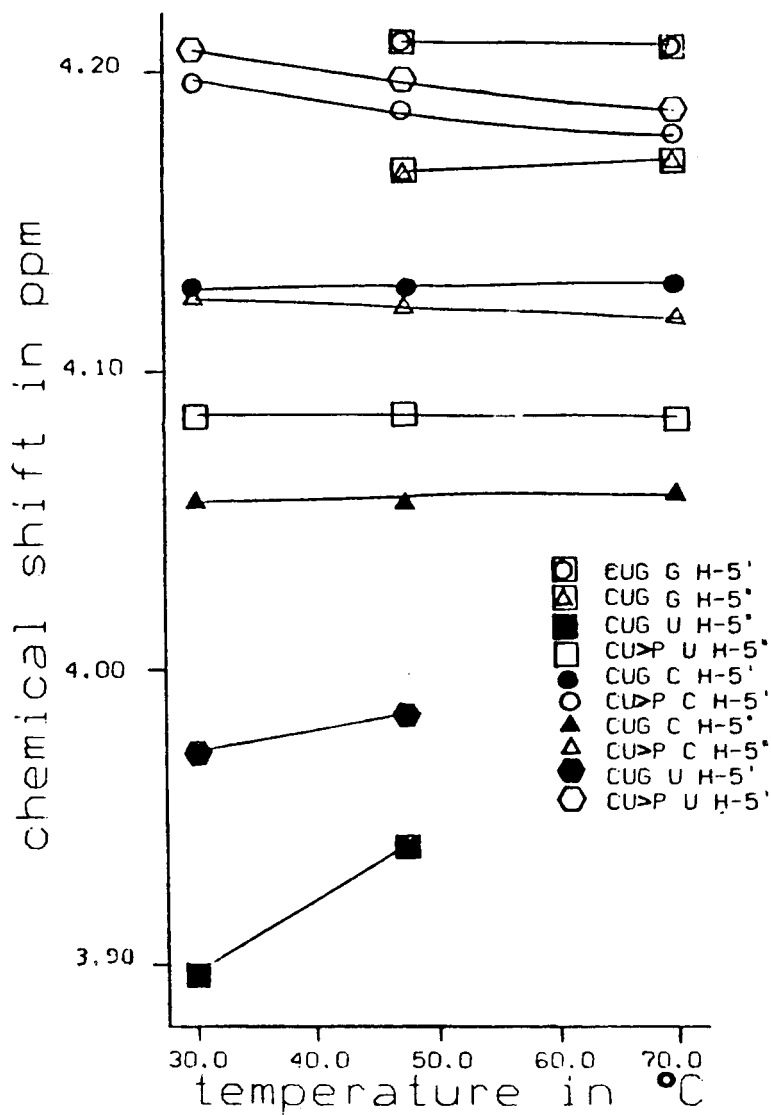


Fig. 42. Variable temperature plots comparing the H-5'/H-5\* protons of CUG high (3.31 mM) and CU>P high (3.90 mM).

concept.

Another observation of these calculations is that the 5'-5' link does not alter the orientation of the 3'-5' link in the UpG portion significantly. This is seen in the  $\epsilon_{ap}$  population about C3'-O3' where both isomers are almost equally populated (63% to 62%). This is in agreement with the phosphorus data which suggests that both phosphorus atoms behave similarly in the two isomers. Effects upon the G base and H-1' protons are therefore due to an altered orientation of the base U above it or a difference in G's position relative to the ribose.

With this information, the H-5'/H-5" chemical shift versus temperature graphs may be interpreted. These are produced in Figures 41 and 42. As discussed in the Introduction, information on  $\alpha$  and  $\zeta$  can only be inferred from trends present in these plots. The information obtained will indicate whether a right or left handed helix is being formed. For a right handed helix H-5' is shifted downfield with decreasing temperature as it is brought nearer the 2' hydroxyl group (Ezra et al., 1977, Lee et al., 1976). In the low isomer such a trend is observed for each set of H-5'/H-5" protons. H-5" moves little over the 70 to 5°C range. In C and G it moves marginally upfield while in U the movement is slightly downfield. By comparison all the H-5' protons move markedly downfield, consistent with the right handed helical model that would confine  $\alpha$  and  $\zeta$  into the -sc and -ap range.

The high isomer behaves quite differently. First, neither C H-5'/H-5" protons move much over the same temperature range. This would suggest nothing is happening to alter the H-5'/H-5" orientation with regards to the rest of the molecule. This is consistent with model studies with the available torsion angles that show these protons projecting out towards the solvent. Even if some base stacking were to occur, they still would not be ushered into a deshielding or shielding zone.

The U H-5'/H-5" in CUG high behave more radically, they move upfield with decreasing temperature. Additionally, at 70°C, both of the protons have nearly the same chemical shifts and appear as one broad signal with only a few coupling constants distinguishable (not extrapolated on Figure 41). In the CU>P high dimer such similar behaviour was not seen with the G removed. Its absence resulted in a typical ABMX system over the same temperature range. As well, the H-5'/H-5" protons of the dimer behave like a typical right handed helix, as Figure 42 illustrates. Both H-5's move downfield to a greater extent than H-5"s with decreasing temperature. This reveals an important feature of the CpU 5'-5" unit when bound to G. That is, the same type of pseudo-symmetrical right handed helix proposed for the CU>P dimer cannot exist in the dimer unit of CUG high. Instead of the C ribose being tilted towards the U such that the H-1' is towards the inside of the stack, it is orientated

with the H-1' shifted away from the stack as Figure 43 illustrates. Adding a G to the 3' end of the dimer unit results in the U C-5' position changing sufficiently to equalize the chemical shifts of both H-5'/H-5" protons at high temperatures. As temperature is decreased, sharp upfield movement occurs, reflecting a preference for  $\gamma_{+sc}$  because this would place these protons furthest away from the deshielding effects of the ribose ring oxygen and the phosphorus bonded oxygens. This is in accord with the 71% population of this state calculated at 47.7°C. The H-5" moves downfield more as well, in agreement with this proton being further away from the ribose in the  $\gamma_{+sc}$  position.

This ribose orientation would help explain the small upfield shift of CUG high's C H-1' with temperature compared to the large shift seen in the CUG low counterpart because the proton is directed away from the center of base-stacking.

It was unfortunately not possible to compare the chemical shifts of both G H-5'/H-5" protons of the two CUG isomers because at 250 MHz the outer quartets were not visible in the high isomer. However, from 500 MHz spectra, plotted in Figure 42, a weak trend appears to be emerging. The H-5' proton drifts marginally upfield while the H-5" is seen to move slightly downfield. This would be consistent with the effect seen in a right handed helix for CUG low and expected from the phosphorus data which suggests the UpG part

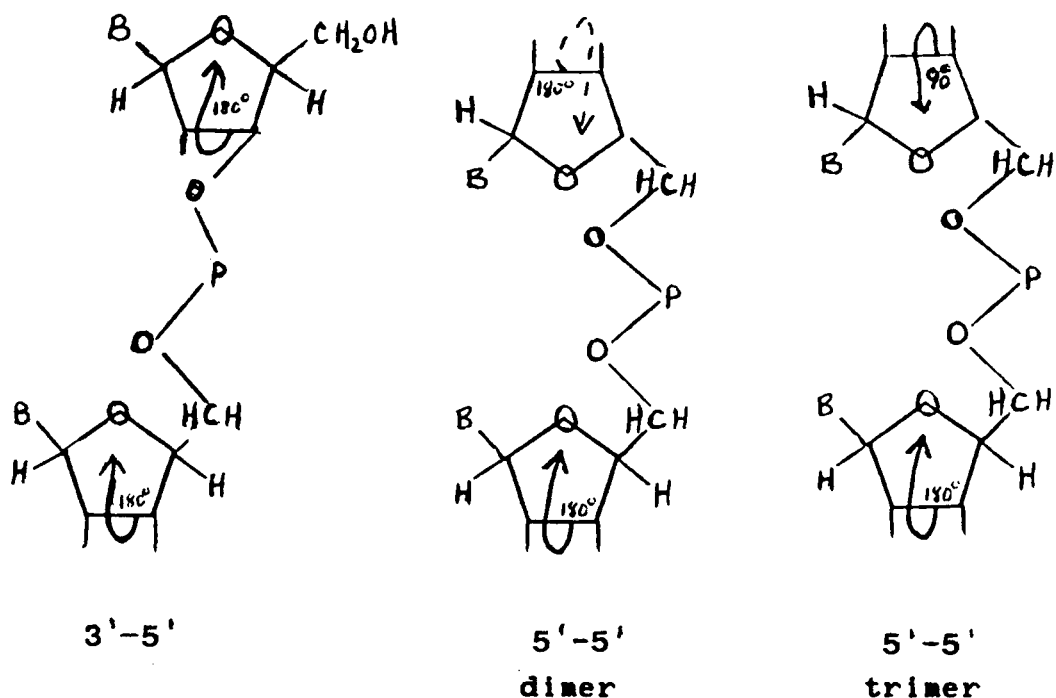


Fig. 43.

Comparison of the orientation of the ribose rings in three different situations. The first is a 3'-5' phosphodiester bond typical of those in CUG low and the CpU dimer. The second involves the 5'-5' phosphodiester bond in the CpU>P dimer. The third is the 5'-5' phosphodiester bond in the CUG high trimer. The bond at the origin of the arrow is to be rotated towards the ring oxygen by the indicated number of degrees. Dashed lines indicate rotation behind the plane of the paper, solid lines in front.

behaves similarly in both isomers.

One additional feature to note is the long range four bond coupling between phosphorus and H-2'. It is possible to observe this when the phosphodiester backbone assumes a "W" type conformation with the 3' ribose in the S pucker. In the ideal case a coupling of 2.7 Hz is expected (Sarma et al., 1973b). In both isomers a coupling of approximately 1 Hz was seen at 50°C. Considering that there is only a slight N preference for both Us at this temperature, such a decreased coupling would be expected. The near identical coupling seen in both isomers is additional proof, consistent with phosphorus and proton NMR data, that suggest the phosphorus is in very similar chemical environments in both molecules.

#### 4.9.1 The N/S Equilibrium

As described in the Introduction, right handed A-RNA adopts the 3' endo (N) conformation when duplexing and/or base-stacking (Lee and Tinoco, 1980). Figure 44 is a plot of the  $3J(H1',H2')$  coupling constants versus temperature for both CUG isomers. Because small values of this coupling constant are associated with less S character, such a plot is a reflection of the shift in the N/S equilibrium. From Figure 44 it is apparent that the low isomer stacks from the 5' end, with both C and U taking on more N character. In contrast, G shows little change suggesting it is doing the

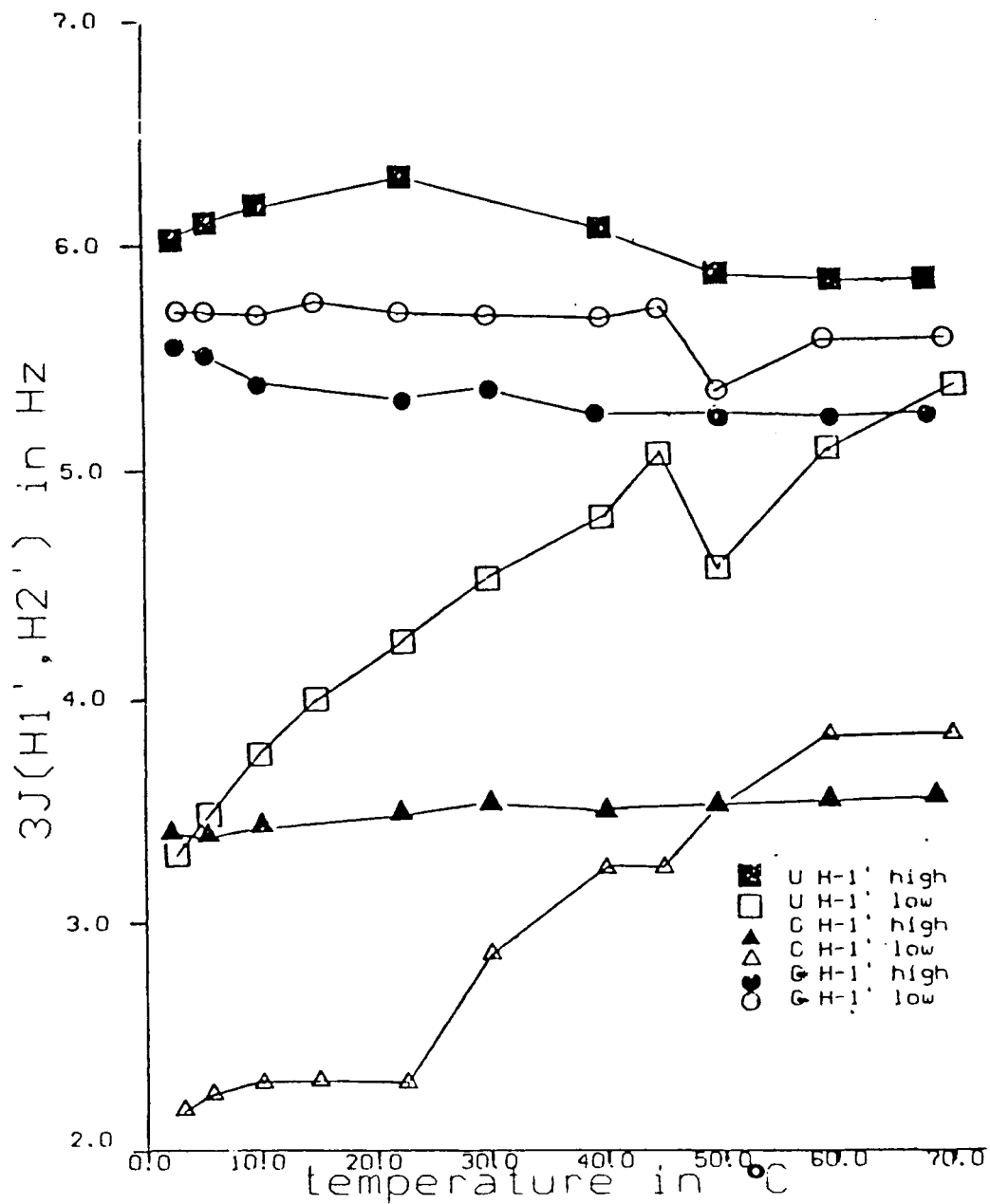


Fig. 44. Variable temperature plots of the  $3J(H1', H2')$  coupling constants of CUG high and low.

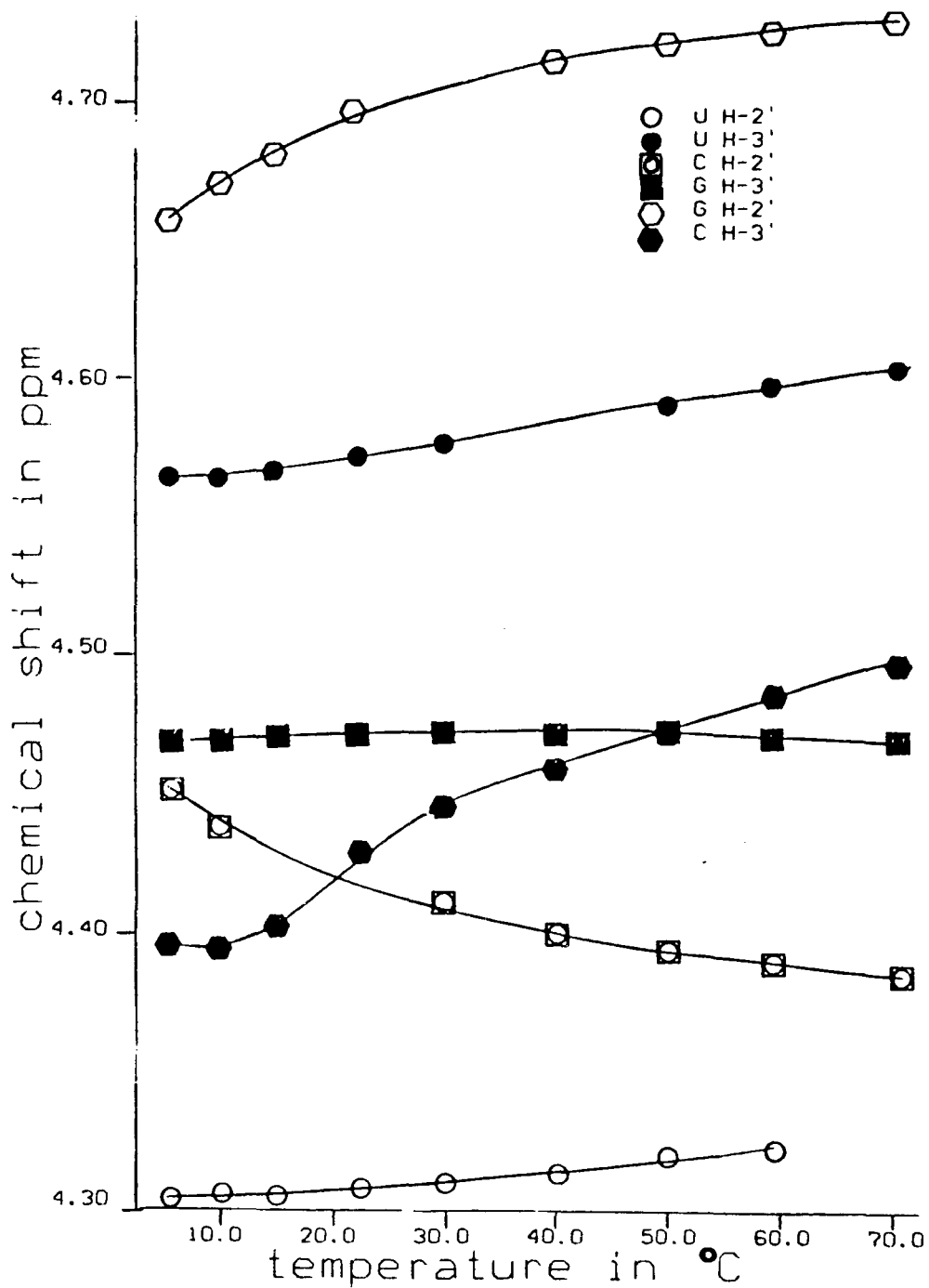


Fig. 45. Variable temperature plots of the H-2' and H-3' protons of CUG low.

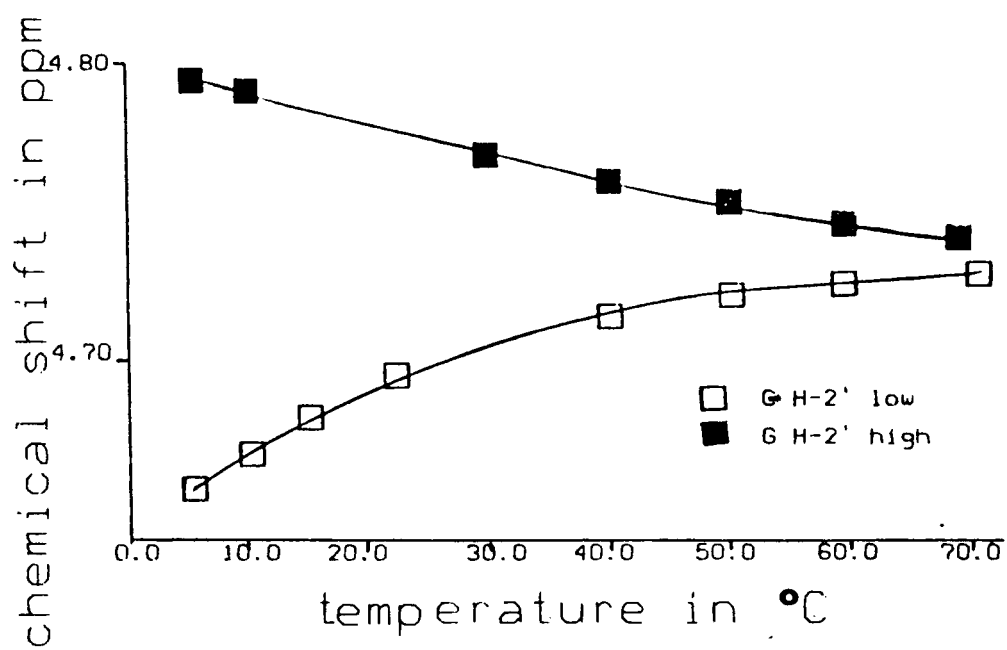


Fig. 46. Variable temperature plots comparing the G H-2' protons of CUG high and low.

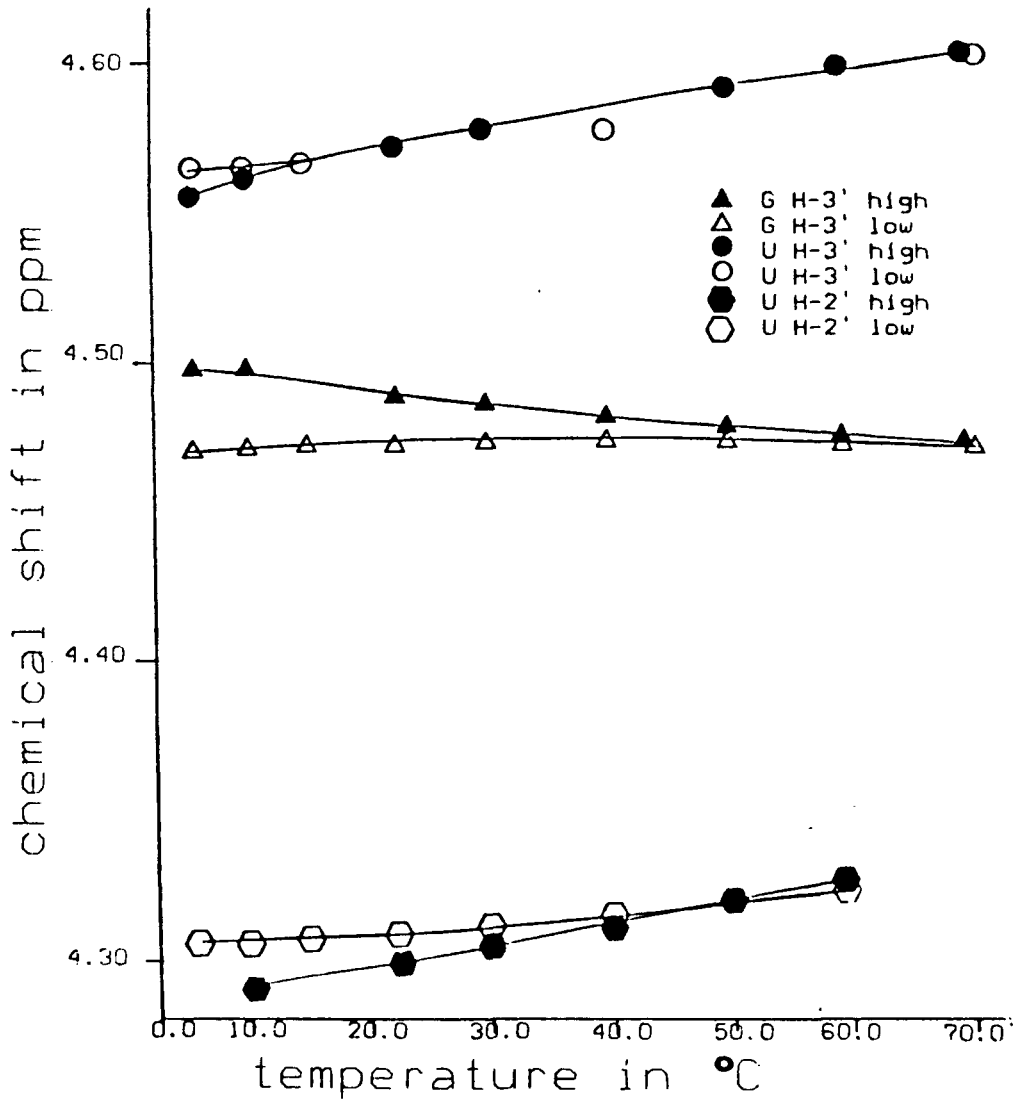


Fig. 47.

Variable temperature plots comparing the H-2' protons of U and the H-3' protons of U and G in CUG high and low.

least amount of stacking or that the 3' endo conformation is not as critical for base-stacking to occur. It is interesting to note that this same trend is seen for UUG by Lee and Tinoco (1980). This would be expected since both sequences are pyrimidine-pyrimidine-purine.

Variable temperature plots of H-2' and H-3' are reproduced in Figure 45 for CUG low. These data are the most difficult to assess because the ribose ring pucker, base stacking, and the position of the phosphodiester backbone all contribute to the chemical shifts of these protons (Lee et al., 1976). One feature to note is that all the protons, except C H-2', move upfield, or show no change, to various degrees with decreasing temperature. Only a comparison of the CUG high and low isomers will therefore be described because it illustrates an important point.

Variable temperature plots of the H-2' and H-3' protons are compared in Figures 46 and 47. Unfortunately the C H-2' and H-3' protons of CUG high were not obtainable because they possessed near identical chemical shifts. This in itself is a forceful indicator that the chemical environment of these protons differ markedly in both isomers. The chemical shifts of these high isomer C H-2' and H-3' protons were upfield of those in the low isomer indicating less deshielding interference from the phosphodiester backbone or any other such group because these protons are directed more towards the solvent in this model.

This contrasts to the sandwich type position of these protons in the low isomer which would allow for their deshielding.

For the protons of U and G, the striking feature is that both plots are nearly identical in both isomers for U. The H-3' proton of G also behaved similarly in both molecules. The only major difference lay in the G H-2' proton. Such a similar behaviour would be expected if the UpG part mimicked each other in both isomers, as the H-5'/H-5" and phosphorus data suggests. Differences were seen in their base and H-1' protons however. This would indicate that while the phosphodiester backbone may be similar, the base-stacking is different. In the high isomer stacking appears less prominent overall with no real base pucker changes with temperature (Figure 44). Hence the chemical shift differences over temperature for G H-2' must be due to a different  $\chi$  torsion angle in the two isomers. In earlier parts of the Discussion the H-8 upfield shift was explained as possibly being due to a shift towards more syn character. In this position the bulk of the purine will be over top the ribose, particularly the H-2'. In such a position the plane of the base is in the plane of H-2'. This would have a deshielding effect on this proton. As a result the evidence for a predominant syn orientation of the G base in the high isomer is given more support. It would also explain the observation in the exchangeable proton data which

indicated the amino protons of the high isomer were more upfield of those seen in the low isomer. In the syn position, the amino group of G would be in a better position to feel base/base-stacking shielding effects. It would also be consistent with the  $3J(H1',H2')$  plot (Figure 44) which indicates that G in the high isomer is the only nucleotide to show a shift towards the S equilibrium with decreasing temperature.

It should be stressed that neither isomer exists in a 100% stacked form at any one time as is evident by the lack of a sigmoidal variable temperature plot of any of the H-1' or H-5 protons. However, some stacking is occurring with the low isomer doing this more readily than the high isomer. Furthermore, the position of the C base in the high isomer appears to be such that it is not involved in much stacking interactions. This allows the UpG part to preferably stack over CpU. This in itself would necessitate a different type of stacking between U and G, for the C is not playing a significant role. This is further credence for different UpG stacking behaviour in the two isomers.

### 5.1.1. CONCLUSIONS

Through the use of proton, phosphorus and carbon NMR it has been possible to follow the behaviour of short ribo-oligonucleotides in solution. The position of chemical shifts, their change with temperature, and their coupling to other nuclei all revealed information concerning the micro-environment of the effected atom. The manner by which these nuclei relaxed was harnessed with COSY, RCT, decoupling, and NOE experiments to obtain proton connectivity through bonds and space. The ability to show that two nuclei are related by any of these methods allowed for the assignment of resonances to a particular atomic site in the molecule. From here it was possible to use "Karplus-styled" equations and variable temperature chemical shift plots to obtain insights into the relative position of these nuclei in relation to each other.

The first major result of these efforts was the characterization of the CUG high isomer. Through the use of HPLC it was possible to separate this species from a mixture containing the desired product (5'C3'-5'U3'-5'G3'). Using NMR as an analytical tool it was possible to determine that this side-product was 3'C5'-5'U3'-5'G3'. This primary structure was further verified through the use of endo- and

exo-nuclease which revealed the high isomer was resistant to spleen phosphodiesterase. However, it was susceptible to snake venom phosphodiesterase and Phy M which suggested that the terminal 5'-5' phosphodiester bond does not play a critical role in the active site of these two enzymes. Kinetic studies would be required to determine if such a bond effected the rate of these reactions.

Carbon-13 NMR studies on oligoribonucleotides are still in their early stages. The spectra and the nearly complete assignment of the two CUG isomers represented an addition to the short list. These assignments were based largely on the effect a 5'-5' link had on the carbon chemical shifts. It may be advantageous to specifically synthesise molecules with a 5'-5' phosphodiester bond to aid in the assignment of carbon-13 spectra of 3'-5' linked nucleotides. This would be particularly useful in larger sequences because of the narrow spectral range of most of the C3' and C5' carbons.

The use of selective CW proton decoupling to assign the phosphorus signals of CUG low represented the first time, as far as it is known, that these signals have been unambiguously assigned. These assignments will enable a more detailed study, and possibly confirmation, of the effect of frame shift mutagens, such as acridine and ethidium, upon short RNA minihelices. In particular, Lee and Tinoco Jr. (1978) have suggested that CUG forms duplexes with itself,

with the U bulged out, upon the addition of ethidium. Phosphorus NMR following the titration of CUG with ethidium and other drugs will allow for a analysis of this behaviour and evidence for its occurrence.

The phosphorus resonance of the 5'-5' phosphodiester in CUG high was observed to exist radically downfield of the corresponding 3'-5' linked signal in the low isomer. It is possible that specific synthesis involving a 5'-5' phosphodiester bond may be used for assignment purposes because it may be more economical than oxygen isotopes and more feasible when complete proton assignment is unavailable.

Biologically, as far as it is known, single 5'-5' phosphodiester bonds do not exist in vivo. However, such bonds exist with three or more phosphorus atoms in between the linkage. The most widespread occurrence is their presence upon the 5' end of most eucaryote mRNAs in the form of 7-methylguanosine triphosphate. Its function is not certain, but data suggests that it may be involved in ribosome binding of the mRNA and/or protection of the mRNA from enzymatic destruction (Shatkin, 1976). Its other presence is in the form of diadenine tetra and pentaphosphates. These dimers appear to act as positive growth signals, binding to the  $\epsilon$  unit of DNA polymerase (Arter and Schmidt, 1976). Analysis of the effect of a single 5'-5' phosphodiester bond in a trimer sequence may therefore help explain its biological non-function.

In the CpU dimers studied, it was observed that the 5'-5' linked molecule, with a cyclic unit upon the U, behaved like a right handed pseudo-symmetrical helix and showed signs of stacking. The 3'-5' linked counterpart behaved more like an A-RNA helix. Neither of the dimers with a cyclic phosphate upon the U stacked as well as 3'-5' CpU without such a group. The data agreed with Gerald's and Williams' (1978) conclusion that 2'/3' cyclic U, in monomers, had the base in the syn position, because it appeared to exist as such in the dimers.

In the trimers, a 5'-5' phosphodiester bond altered the manner by which the 3'-5' linked part of the molecule base-stacked. In the low isomer stacking occurred from the 5' end, but changing the nature of the CpU phosphodiester linkage resulted in the molecule stacking from the other end. This was due to the C's inability to influence base-stacking because of its distance from U. It additionally allowed the G to assume more syn character in the high isomer.

The 5'-5' phosphodiester bond did not measurably effect the phosphodiester backbone of the 3'-5' linked part. This was indicated by phosphorus NMR data, which revealed near identical variable temperature plots, and analysis of coupling constants, which indicated near identical  $\zeta$  and  $\epsilon$  torsion angles.

The 5'-5' phosphodiester unit did not exist with the riboses in the same orientation as in the CU>P high dimer.

The C ribose was twisted such that the H-1' proton was exposed more to the solvent and not sandwiched between nucleotides. However, the  $\beta_{ap}$  and  $\delta_{+sc}$  populations were similar to those seen in 3'-5' oligonucleotides, indicating that the backbone conformation of the 5'-5' link adopted a similar zig-zag orientation extended one bond more. This placed the C more distant from the U, accounting for the decrease in C/U base-stacking in the high isomer.

Adding a G to one end of the 5'-5' dimer did not allow the CpU part to stack as they did in CU>P high. Hence the U/G base-stacking must have been involved in effecting the structure of the CpU part. This could be why the biologically active diadenine tetra and pentaphosphates do not contain another bound nucleotide. In the phosphorus elongated dimers, the As stack upon each other (Kolodny et al., 1979). Adding another nucleotide might create a competition for stacking and disrupt the tertiary structure of the complex.

These results indicated that a 5'-5' phosphodiester bond in a trimer effects the base-stacking and the orientation of the ribose of the alternatively linked nucleotide. The phosphodiester backbone, however, still assumed torsion angle populations consistent with Sundaralingam's "rigid" nucleotide concept (1973). This change may be sufficient to alter the structure of the oligoribonucleotide to make its primary in vivo use as the

intermediate of transcription and translation faulty. As a result any such oligoribonucleotide is probably quickly destroyed by nucleases to prevent errors in protein synthesis. Hence the major 5'-5' bond involved in capping is a triphosphate which differs much more significantly so as to not be confused with anything else.

## BIBLIOGRAPHY

- Akasaka, K., Imoto, T., Shibata, S. and Hatano, H. (1974)  
J. Magn. Reson. 18, 328.
- Alderfer, J.L. and Ts'o, P.O.P. (1977) Biochemistry 16,  
2410.
- Alkema, D. (1982) Ph. D. Thesis, McMaster University,  
Hamilton, Ontario.
- Alkema, D., Hader, P.A., Bell, R.A. and Neilson, T. (1982)  
Biochemistry 21, 2109.
- Altona, C. and Sundaralingam, M. (1972) J. Am Chem. Soc.  
94, 8205.
- Altona, C. and Sundaralingam, M. (1973) J. Am. Chem. Soc.  
95, 2333.
- Andrew, A.P. and Bolton, P.H. (1984) J. Am. Chem. Soc. 106,  
437.
- Arnott, S., Dover, S.D. and Wonacott, A.J. (1969) Acta.  
Crystallography, Sec. B 25, 2192.
- Arnott, S. and Hukins, D.W.L. (1969) Nature 224, 886.
- Arnott, S. (1970) Biophys. Mol. Biol., 265.
- Arnott, S., Hukins, D.W.L., Dover, S.D., Fuller, W. and  
Hodgson, A.R. (1973) J. Mol. Biol. 81, 107.
- Arter, D.B. and Schmidt, P.G. (1976) Nucleic Acid Res. 3,  
1437.
- Assa-Munt, N., Granot, J., Behling, R.W. and Kearns, D.R.

- (1984) *Biochemistry* 23, 944.
- Astbury, W.T. (1947), *Symp. Soc. Exp. Bio. (Nucleic Acids)* 1, 66.
- Aue, W.P., Bartholdi, E. and Ernst, R.R. (1976) *J. Chem. Phys.* 64, 2229.
- Avery, O.T., MacLeod, C.M. and McCarty, M. (1944) *J. Exp. Med.* 79, 137.
- Barfield, M. and Grant, D.M. (1965) in "Advances in Magnetic Resonance". Waugh, J.S., ed., 1, 149.
- Bax, A. and Freeman, R. (1981) *J. Magn. Reson.* 42, 164.
- Bax, A. and Drobny, G. (1985) *J. Magn. Reson.* 61, 306.
- Beckett, O. and Uhlenbeck, O.C., in "Oligonucleotide Synthesis...A Practical Approach". Gait, M.J., ed., IRL Press Limited, Oxford, England, 190.
- Bell, R.A. and Saunders, J.K. (1973) in "Topics in Stereodynamics". Allinger, N.L. and Eliel, L., eds., Wiley, N.Y., Vol. 7, 1.
- Bell, R.A., Alkema, D., Coddington, J.M., Hader, P.A., Hughes, D.W., and Neilson, T. (1983) *Nucleic Acid Res.* 11, 1143.
- Bell, R.A., Everett, J.R., Hughes, D.W., Coddington, J.M., Alkema, D., Hader, P.A. and Neilson, T. (1985) *J. Biomol. Struct. Dynam.* 2, 693.
- Blackburn, B.J., Grey, A.A., Smith, I.C.P. and Hruska, F.E. (1970), *Can. J. Chem.* 48, 2866.
- Bodenhausen, G. and Freeman, R. (1977) *J. Magn. Reson.* 28,

471.

- Bolton, P.H. (1982) *J. Magn. Reson.* 48, 336.
- Borer, P.N., Dengler, B., Tinoco, Jr., I. and Uhlenbeck, P.C. (1974) *J. Mol. Biol.* 66, 843.
- Borer, P.N., Kan, L.S. and Ts' O, P.O.P. (1975), *Biochemistry* 14, 4847.
- Breitmaier, E., Spohn, K.H. and Berger, S. (1975) *Agnew. Chem. Internat. Edit.* 14, 144.
- Bridge, S., Wartell, R., Stellman, S., Hingenty, B. and Langridge, R. (1975) *Biopolymers* 14, 1597.
- Bury, C.D., Nurth, A.C.T., Glasel, J.A., Williams, R.J.P. and Xavier, A.V. (1980) *Nature* 232, 236.
- Cantor, E.R. and Schimmel, P.R. (1980) in "Biophysical Chemistry, Part III, The Behaviour of Macromolecules". W.H. Freeman and Company, San Francisco, 1109.
- Chachaty, C., Zamb, T., Langlet, G., Tran-Dinh Son, Buc, H. and Morange, M. (1976) *Eur. J. Biochem.* 62, 45.
- Chan, S.I. and Neilson, J.H. (1969) *J. Am. Chem. Soc.* 91, 168.
- Cheng, D.M., Kan L.-S., Iuorno, V.L. and Ts'o, P.O.P. (1984) *Biopolymers* 23, 575.
- Chou, S.-H., Wenner, D.E., Hare, D.R. and Reid, B.R. (1984) *Biochemistry* 23, 2257.
- Clore, G.M., Kimber B.J. and Gronenborn, A.M. (1983) *J. Magn. Reson.* 54, 170.

- Clore, G.M. and Gronenborn, A.M. (1984) *Eur. J. Biochem.* 141, 119.
- Clore, G.M., Lauble, H., Frenkiel, T.A. and Gronenborn, A.M. (1984) *Eur. J. Biochem.* 145, 629.
- Coddington, J. and Bell, R.A. (1983) in unpublished data.
- Cruz, P., Hall, K., Puglisi, J.D., Davis, P., Hardin, C.C., Trulson, M.O., Mathies, I., Tinoco, Jr., I. and Neilson, T. (1985) in "The Fourth Conference of Biomolecular Stereodynamics". Sarma, R.H. ed., Adenine Press, N.Y., 268.
- Davies, D.B., (1976) *Stud. Biophys.* 55, 29.
- Davies, D.B. (1978) *Prog. NMR Spec.* 12, 135.
- de Leeuw, H.P.M., Haasnoot, C.A.G. and Altona, C. (1980) *Isr. J. Chem.* 20, 108.
- Delsuc, M.A., Guittet, E., Trotin, N. and Lallemand, N.Y. (1984) *J. Magn. Reson.* 56, 163.
- Donner-Keller, H., Maxam, A.M. and Gilbert, W. (1977) *Nucleic Acid Res.* 4, 2527.
- Dorman, D.E. and Roberts, J.D. (1970) *Proc. Natl. Acad. Sci. USA* 65, 19.
- Eich, G., Bodenhausen G. and Ernst, R.R. (1982) *J. Am. Chem. Soc.* 104, 3731.
- England, T.E. and Neilson, T. (1976) *Can. J. Chem.* 54, 1714.
- England, T.E. and Neilson, T. (1977) *Can. J. Chem.* 55, 365.
- Everett, J.R., Hughes, D.W., Bell, R.A., Alkema, D., Nelson, T. and Romaniuk, P.J. (1980) *Biopolymers* 19, 557.

- Ezra, F.S., Lee, C.-H., Kondo, N.S., Danyluk, S.S., and  
Sarma, R.H. (1977) *Biochemistry* 16, 1977.
- Fazakerley, G.V., van der Marel, G.A., van Boom, J.H. and  
Guschlbauer, W. (1984) *Nucleic Acid Res.* 12, 8269.
- Fukushima, E. and Roeder, S.B.W. (1981) in "Experimental  
Pulse NMR; A Nuts and Bolts Approach". Addison-  
Wesley Publishing Company, Inc., Don Mills,  
Ontario, 163.
- Gaven, H. and Levinthal, C. (1960) *Biochem. et Biophys.*  
*Acta.* 38, 470.
- Geissner-Prettre, C., Pullman B., Borer, P.N., Kan, L. and  
Ts'o, P.O.P. (1976) *Biopolymers* 15, 2277.
- Geraldes, C.F.G.G. and Williams, R.J.P. (1978) *Eur. J.*  
*Biochem.* 85, 471.
- Glover, D.M. (1980) in "Genetic Engineering: Cloning  
DNA". Chapman and Hall, N.Y., 1.
- Gorenstein, D.G. and Kar, D. (1975) *Biochem. Biophys. Res.*  
*Commun.* 65, 1073.
- Gorenstein, D.G., Findlay, J.B., Momii, R.K., Luxon, B.A.  
and Kar D. (1976) *Biochemistry* 15, 3796.
- Gorenstein, D.G., Luxon, B.A., Goldfield, E.M., Lai, K. and  
Vegeais, D. (1982) *Biochemistry* 21, 580.
- Gorenstein, D.G., Lai, K. and Shah, D.O. (1984) *Biochemistry*  
23, 6717.
- Gorenstein, D.G. (1984) in "P-31 NMR: Principles and  
Applications". Gorenstein, D.G. ed., Academic Press

Orlando, Flor., 1.

- Gralla, J. and Crothers, D.M. (1973) *J. Mol. Biol.* 78, 301.
- Gregoire, R.J. and Neilson, T. (1978) *Can. J. Chem.* 56, 487.
- Griffen, J.H., Schechter, A.N. and Cohen, J.S. (1973) *Ann. N.Y. Acad. Sci.* 222, 693.
- Gueron, M. and Shulman, R.G. (1975) *Proc. Natl. Acad. Sci. USA* 72, 3482.
- Guittet, E., Piveteau, D. and Lallemand, N.Y. (1984), *Nucleic Acid Res.* 12, 5927.
- Guschlbauer, W. and Trans-Din Son (1975) *Nucleic Acid Res.* special publication #1, 585.
- Haasnoot, C.A.G. and Altona, C. (1979) *Nucleic Acid Res.* 6, 1135.
- Hader, P.A., Alkema, D., Bell, R.A. and Neilson, T. (1982) *J. Chem. Soc. Chem. Commun.*, 10.
- Hahn, U., Desai-Hahn, R. and Ruterjans, H. (1985) *Eur. J. Biochem.* 146, 705.
- Hall, K., Cruz, P., Tinoco, Jr., I., Jovin, T.M. and van de Sandt, J.H. (1984) *Nature* 311, 584.
- Hare, D.R. and Reid, B.R. (1982) *Biochemistry* 21, 1835.
- Harris, R.K. (1983) in "Nuclear Magnetic Resonance Spectroscopy". Pitman Publishing Inc., Toronto, 105.
- Hiramaru, M., Uchida, T. and Egami, F. (1969) *J. Biochem. (Tokyo)* 65, 697.
- Hoffman, R.A. and Forsen S. (1966) *Prog. Nucl. Reson. Spec.*

- 1, 15.
- Holley, R.W., Apgar, J., Everett, G.A., Madison, J.T.,  
Marquise, M., Merrill, S.J., Penwick, J.R. and  
Zamir, A. (1965) *Science* 147, 1462. †
- Hore, P.J. (1983) *J. Magn. Reson.* 54, 539.
- Hruska, F.E. (1973) in "Conformations of Biological  
Molecules and Polymers". Bergmann, E.D. and  
Pullman, B., ed., Academic Press, N.Y., 345.
- Hruska, F.E. and Blonski, W.J.P. (1982) *Can. J. Chem.* 60,  
4026.
- IUPAC-PAC Joint Commission on Biochemical Nomenclature (1983)  
*Eur. J. Biochem.* 131, 9.
- Jardetzky, C.D. (1960) *J. Am. Chem. Soc.* 82, 229.
- Jones, A.J., Winkley, M.W., Grant, D.M. and Robins, R.K.  
(1970) *Proc. Natl. Acad. Sci. USA* 65, 27.
- Kallenback, N.R. and Bermann, H.M. (1977) *Quarterly Rev.  
Biophys.* 10, 138.
- Karplus, M. (1969) *J. Chem. Phys.* 33, 1842.
- Kearns, D.R., Patel D.J. and Shulman, R.G. (1971) *Nature* 229,  
338.
- Kearns, D.R. and Shulman, R.G. (1974) *Accounts Chem. Res.* 7,  
33.
- Kitamura, K., Wakahara, A., Mizuno, H., Baba, Y. and  
Tomita, K.-I. (1981) *J. Am. Chem. Soc.* 103, 3899.
- Klyne, W. and Prelog, V. (1960) *Experientia* 16, 521.
- Kolodny, N.H., Kisteneff, E., Redfield C. and Rapaport E.

- (1979) FEBS Letters 107, 121..
- Kondo, N.S., Holmes, H.M., Stempel, L.M. and Ts'ao, P.O.P.  
(1970) Biochemistry 9, 3479.
- Kornberg, A. (1960) Science 131, 1503.
- Lankhorst, P.P., Haasnoot, C.A.G., Erkelen, C., Westerink,  
J.H., van der Marel, G.A., van Boom, J.H. and  
Altona, C. (1985) Nucleic Acid Res. 13, 927.
- Lapper, R.D. and Smith, I.C.P. (1973) J. Am. Chem. Soc. 95,  
2880.
- Lee, C.-H. and Sarma, R.H. (1976) J. Am. Chem. Soc. 98,  
3541.
- Lee, C.-H., Ezra, F.S., Kondo, N.S., Sarma, R.H. and  
Danyluk, S.S. (1976) Biochemistry 15, 3627.
- Lee, C.-H. and Tinoco, Jr., I. (1978) Nature 274, 609.
- Lee, C.-H. and Tinoco, Jr., I. (1980) Phys. Chem. 11, 283
- Le Goff, E. (1964) J. Organic Chem. 29, 2048.
- Lown, J.W. and Hanstock, C.C. (1985) J. Biomol. Struct.  
Dynam. (in press).
- Macura, S. and Ernst R.R. (1980) Mol. Phys. 41, 95.
- Martin, F.H., Uhlenbeck, O.C. and Doty, P. (1971) J. Mol.  
Biol. 57, 201.
- Maudsley, A.A., Muller, L. and Ernst, R.R. (1977), J. Magn.  
Reson. 28, 463.
- Meselson, M. and Stahl, F.W. (1958) Proc. Natl. Acad. Sci.  
USA 44, 671.
- Miller, J., Kumar, A. and Ernst, R.R. (1975) J. Chem. Phys.

- 63, 5490.
- Mizuno, H., Tomita, K. and Nakagawa, E. (1981) *J. Mol. Biol.* 148, 103.
- Morris, G.A. and Freeman, R. (1979) *J. Am. Chem. Soc.* 101, 760.
- Nagayama, K., Wuthrich, K. and Ernst, R.R. (1979) *Biochem. Biophys. Res. Commun.* 90, 305.
- Nagayama, K., Kumar, A., Wuthrich, K. and Ernst, R.R. (1980) *J. Magn. Reson.* 40, 321.
- Neilson, T. (1969) *Chem. Comm.*, 1139.
- Neilson, T. and Werstiuk, E.S. (1971) *Can. J. Chem.* 49, 493.
- Neilson, T., Wastrodowski, F.V. and Werstiuk, E.S. (1973) *Can. J. Chem.* 51, 1068.
- Neilson, T. and Werstiuk, E.S. (1974) *J. Am. Chem. Soc.* 96, 2295.
- Neilson, T., Deugau, K.V., England T.E. and Werstiuk, E.S. (1975) *Can. J. Chem.* 53, 1093.
- Noggle, J.H. and Schirmer, R.F. (1971) in "The Nuclear Overhauser Effect". Academic Press, N.Y., 1.
- Ott, J. and Eckstein, F. (1985) *Biochemistry* 24, 2530.
- Pardi, A. and Tinoco, Jr., I. (1982) *Biochemistry* 21, 4686.
- Pasto, D.J. and Johnson C.R. (1969) in "Organic Structure Determination". Prentice-Hall Inc., Englewood Cliffs, N.J.
- Patel, D.J., and Tonelli, A.E. (1974) *Biopolymers* 13, 1943.
- Patel, D.J. (1976) *Biopolymers* 15, 533.

- Patel, D.J., Kozlowski, S.A., Nordheim, A. and Rich, A.  
(1982) Proc. Natl. Acad. Sci. USA 79, 1413.
- Patel, D.J., Kozlowski, S.A., Weiss, M. and Bhatt, R.  
(1984) Biochemistry 24, 936.
- Perkins, S.J. (1982) in "Biological Magnetic Resonance".  
Berliner, L.J. and Reuben, J., eds., Plenum Press,  
N.Y., 193.
- Petersheim, M., Shujaath, M. and Geilf, J.A. (1984) J. Am.  
Chem. Soc. 106, 439.
- Philippsen, P. and Zachau, H.G. (1974) in "Methods in  
Enzymology". Vol. 19, Academic Press, N.Y., 473.
- Plateau, P. and Gueron, M. (1982) J. Am. Chem. Soc. 104,  
7310.
- Pradd, F.R., Giessner-Prettre, C. Pullman, B. and Daudex,  
J.-P. (1977) J. Am. Chem. Soc. 101, 1737.
- Razzell, W.E. and Kharana, H.G. (1959) J. Biol. Chem. 234,  
2105.
- Razzell, W.E. and Kharana, H.G. (1961) J. Biol. Chem. 236,  
1144.
- Redfield, A.G., Kunz, S.D. and Ralph, E.K. (1975) J. Magn.  
Reson. 19, 114.
- Redfield, A.G., Roy, S., Sanchez V., Tropp J. and Figueroa,  
N. (1981) in "The Second SUNYA Molecular  
Sterodynamics Conference". Sarma, R.H. ed., Pergamon  
New York, 195.
- Reinhard, B. and Gunther, H. (1983) Angew. Chem. Internat.

- Edit. 22, 350.
- Romaniuk, P.J. (1979) Ph. D. Thesis, McMaster University, Hamilton, Ontario.
- Rosenberg, J.M., Seeman, N.C., Kim, J.J.P., Suddath, F.L., Nicholas, H.B. and Rich, A. (1973) *Nature* 243, 150.
- Roth, K., Kimber B.J. and Feeney J. (1980) *J. Magn. Reson.* 41, 283.
- Saenger, W. (1984) in "Principles of Nucleic Acid Structure". Springer-Verlag, N.Y. Inc., 16.
- Sanger, F., Brownlee, G.G., and Barrell, B.G. (1967) in "Struct. Funct. Transfer RNA 5S-RNA, Proc. Meet. Fed. Euro. Biochem. Soc., 4th 1967". Froeholm, L.O. ed., Academic Press: London, England, 1.
- Sarma, R.H., Lee, C.-H., Hruska, F.E. and Wood, D.J. (1973a) *FEBS Lett.* 36, 157.
- Sarma, R.H., Mynott, R.J., Wood, D.J. and Hruska, F.E. (1973b) *J. Am. Chem. Soc.* 95, 6457.
- Schweizer, M.P., Banta, E.B., Witkowski, J.T. and Robins, R.K. (1973) *J. Am. Chem. Soc.* 95, 3770.
- Seeman, N.C. (1980) in "Nucleic Acid Geometry and Dynamics". Sarma, R.H. ed., Elmsford, N.Y., Pergamon Press, 47.
- Scheek, R.M., Sniderweg, E.R.P., Klappe, K.J.M., van Boom, J.H., Kaptein, R., Rutenjans, H. and Beyreuther, K. (1983) *Biochemistry* 22, 228.
- Schleich, T., Cross, B.P. and Smith, I.C.P. (1976) *Nucleic Acid Res.* 3, 355.

- Shah, D.O., Lai, K. and Gorenstein, D.G. (1984) *J. Am. Chem. Soc.* 106, 4302.
- Shatkin, A.J. (1976) *Cell* 9, 645.
- Sklenar, V. and Starcuk, Z. (1982) *J. Magn. Reson.* 50, 495.
- Stannard, B.S. and Fesenfeld, G. (1975) *Biopolymers* 14, 299.
- Starcuk, Z. and Sklenar, V. (1985) *J. Magn. Reson.* 61, 567.
- Sundaralingam, M. (1973) in "Conformations of Biological Molecules and Polymers". Bergmann, E.D. and Pullman, B., ed., Academic Press, N.Y., 417.
- Sussman, J.L., Seeman, N.C., Kim, S.H. and Berman, H.M. (1972) *J. Mol. Biol.* 61, 403.
- van Boom, J.H. and Wreesman, C.T.J. (1984) in "Oligonucleotide Synthesis...A Practical Approach". Gait, M.J., ed., IRL Press Limited, Oxford, England, 153.
- Ts'o, P.O.P., Kondo, M.S., Schweizer, M.P. and Hollis, D.P. (1969) *Biochemistry* 8, 997.
- Wastrodowski, E.V. (1972) Masters Thesis, McMaster University, Hamilton, Ontario.
- Watson, J.D. and Crick, F.H.C. (1953a) *Nature* 171, 737.
- Watson, J.D. and Crick, F.H.C. (1953b) *Nature* 171, 694.
- Wehilri, F.W. and Wirthlin, T. (1976) in "Interpretation of C-13 NMR Spectroscopy". Heyden and Son Ltd., London.
- Werstiuk, E.S. and Neilson, T. (1973) *Can. J. Chem.* 51, 1889.
- Werstiuk, E.S. and Neilson, T. (1976) *Can. J. Chem.* 54, 2689.

- Wiberg, K.B. and Nist, B.J. (1962) in "Interpretation of NMR Spectra". W.A. Benjamin, Inc., N.Y.
- Wong, A.H.J., Quigley, G.J., Kolpak, F.J., Crawford, J.L., van Boom, J.H., van der Marcel, G. and Rich, A. (1979) Nature 282, 680.
- Yokoyama, S, Inagaki, F. and Miyazawa, T. (1981) Biochemistry 20, 2981.
- Hughes, D.W., Bell, R.A., Neilson, T., and Bain, A.D. (1985) Can. J. Chem. 63, 3133.